

LIBRARY
SEP 15 1958

JOURNAL OF THE
**Electrochemical
Society**

Vol. 105, No. 9

September 1958

แผนกห้องสมุด กรมวิทยาศาสตร์
กระทรวงอุตสาหกรรม





Quiet, please—skill at work!

The quiet efficiency of a skillfully operated cell room has the rewarding effect of extra returns.

The technical know-how of the man on the job contributes greatly to a profitable operation. Equally important is the superior performance of **GLC anodes**, which are "custom-made" to individual cell requirements.

FREE — This illustration of anode adjustment has been handsomely reproduced with no advertising text. We will be pleased to send you one of these reproductions with our compliments. Simply write to Dept. J 9.

ELECTRODE

DIVISION

GREAT LAKES CARBON CORPORATION

18 EAST 48TH STREET, NEW YORK 17, N.Y. OFFICES IN PRINCIPAL CITIES

EDITORIAL STAFF

R. J. McKay, Chairman, Publication Committee

Cecil V. King, Editor

Norman Hackerman, Technical Editor

Ruth G. Sterns, Managing Editor

U. B. Thomas, News Editor

H. W. Salzberg, Book Review Editor

Natalie Michalski, Assistant Editor

DIVISIONAL EDITORS

W. C. Vosburgh, Battery

Milton Stern, Corrosion, I

R. T. Foley, Corrosion, II

T. D. Collinan, Electric Insulation

Abner Brenner, Electrodeposition

H. C. Froelich, Electronics

D. H. Baird, Electronics—Semiconductors

Sherlock Swann, Jr., Electro-Organic, I

Stanley Wawzonek, Electro-Organic, II

John M. Blocher, Jr., Electrothermics and Metallurgy, I

A. U. Seybolt, Electrothermics and Metallurgy, II

N. J. Johnson, Industrial Electrolytic

C. W. Tobias, Theoretical Electrochemistry, I

A. J. deBethune, Theoretical Electrochemistry, II

REGIONAL EDITORS

Howard T. Francis, Chicago

Joseph Schuelein, Pacific Northwest

J. C. Schumacher, Los Angeles

G. W. Heise, Cleveland

G. H. Fetterley, Niagara Falls

Oliver Osborn, Houston

Earl A. Gulbransen, Pittsburgh

A. C. Holm, Canada

J. W. Cuthbertson, Great Britain

T. L. Rama Char, India

ADVERTISING OFFICE

ECS

1860 Broadway, New York 23, N. Y.

ECS OFFICERS

Sherlock Swann, Jr., President
University of Illinois, Urbana, Ill.

W. C. Gardiner, Vice-President
Olin Mathieson Chemical Corp., Niagara
Falls, N. Y.

R. A. Schaefer, Vice-President
Cleveland Graphite Bronze Div., Clevite
Corp., Cleveland, Ohio

Henry B. Linford, Vice-President and
Interim Secretary
Columbia University, New York, N. Y.

Lyle I. Gilbertson, Treasurer
Air Reduction Co., Murray Hill, N. J.

Robert K. Shannon, Executive Secretary
National Headquarters, The ECS, 1860
Broadway, New York 23, N. Y.

Journal of the Electrochemical Society

SEPTEMBER 1958

VOL. 105 • NO. 9

CONTENTS

Editorial

September 28–October 2, 1958. *J. Convey* 184C

Technical Papers

The Reaction of Germanium with Nitric Acid Solutions

I. The Dissolution Reaction. *M. C. Cretella and H. C. Gatos* 487

II. Passivity of Germanium. *M. C. Cretella and H. C. Gatos* 492

Studies of the Anodic Behavior of Aluminum

I. The Direction of Ionic Movement. *J. E. Lewis and
R. C. Plumb* 496

II. Coulometry of Barrier Layer Production. *R. C. Plumb* 498

III. The Specific Surface Area of Aluminum with Variable
Resolution from 20Å to 1000Å. *R. C. Plumb* 502

Schlieren Studies of Concentration Gradients at a Cu|HCl Anode.

R. S. Cooper 506

The Electrodeposition of Iron–Molybdenum Alloys. *L. O. Case*

and A. Krohn 512

Isolation of the Diffusion Layer at an Electrode and the Deter-

mination of Concentration Polarization. *T. Yannakopoulos
and A. Brenner* 521

Phase Equilibria and Fluorescence in a Portion of the System

ZnO–MnO–P₂O₅. *F. A. Hummel and F. L. Katnack* 528

Preparation and Properties of Aluminum Antimonide.

A. Herczog, R. R. Haberecht, and A. E. Middleton 533

Anodic Polarography with a Rotating Platinum Microelectrode,

II. Oxidation of Various Indole Alkaloids. *M. J. Allen and
V. J. Powell* 541

The Preparation of Cadmium Niobate by an Anodic Spark Re-

action. *W. McNeill* 544

Technical Notes

The Nature of Anode Slime. *D. A. Vermilyea* 547

Transport Numbers of the Pure Fused Salts, LiNO₃, NaNO₃,
KNO₃, and AgNO₃. *F. R. Duke and B. Owens* 548

Technical Review

Report of the Chlor-Alkali Committee of the Industrial Electro-
lytic Division for the Year 1957. *J. C. Cole and
R. B. MacMullin* 550

Current Affairs

Ottawa Meeting, September 28–October 2, 1958 187C

J. J. Lander to Receive Battery Division's First Research Award 189C

High Lights of April 1958 Board of Directors' Meeting 189C

Section News 190C Literature from Industry 195C

Division News 190C Book Reviews 196C

New Members 191C Announcements from

Personals 192C Publishers 199C

News Items 192C Employment Situation 199C

Changes in E & M Program,
Ottawa Meeting 193C ECS Future Meeting Dates 182C

Published monthly by The Electrochemical Society, Inc., from Manchester, N. H., Executive Offices, Editorial Office and Circulation Dept., and Advertising Office at 1860 Broadway, New York 23, N. Y., combining the JOURNAL and TRANSACTIONS OF THE ELECTROCHEMICAL SOCIETY. Statements and opinions given in articles and papers in the JOURNAL OF THE ELECTROCHEMICAL SOCIETY are those of the contributors, and The Electrochemical Society assumes no responsibility for them. Noneductible subscription to members \$6.00, subscription to nonmembers \$18.00. Single copies \$1.25 to members, \$1.75 to nonmembers. Copyright 1958 by The Electrochemical Society, Inc. Entered as second-class matter at the Post Office at Manchester, N. H., under the act of

181C

สมุดรายนามสมาชิก

FUTURE MEETINGS OF The Electrochemical Society



Ottawa, Canada, September 28, 29, 30, October 1, and 2, 1958

Headquarters at the Chateau Laurier

Sessions will be scheduled on

Batteries, Corrosion, Electrodeposition (including symposia on "Electrodeposition on Uncommon Metals" and "Electrodeposition from Fused Salts"

Electronics (Semiconductors),

Electrothermics and Metallurgy,

and a symposium on "Films Formed in Contact with Liquids"

sponsored by Theoretical Electrochemistry, Battery, and Corrosion Divisions

★ ★ ★

Philadelphia, Pa., May 3, 4, 5, 6, and 7, 1959

Headquarters at the Sheraton Hotel

Sessions probably will be scheduled on

Electric Insulation, Electronics (including Luminescence and Semiconductors), Electrothermics and Metallurgy

(including a Projected Symposium on "Mechanical Properties of Intermetallic Compounds"),

Industrial Electrolytics, and Theoretical Electrochemistry

★ ★ ★

Columbus, Ohio, October 18, 19, 20, 21, and 22, 1959

Headquarters at the Deshler-Hilton Hotel

★ ★ ★

Chicago, Ill., May 1, 2, 3, 4, and 5, 1960

Headquarters at the Lasalle Hotel

★ ★ ★

Houston, Texas, October 9, 10, 11, 12, and 13, 1960

Headquarters at the Shamrock Hotel

★ ★ ★

Papers are now being solicited for the meeting to be held in Philadelphia, Pa., May 3-7, 1959. Triplicate copies of each abstract (*not exceeding 75 words in length*) are due at Society Headquarters, 1860 Broadway, New York 23, N. Y., *not later than January 2, 1959* in order to be included in the program. *Please indicate on abstract for which Division's symposium the paper is to be scheduled, and underline the name of the author who will present the paper.* Complete manuscripts should be sent in triplicate to the Managing Editor of the JOURNAL at 1860 Broadway, New York, 23, N. Y.

ANODE UNIFORMITY

**...that
really
pays-off!**

... from a Maintenance Standpoint

the uniform structure of Stackpole GraphAnodes assures slow, even graphite consumption with reduced cell contamination. GraphAnodes are carefully planed for perfect cell alignment, longer life, uniform wear. Moreover, the superior chemical resistance of their Stackpole oil impregnants materially lengthens diaphragm life.

... from Cost and Performance Standpoints

Stackpole GraphAnodes deliver more for the money in terms of longer life, lower cell maintenance . . . and with the added economy of low-voltage operation. Let Stackpole engineers arrange for a convincing demonstration on your equipment. *Stackpole Carbon Company, St. Marys, Penna.*



STACKPOLE

GRAPHANODES

**graphite anodes in grades, sizes
and shapes for all electrolytic cells**

TUBE ANODES • CATHODIC PROTECTION ANODES • FLUXING & DE-GASSING TUBES • BRUSHES for all rotating electrical equipment • ELECTRICAL CONTACTS • VOLTAGE REGULATOR DISCS • "CERAMAGNET"® CERAMIC MAGNETS • ROCKET NOZZLES • BEARINGS • SALT BATH RECTIFICATION RODS • SEAL RINGS • FRICTION RINGS • ELECTRODES & HEATING ELEMENTS • MOLDS & DIES • WELDING CARBONS • POROUS CARBON • and many other carbon, graphite, and electronic components.



September 28-October 2, 1958

*T*HE Ontario-Quebec Section of The Electrochemical Society will be happy to welcome you to Ottawa, the Capital city of Canada.

It is seven years since the Society held its convention in Canada and, on that occasion, Montreal, the largest commercial and industrial city, was visited. Ottawa has a different setting; its pioneer industry of lumbering is represented today by the pulp and paper industries in its environs, while its gothic Parliament Buildings, Chateau Laurier, and the magnificent Ottawa River are the outstanding sights in the view embracing the Gatineau Hills and the rugged Gatineau National Park.

You may think of Ottawa as beyond the northerly limit of the United States, whereas, in fact, its latitude is practically that of Minneapolis and St. Paul, and most of our cold weather of last winter, we are led to believe, originated to the south and west of us. Ottawa usually has incomparable autumn weather and we planned the Fall Convention dates with that thought uppermost in our minds.

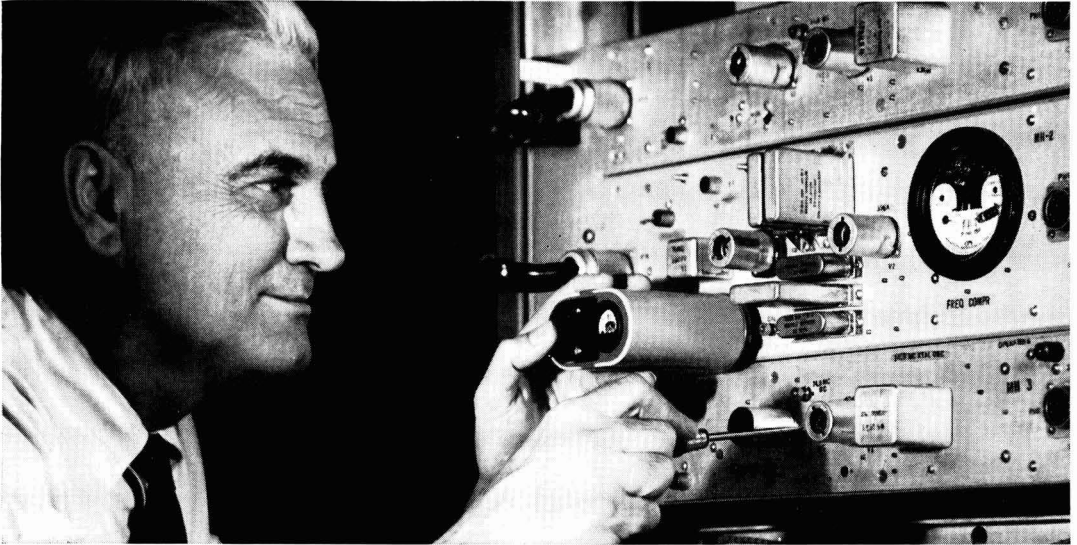
We are sure you will enjoy the scenic beauties of Ottawa and understand why it was selected as the Capital. Hordes of visitors from south of the line were with us recently for the world-famous Spring Tulip Festival. Though you may have missed that display, we know you will enjoy the autumn colors in the numerous parks and along the driveways. A short drive along the Ottawa River takes one into the sports and recreation area beloved by both summer tourist and winter ski enthusiast.

Our headquarters hotel is justly named the "Chateau" because its architecture and its hospitality make it more than merely a hotel. The other accommodations are also famous for their hospitality. Perhaps, when you have once visited Ottawa, you will return to see why we enjoy our Capital not only in autumn but in spring, summer, and winter.

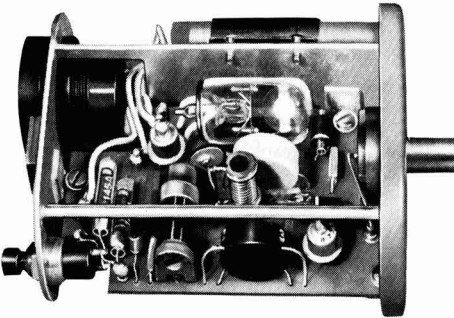
JOHN CONVEY¹

¹ General Chairman, Ottawa Convention Committee.

Bell Laboratories Announces Pocket-Sized Frequency Standard for Microwave Systems



Lawrence Koerner, who developed the portable frequency standard, demonstrates how the device can be plugged in at a radio relay station to supply a checking frequency. Battery-powered, the device maintains precision calibration for several months.



Inside the portable frequency standard. Four Laboratories-developed devices make it possible: (1) transistor, which converts the power from a battery to radio frequency oscillations; (2) voltage reference diode, which maintains constant voltage; (3) piezoelectric crystal unit of superlative stability; (4) thermistor, which corrects for temperature variations.

Microwave radio relay systems depend critically on the accuracy of their "carrier" frequencies. At scores of relay stations along a route, carrier frequency oscillators must be checked periodically against a signal from a precise standard.

In the past, the maintenance man has had to obtain his checking frequency by picking up a standard radio signal from a government station. This operation takes time—and requires elaborate equipment.

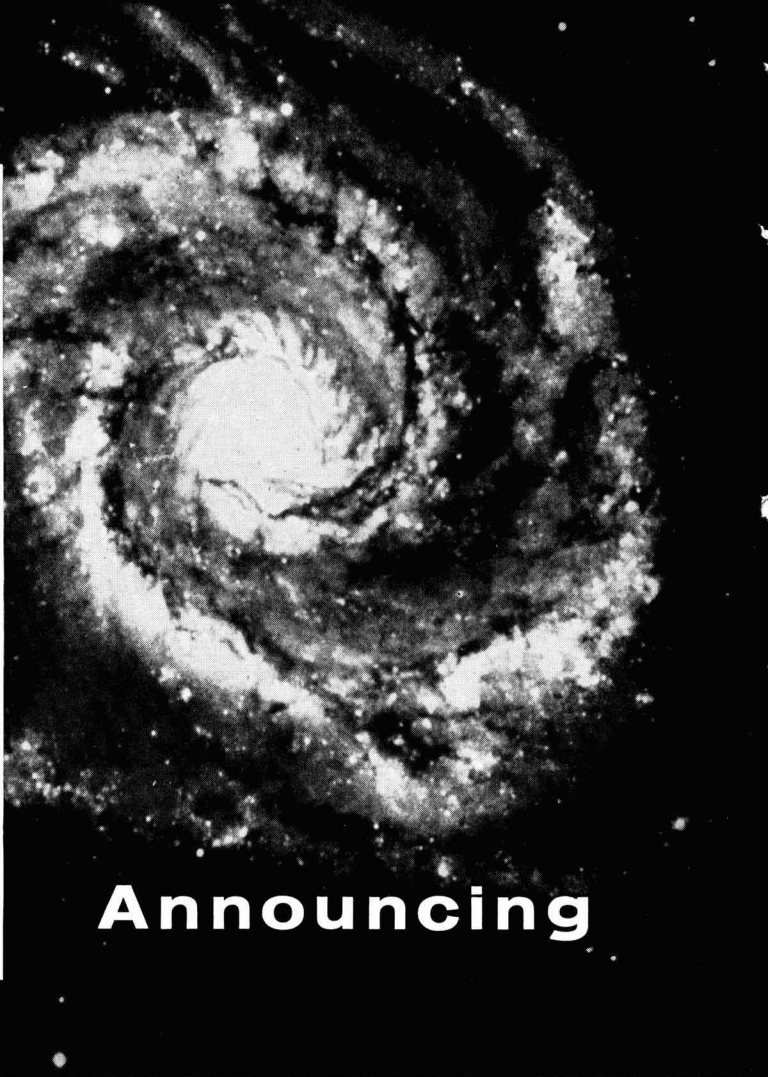
With a new *portable* frequency standard developed by Bell Laboratories engineers, the job is much simplified. To check an oscillator, the portable standard is plugged in, and a button is pressed. In seconds, it supplies a checking frequency accurate to one part in a million.

Until now, such precision in a frequency standard has been obtainable only in a laboratory. The new portable standard makes it available for routine use in the Bell System. First use of the standard will be to maintain frequency control in a new microwave system for telephone and TV, now under development at Bell Laboratories.



BELL TELEPHONE LABORATORIES

WORLD CENTER OF COMMUNICATIONS RESEARCH AND DEVELOPMENT



Announcing

GRACE SILICON

(ultra-high purity)

Whether you make or use silicon devices, a new standard of quality is now available to you through Grace—leader in chemical research and development.

Grace Silicon, manufactured by the Pechiney process, has an extremely low boron content as well as over-all ultra-high purity.

Other characteristics of Grace Silicon include uniform quality as verified by some of the nation's leading electronic manufacturers.

Wherever a semi-conductor of top quality is desired for rectifiers, transistors, diodes—get in touch with GRACE ELECTRONIC CHEMICALS, INC., at PLaza 2-7699 in Baltimore.

GRACE ELECTRONIC CHEMICALS, INC.

101 N. Charles St., Baltimore, Maryland



Subsidiary of W. R. GRACE & CO.

The Reaction of Germanium with Nitric Acid Solutions

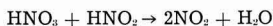
I. The Dissolution Reaction

Mary C. Cretella and Harry C. Gatos

Lincoln Laboratory, Massachusetts Institute of Technology, Lexington, Massachusetts

ABSTRACT

The reaction of single-crystal germanium with HNO_3 was studied as a function of concentration, stirring rate, and temperature. The reaction rate increased with increasing HNO_3 concentration, reaching a maximum at approximately 6*N*. At a given HNO_3 concentration the dissolution rate decreased with stirring and increased with time. The initial rate was found to be proportional to the product of the concentrations of undissociated HNO_3 and HNO_2 . The dissolution potential of the germanium became more noble (cathodic) with increasing HNO_3 concentration. It is proposed that the rate-determining step of the dissolution process is



The germanium dissolution rate in HNO_3 solutions ($N < 6$) was not affected by the presence of HF unless the concentration of the latter exceeded approximately 6*N*.

Chemical reactions of semiconductor surfaces with aqueous solutions have become of considerable interest in recent years. The preparation of consistently clean and reproducible surfaces, particularly those of germanium and silicon, is extremely important in many studies of semiconductor physics and in the fabrication of solid-state devices. Mechanical means of surface preparation usually result in contamination and, especially, in structural distortion of the surfaces. Chemical methods, on the other hand, have been employed satisfactorily by and large. A number of solutions have been developed for chemical polishing and etching, primarily on an empirical basis. Since germanium and silicon are generally not attacked by nonoxidizing media over a wide range of pH, effective etches for these two elements contain at least one oxidizing agent. Nitric acid is the principal oxidizing agent in the relatively successful and most commonly used etching or polishing solution for germanium and silicon. Known as the CP-4 etch, it contains hydrofluoric acid, acetic acid, and bromine in addition to nitric acid. The action of this chemical polishing agent or that of its individual components is little understood.

The present study represents an attempt to elucidate the action of HNO_3 , undoubtedly the most important component of CP-4 etch, with elemental semiconductors. Germanium was chosen since it was more readily available at high purity than silicon. In order to clarify certain aspects of the action of nitric acid on germanium, nitric-hydrofluoric acid solutions were employed. Thus, to some extent, the action of hydrofluoric acid on germanium was also studied.

Experimental

Germanium samples.—The samples used were prepared from single crystals grown in this lab-

oratory from high-purity, zone-refined germanium. Slabs with uniform resistivity of about 20 ohm-cm were cut from p-type crystals and 40 ohm-cm from n-type. The crystals were grown along the $\langle 111 \rangle$ axis, and slabs were cut perpendicular to this axis. All samples employed were rectangular in shape and measured 1 cm x 2 cm x 0.06 cm, affording a large face-to-edge ratio. The two large faces were {111} surfaces. Unless otherwise stated, the data reported in the paper refer to p-type material.

Surface treatment consisted of grinding the faces with No. 600 Carborundum, etching for 1 min in CP-4 etch to remove the distorted layers and immediately rinsing thoroughly with doubly distilled water. This treatment resulted in smooth and reproducible surfaces. The samples were desiccated prior to weighing. Frequently the samples were reused, but their surfaces were prepared in the same manner as above prior to each run.

Solutions.—Stock solutions of the desired HNO_3 normality were prepared, and their exact concentration was determined analytically. The $\text{HNO}_3 + \text{HF}$ solutions were prepared just before use by weighing standard HNO_3 and HF solutions into the reaction vessel. Prior to weighing, the concentrations of the individual solutions were determined analytically. All solutions were prepared from reagent grade chemicals and doubly distilled water.

Apparatus for dissolution experiments and potential measurements.—The apparatus employed for the dissolution experiments, potential measurements, and the effect of stirring is shown in Fig. 1. The main vessel was constructed of glass in the HNO_3 experiments and of "Kel-F" when HF solutions were employed. A Kel-F sample holder permitted rotation of the germanium samples and electrical connection for electrode potential measurements. Ohmic contacts between platinum leads and

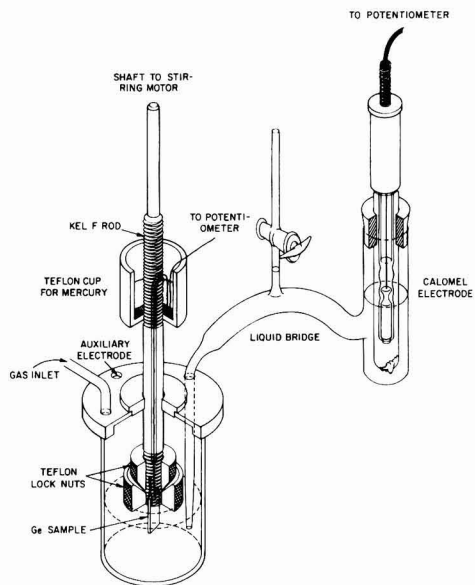


Fig. 1. Apparatus for dissolution experiments and potential measurements.

the germanium samples were obtained by soldering. In cases of vigorous or extensive dissolution the small portion of the sample masked by the holder was attacked, and its area was then included in computing the rates. Ordinarily, however, the clamped portion underwent very slight attack. Excellent agreement was found between dissolution rates determined without stirring, using the holder shown in Fig. 1, and those determined using a four-point contact sample holder made of glass rod.

Movement of solution over the sample surface was provided by coupling the Kel-F sample holder to the shaft of a stirring motor.

The apparatus was maintained to constant temperature $\pm 0.1^\circ\text{C}$. Before sample immersion the solutions were allowed to reach the desired temperature. Unless otherwise specified the data discussed in this paper were obtained at 27.5°C .

Rate determinations.—The dissolution rates were determined principally from weight-loss measurements (to ± 0.005 mg) employing an Oertling microbalance and the geometric area of the samples. Generally the weight losses fell between 0.06 and 200 mg for a sample area of approximately 4.5 cm^2 . The weight-loss data were compared with data obtained by analysis of the solutions for germanium using the spectrophotometric hematoxylin method (1) suitably modified for this work. The results of the two methods were in very good agreement. It was necessary to resort to the analytical method for all samples bearing electrical connections. Since in most cases dissolution rates remained constant for the first few hours, rates were calculated from the weight loss after 1-hr immersion and are expressed throughout in units of $\text{mg}/\text{cm}^2/\text{hr}$.

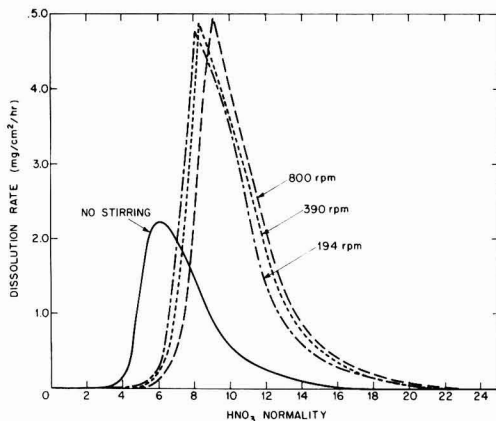


Fig. 2. Dissolution rate of germanium in HNO_3 as a function of HNO_3 concentration and stirring at 27.5°C .

Introduction of gases into the solutions.—Gases obtained commercially, mainly prepurified nitrogen, nitrogen dioxide, or mixtures of the two, were introduced through calibrated flow meters. In general, gas was bubbled through the solution for at least 1 hr prior to immersion of the samples; total gas flow was maintained at 80 ml/min. The agitation caused by gas bubbling could not be directly calculated in terms of sample rotation, which was the main form of agitation employed in this study. However, an estimate of equivalent stirring rate could be made by comparing dissolution rates during nitrogen bubbling with rates measured at various stirring rates. Nitrogen was used in this study since it could not chemically participate in the reaction mechanism.

Results and Discussion

Dependence of Dissolution Rate on Acid Concentration and Agitation

The dissolution rate of germanium as a function of HNO_3 concentration is shown for several stirring rates in Fig. 2. For all stirring rates (including zero) the dissolution rate at first increases with increasing HNO_3 concentration, reaches a maximum and then decreases, approaching zero at sufficiently high HNO_3 concentrations.

The HNO_3 concentration at which the dissolution rate is essentially zero in 1 hr or less is approximately $17N$ with no stirring; this value is shifted to approximately $23N$ (fuming HNO_3) with stirring. No hydrogen was evolved² during dissolution either with or without stirring. Stirring increases the dissolution rate at HNO_3 concentrations below about $8N$, but it has the reverse effect above $8N$ as shown for two representative concentrations in Fig. 3. The velocities indicated are the average for all parts of the sample faces as calculated from the rpm and the geometry of the sample.

The above behavior of germanium resembles closely the behavior of some of the more common

² Analysis for evolved hydrogen was performed by sweeping the reaction chamber with a stream of nitrogen and employing standard oxidation and adsorption techniques.

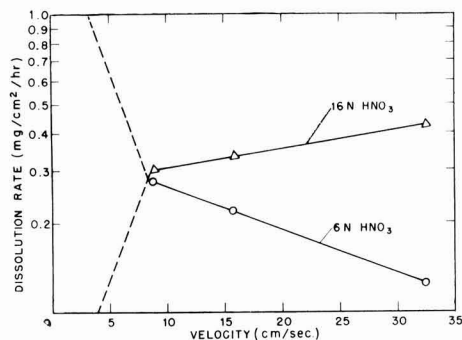


Fig. 3. Germanium dissolution in HNO_3 as a function of sample velocity at 27.5°C .

metals such as iron (2) and aluminum (3) in HNO_3 solutions. These metals are known to dissolve in dilute HNO_3 solutions and to become passive in concentrated HNO_3 . Furthermore, stirring has been found to affect their dissolution rates (4) in a way similar to that observed for germanium.

The foregoing results lead to the following conclusions.

In HNO_3 concentrations corresponding to the ascending branch of the dissolution curves (Fig. 2) intermediate products formed by the interaction of germanium and nitric acid participate in the overall dissolution reaction. Thus, stirring decreases the dissolution rate because it brings about a lower steady-state concentration of intermediates at the germanium-solution interface than does diffusion alone.

In HNO_3 concentrations corresponding to the descending branch of the dissolution curves, stirring increases the dissolution rate by reducing concentration polarization, as is often the case in metal dissolution reactions.

Apparently, different mechanisms operate in the ascending and descending branches of the dissolution curves. Furthermore, the mechanism of the descending branch must lead to passivation of germanium.

The experiments described below were carried out in an attempt to clarify these two mechanisms. The semiconductor properties of germanium have been taken into consideration.

Role of Nitrous Acid in the Dissolution Reaction

Since HNO_2 is recognized as an important intermediate in the reduction of HNO_3 , a study of the role of HNO_2 was considered essential to an understanding of the Ge-HNO_3 reaction.

In addition to HNO_2 , NO_2 has been considered an important intermediate in the reduction of HNO_3 (5). Actually, an equilibrium exists among the species HNO_2 , NO_2 , and HNO_3 in aqueous solutions as shown in Eq. [1]



Vetter (6) showed that the ratio $\frac{[\text{NO}_2]^2}{[\text{HNO}_2]}$ varies

from 10^{-7} to 10^{-5} in HNO_3 solutions ranging from 7 to 14.5N at 25°C , and hence $[\text{HNO}_2] \gg [\text{NO}_2]$. Thus,

Table I. Dissolution of germanium in dilute HNO_3 solutions at 27.5°C

Dissolution rate mg/cm ² /hr	HNO_3 Normality	C_{HNO_2} mole/liter $\times 10^3$	$\text{C}_{\text{HNO}_2}^*$ mole/liter	$\text{C}_{\text{HNO}_2} \times \text{C}_{\text{HNO}_3}$ $\times 10^5$
With stirring, 194 rpm				
0.06	5.46	—	1.26	—
0.20	5.95	0.12	1.49	17.9
0.90	6.36	0.41	1.75	71.7
1.75	6.94	0.57	2.05	116.8
3.00	7.46	0.82	2.41	197.6
Without stirring				
0.15	4.00	0.18	0.67	12.1
0.33	4.50	0.22	1.04	35.4
1.50	5.05	0.34	1.26	21.4
2.15	5.70	0.65	1.49	96.9

* Concentration of undissociated HNO_2

virtually all of the NO_2 introduced into a moderately concentrated HNO_3 solution is immediately converted to $\text{HNO}_2 + \text{HNO}_3$.

In view of this equilibrium, it is possible to determine the amount of HNO_2 present in HNO_3 solutions by means of a suitable oxidizing agent, without introducing any significant uncertainty due to the presence of dissolved free NO_2 . Furthermore, addition of HNO_2 to HNO_3 solutions can be conveniently accomplished by bubbling NO_2 through the solution. This technique is preferable to adding a nitrite salt since no foreign cation is introduced into the system under study; however, it is necessary to determine both HNO_2 and HNO_3 after NO_2 bubbling.

In HNO_3 solutions resulting from dissolution runs with stirring the amount of HNO_2 present was determined by introducing aliquot portions of the solution into a Ce^{IV} solution and titrating the excess of Ce^{IV} with FeSO_4 . The solutions resulting from runs without stirring were homogenized before aliquots were taken for analysis. The analytical results are presented in Table I. No significant change in HNO_2 concentration was found during the 1-hr duration of the experiments. The HNO_2 concentration remained essentially constant in the vicinity of one hour.

The dissolution rates tabulated in Table I pertaining to stirred solutions are plotted in Fig. 4 against the product of the concentrations of HNO_2 and HNO_3 . The dependence of rate on concentration is expressed by the following relationship:

$$V = K\text{C}_{\text{HNO}_2}\text{C}_{\text{HNO}_3} \quad [2]$$

where V is the dissolution rate, and C_{HNO_2} and C_{HNO_3} are the concentrations of undissociated HNO_2 and

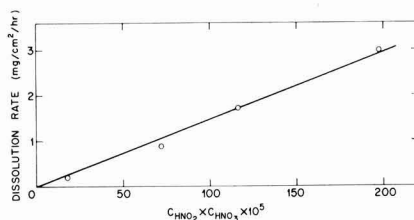


Fig. 4. Dissolution rate of germanium as a function of the product of concentrations of undissociated HNO_2 and HNO_3 at 27.5°C .

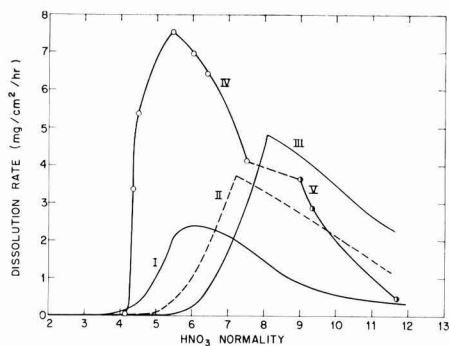


Fig. 5. Dissolution of germanium in HNO_3 solutions at 27.5°C . The effect of HNO_2 . Curve I, no stirring (as in Fig. 2); curve II, stirring resulting from N_2 bubbling; curve III, stirring, 194 rpm (as in Fig. 2); curve IV, mixtures of $\text{NO}_2 + \text{N}_2$ bubbling through HNO_3 solution. Initial concentration 4.29N HNO_3 . Stirring equivalent to curve II; curve V, as in curve IV except initial HNO_3 concentration was 8.1N.

HNO_3 , respectively. The values of C_{HNO_3} were calculated from the HNO_3 normality using the data of Hood, Redlich, and Reilly (7). The values of C_{HNO_2} were assumed to be the same as the corresponding HNO_2 normalities since the dissociation constant of HNO_2 is relatively small (4×10^{-4}) and ionization is further repressed by the presence of HNO_3 . It is of interest to note that Eq. [2] does not apply to the rates obtained without stirring (Table I). This result is not surprising since, without stirring, the average HNO_2 concentration in the bulk of the solution does not represent, even approximately, the concentration in the immediate vicinity of the germanium surface. In fact, if it is assumed that Eq. [2] applies to the dissolution without stirring, it can be estimated from the data of Table I that the concentration of HNO_2 at the germanium-solution interface may be 10 to 30 times greater than the over-all concentration.

The influence of HNO_2 is further brought out by the results plotted in Fig. 5. Curve II was obtained in HNO_3 solutions through which N_2 was bubbling and curve IV in solutions through which NO_2 and N_2 mixtures were bubbling. In both cases the over-all rate of gas flow and, therefore, the rate of stirring was the same. The HNO_3 solutions corresponding to curve IV, therefore contained appreciably more HNO_2 than those of curve II. Curves I and III already shown in Fig. 2, are replotted for comparison. Curve V will be discussed later.

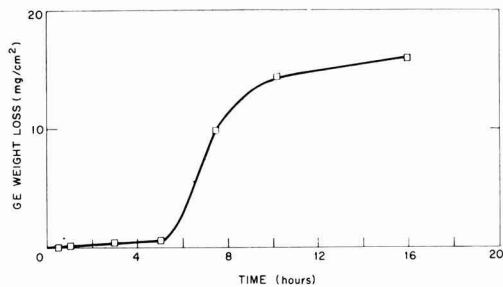


Fig. 6. Dissolution of germanium in 5.5N HNO_3 as a function of time at 27.5°C with stirring (194 rpm).

A comparison of curves II and IV (Fig. 5) shows that for a given HNO_3 concentration HNO_2 increases the dissolution rate and also shifts the position of maximum dissolution rate toward lower HNO_3 concentrations. The observed increase in dissolution rate by a factor of approximately 100 in going from curve II to curve IV for the concentrations 4.37N and 4.54N (experimental points on curve IV) resulted from an increase in HNO_2 concentration by a factor of approximately 200. In view of the fact that the amount of stirring in these runs was not sufficient to prevent entirely concentration polarization at the germanium-solution interface, the results are in reasonable agreement with Eq. [2].

Since HNO_2 is formed during the dissolution process and is itself a reactant, the dissolution rate should increase with time, i.e., the reaction should be autocatalytic. Such increase in rate has been observed for a number of common metals (4). Results obtained with germanium in 5.5N HNO_3 are shown in Fig. 6. The dissolution rate (slope) with stirring remains constant for the first 5 hr, then it increases sharply and finally decreases. Accordingly, the HNO_2 concentration at the end of $7\frac{1}{2}$ hr was found to be approximately five times larger than that at the end of 5 hr. The latter concentration, on the other hand, was found to be only 10% larger than that at the end of 3 hr. The reasons for the several hour interval prior to the sharp increase in HNO_2 concentration are not clear at this time. A sharp increase in HNO_2 concentration, however, is reflected in a sharp increase in dissolution rate. The subsequent decrease in dissolution rate will be discussed later.

Dissolution Potential

The instantaneous electrode potential of germanium obtained within 10 sec after immersion in unstirred HNO_3 solutions is plotted as a function of HNO_3 normality in Fig. 7. In the concentration range 5 to 7N, where the maximum in dissolution rate occurs, the potential shifts towards more noble (positive) values by approximately 0.2 v.

The cathodic shift of the potential with increasing HNO_3 concentration, accompanied by an increase in dissolution rate, is indicative of a decrease in ca-

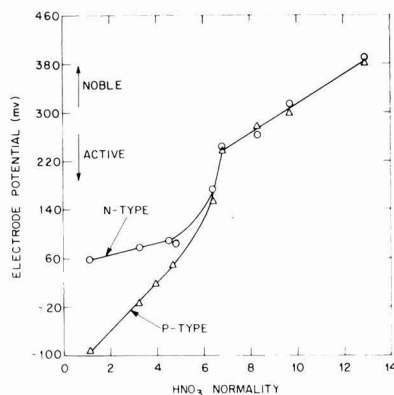


Fig. 7. Instantaneous potential of germanium in HNO_3 solutions at 27.5°C vs. standard hydrogen electrode; no stirring.

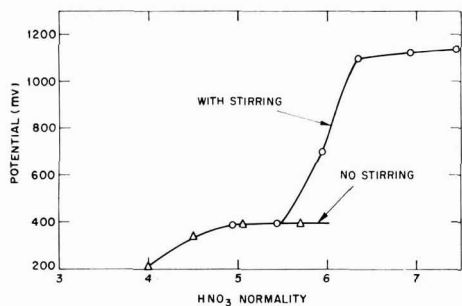


Fig. 8. Dissolution potential of germanium in HNO_3 solutions at 27.5°C vs. standard hydrogen electrode.

thodic polarization (8). On the other hand, above approximately 7N HNO_3 the cathodic shift of the dissolution potential, associated with a decrease in dissolution rate, is indicative of an increase in anodic polarization which, at higher HNO_3 concentrations, leads to germanium passivity as will be discussed later.

The steady-state dissolution potential, essentially attained within 1 hr after immersion, is shown in Fig. 8 as a function of HNO_3 normality. In this case, both with and without stirring, the pronounced cathodic shift occurs at smaller concentrations than in the case of instantaneous potential, probably owing to the accumulation of HNO_2 . This behavior is consistent with the observed cathodic shift of the potential with time for a given HNO_3 concentration. As shown in Fig. 8, in 5N and 5.5N HNO_3 the dissolution potential is the same with and without stirring, indicating that stirring does not significantly affect the anodic reaction. At higher concentrations, however, where the cathodic reaction controls the dissolution potential (see below) stirring shifts the potential toward more noble values by causing a decrease in the cathodic polarization.

It is of interest to note in Fig. 7 that in dilute HNO_3 solutions the instantaneous potential of n-type germanium is more noble than that of p-type. During metal dissolution in acids the dissolution potential (mixed potential) usually remains near the reversible potential of the metal (9) because the exchange current for the metal-oxidation reaction is usually much larger than the exchange current for the hydrogen-reduction reaction, or in this case the HNO_3 reduction reaction. Thus, the dissolution potential is usually controlled by the anodic reaction. In the present case, the over-all anodic reaction could be represented as (10):



where e^+ is a positive hole, or electron deficiency in the valence band in germanium. According to this mechanism the instantaneous potential of p-type germanium should be more active than that of n-type in the same solution owing to the greater supply of holes (cf. Fig. 7). Moreover, the initial dissolution rate (averaged over the first hour of immersion) of p-type germanium has been found to be approximately twice that of n-type at HNO_3 concentrations up to 4N . In more concentrated HNO_3

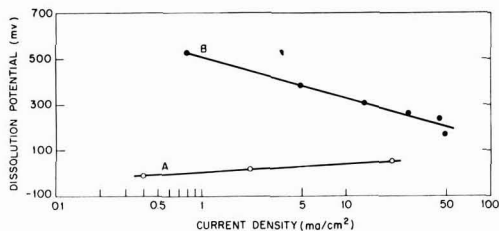


Fig. 9. Potential of germanium in HNO_3 solutions at 27.5°C as a function of current density. Calculated from dissolution rates. A, $\text{HNO}_3 < 6\text{N}$; B, $\text{HNO}_3 > 6\text{N}$.

solutions, on the other hand, where pronounced anodic polarization occurs (anodic control) and the anodic reaction no longer controls the dissolution potential, no difference in potential (Fig. 7) or in dissolution rate was observed between the two types of germanium.

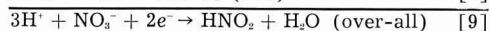
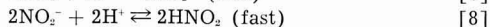
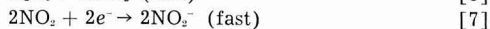
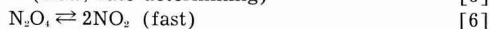
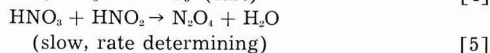
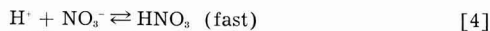
In Fig. 9 the instantaneous potential is plotted against the logarithm of the current density as calculated from the dissolution rates assuming a roughness factor of 1.3 (11). This Tafel-type relationship has been observed earlier by Makrides, Komodromos, and Hackerman (12) and by Gatos (13, 14) for the potential of iron dissolving in oxidizing acid media. For the concentration range indicated (Fig. 9) straight line A approximates the anodic polarization of dissolving germanium since the system is under cathodic control (12) and, correspondingly, B approximates the cathodic polarization.

Interpretation of the Dissolution Process

At low HNO_3 concentrations (nonpassivating) the over-all anodic reaction can be represented by Eq. [3]. No attempt was made in this investigation to determine the mechanism involved in the removal of germanium atoms from their respective lattice sites and their oxidation to the corresponding ions. Turner (15) has recently investigated this aspect in studying the anodic dissolution of germanium under the influence of an externally applied emf. In the present system, as it has been pointed out above, the dissolution process is controlled by the cathodic reaction which will be the subject of the present discussion.

In discussing the role of HNO_2 in the dissolution of metals in HNO_3 , Evans (4) concludes that, in the absence of hydrogen evolution, reaction [1] leads to the formation of NO_2 which is responsible for the oxidation of the surface metal atoms. Similarly, Vetter (16) has found that reaction [1] is rate determining in the reduction of HNO_3 on a platinum electrode.

Thus, the over-all cathodic reaction involves the reduction of HNO_3 to HNO_2 and possibly, although unlikely, to NO . An effort was made to detect free hydrogen among the reaction products, under all experimental conditions, but the results were negative. The reduction of HNO_3 in the present system is believed to proceed according to the mechanism proposed by Vetter (16) for the cathodic reduction of HNO_3 on a platinum electrode:



Reaction [5] is rate determining. Reaction [7] determines the cathodic potential since it is the only reaction involving electron transfer. According to Vetter, this reaction becomes rate determining at low current densities, well below these corresponding to the dissolution rates at hand (0.1 to 1 ma/cm²).

Some of the experimental results described above will now be viewed briefly in the light of this mechanism.

With no stirring the concentration of HNO₂ becomes appreciably higher at the germanium-liquid interface than in the main body of the solution, HNO₂ forming faster than it can diffuse away from the interface. Stirring decreases the dissolution rate (Fig. 2) by removing the HNO₂ forming at the interface. Changes in stirring at high stirring rates have only a small effect on the dissolution rate, indicating that the HNO₂ formation rate approaches the rate of its consumption through reaction [5] and through removal from the interface by stirring. Although no electron exchange with the germanium surface takes place in reaction [5] the action of HNO₂ is essentially limited at the interface for two reasons. First, NO₂ produced in reaction [5] undergoes reduction at the germanium surface according to reaction [7], and second, reaction [5] is catalyzed by metallic surfaces as shown by Vetter (6) in the case of platinum.

On the basis of the above mechanism the HNO₂ concentration must increase with time and, as a result, the dissolution rate must also increase since it is controlled by reaction [5]. The decrease in C_{HNO₃} corresponding to the increase in C_{HNO₂} is of little significance because at time zero C_{HNO₃} >> C_{HNO₂}. In agreement with the above are the results shown

in Fig. 6 where the HNO₂ concentrations, determined analytically as a function of time, were found consistent with the dissolution rates. Furthermore, the potential (*E*) of the Pt|HNO₃, HNO₂ electrode shifted during germanium dissolution, because of HNO₂ formation, as expected from the relationship $E = E_0 - 0.0296 \log [\text{HNO}_2]$, which has been verified experimentally by Monk and Ellingham (17). Also consistent are the results reported on solutions in which the concentration of HNO₂ was appreciably increased by bubbling NO₂ (Fig. 5).

Activation energies were obtained for the dissolution process by determining the dissolution rates 27.5°, 34.4°, and 44.2°C. The results are shown in Table II.³ Vetter (6) determined the activation energy of reaction [5] on platinum and found that it decreases from 16.5 kcal/mole (in 6.9*N* HNO₃) to 14.4 kcal/mole (in 14.5*N*). Our value of 18.0 kcal/mole in 5.5*N* solution, with stirring, is consistent with Vetter's results. In the case of 7.5*N* solution our value of 12 kcal/mole is lower than the corresponding value by Vetter (approximately 16 kcal/mole). This is not surprising, however, since, in the present system, 7.5*N* approaches the passivating region where the above reaction mechanism no longer holds. In 5.5*N* and 7.5*N*, with no stirring, the activation energies are lower than those obtained with stirring (18 and 12 as compared with 10 and 9 kcal/mole). The outstanding difference between a stirred and nonstirred Ge-HNO₃ reaction is that the HNO₂ concentration at the germanium-liquid interface is appreciably less in the former than in the latter. Thus, it appears reasonable that the measured activation energy could also be a function of HNO₂ concentration. Consistent with this is the low value of 5 kcal/mole obtained in 6.0*N* solutions, through which NO₂ had been bubbled. The HNO₂ concentration in this case was appreciably higher than in the previous cases.

³ The activation energy is equal to $\left(\frac{1}{T_1} - \frac{1}{T_2}\right)R \ln \frac{V_2}{V_1}$, where V_1

and V_2 are the rates at the absolute temperatures T_1 and T_2 respectively, assuming that the concentration of the reactants is not sensitive to temperature.

II. Passivity of Germanium

ABSTRACT

Above 6 to 8*N*, HNO₃, the initial dissolution rate of germanium decreased with increasing HNO₃ concentration and increasing stirring rate. The time required to bring about passivation of the germanium in these solutions decreased from several hours to a few seconds in going to higher HNO₃ concentrations. A surface oxide film (very likely GeO₂) is associated with the passivity of germanium. Accordingly, the presence of HF which dissolves GeO₂ but not germanium prevented germanium passivity. Dissolution potential measurements were consistent with the kinetic data.

Dissolution as a Function of Time in Concentrated HNO₃ Solutions

Weight losses of germanium in 7.5, 10.3, and 12.0*N* HNO₃ as a function of time, with no stirring, are shown in Fig. 10. The time necessary to attain a maximum weight loss is seen to decrease with increasing HNO₃ concentration. The gain in weight beyond this point is associated with the formation of a surface film which eventually becomes visible. At

concentrations greater than 18*N* the film forms immediately upon immersion. When sufficiently thick, the film is opaque white and exhibits the properties of the soluble hexagonal GeO₂.⁴ Thus, it can be removed without affecting the substrate, since it is soluble in KOH, NaOH, and HF, solutions which do not attack germanium at room temperature in the

⁴ The extremely inert tetragonal form of GeO₂ was not detected. This form is insoluble in water and is not attacked by HF or NaOH solutions (18).

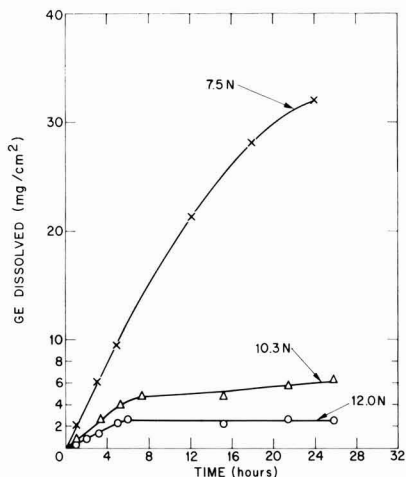


Fig. 10. Dissolution of germanium in HNO_3 solutions as a function of time at 27.5°C .

absence of dissolved oxygen (19). In this respect, the Ge-GeO₂ system affords a unique advantage over the more common metals.

The total amount of germanium reacted was determined from the weight losses plotted in Fig. 10 and the amount of germanium contained in the oxide film. The latter was obtained gravimetrically by immersing the oxide bearing samples in 1N NaOH for approximately 1 hr. Repeated immersions in 1N NaOH resulted in no additional weight loss. The results are shown in Fig. 11. No structural studies of the oxide film were carried out; however, analysis of the germanium oxide solutions for germanium combined with the total weight of the oxide film gave the empirical formula Ge₂O₃. The

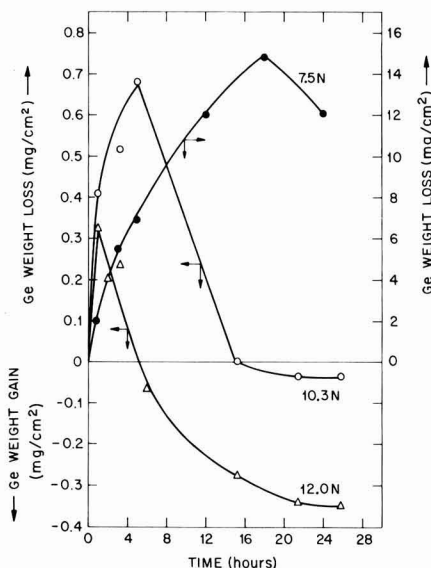


Fig. 11. Dissolution of germanium in HNO_3 solutions as a function of time at 27.5°C (oxide surface film removed).

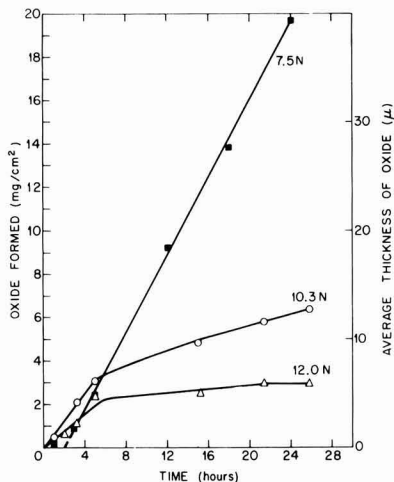


Fig. 12. Oxide film on germanium formed in HNO_3 solutions at 27.5°C as a function of time.

amount of oxide present on the surface and its average thickness, assuming a density (4.7 g cm^{-3}) equal to that of bulk GeO₂, is shown in Fig. 12 as a function of time. In 7.5N solution an extended period of rapid growth begins after approximately 3 hr. For periods shorter than about 3 hr the average thickness of oxide in 7.5N HNO_3 is less than that formed in the more concentrated solutions, although the initial dissolution rate for the latter concentrations is smaller than for the former. Assuming that the nature of the surface film is the same in the various solutions, it is apparent that its solubility and/or rate of solution is greater in 7.5N HNO_3 than in the other two solutions. Accordingly, while the initial rate of germanium dissolution in 10.3N HNO_3 is 2.7 times smaller than in 7.5N solution, the initial rate of oxide growth in the former is only 1.6 times smaller than in the latter considering the linear growth beyond 3 hr. In agreement with the above, semiquantitative experiments showed that the solubility and rate of dissolution in HNO_3 solutions decreases appreciably with increasing HNO_3 concentrations. Pugh (20) has observed similar behavior for GeO₂ in H_2SO_4 solutions over a wide concentration range (0 to 16N).

In stirred concentrated HNO_3 solutions the behavior of germanium is similar to that in non-stirred solutions except that with stirring higher concentrations and/or longer periods are required to bring about passivity.

It should be pointed out that in concentrations lower than 6-8N the dissolution rate can also decrease with time, although it does not become zero. In this case, however, relatively large amounts of germanium dissolve before a surface film is formed. By decreasing the volume of a 5.5N HNO_3 solution from 90 to 20 ml, the decrease in dissolution rate set in after 6 hr rather than after approximately 24 hr. A surface film was ultimately formed in both experiments and, after an additional 24 hr, small amounts of GeO₂ were observed on the walls of the reaction vessel.

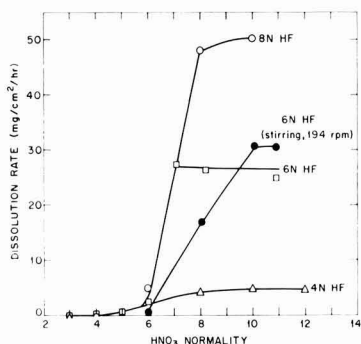


Fig. 13. Dissolution of germanium in HNO_3 solutions containing HF at 27.5°C . The solutions were not stirred except in the case indicated.

Effect of Hydrofluoric Acid

Dissolution rates pertaining to HF + HNO_3 mixtures are summarized in Fig. 13. A comparison of these results with those of Fig. 2 shows that, in general, the dissolution rate is not significantly affected by the presence of HF at HNO_3 concentrations below 6N without stirring and 8N with stirring. An increase in dissolution rate by a factor of approximately 2 is observed in nonstirred 6N HNO_3 + 6N HF solution over 6N HNO_3 , possibly due to a decrease in the degree of dissociation of HNO_3 . An increase in the concentration of undissociated HNO_3 would lead to increased rate according to Eq. [2]. Lack of suitable concentration and dissociation data under the present experimental conditions prevents a quantitative treatment of this effect.

Figure 13 shows further that in the presence of HF, as in the absence of HF (Fig. 2), stirring decreases the dissolution rate at the lower HNO_3 concentrations. Thus, it appears that HF does not interfere with the mechanism of dissolution and that reaction [5] remains rate determining. In accord with this result, the activation energy of the dissolution process in stirred 6N HNO_3 + 6N HF was determined as 19 kcal/mole which compares favorably with the value of 18 kcal/mole found in stirred 5.5N HNO_3 (Table II).

In the higher HNO_3 concentrations where reaction [5] is no longer rate determining, the dissolution rate increases markedly in the presence of HF and reaches a limiting value which, for a given HNO_3 concentration, increases with increasing HF concentration (Fig. 13). As in the absence of HF (Fig. 2), here also stirring increases the dissolution rate.

Table II. Activation energy for the dissolution of germanium in HNO_3 solutions

HNO_3 Normality	Activation energy Kcal/mole
5.5N, 194 rpm	18
7.5N, 194 rpm	12
6.0N + added HNO_3 , 194 rpm	5
5.5N, no stirring	10
7.5N, no stirring	9
6.0N + 6N HF, 194 rpm	19

Inasmuch as the decrease in dissolution rate is associated with surface oxide formation, it is reasonable to assume that the increase in dissolution rate by HF is due to the greater solubility of GeO_2 in HF solutions due to the reaction:



The Nature of the Passivity of Germanium

The facts described above point to a pronounced anodic polarization in concentrated HNO_3 solutions resulting from the formation of a surface oxide which can become protective and lead to passivity. The anodic reaction and related side-reactions may not be precisely described by Eq. [3]. However, in view of the predominantly acidic character of GeO_2 , it is unlikely that ionic or molecular species other than GeO_2 or germanic acids are formed during oxidation of germanium with HNO_3 . The formation of complex compounds between germanium and HNO_3 (or the intermediates of HNO_3 reduction) is essentially excluded since the solubility of GeO_2 decreases with increasing HNO_3 concentration. It is possible that GeO_2 is the first distinct anodic product and that H_2GeO_3 is formed from it by hydration. Alternatively, GeO_2 may form from H_2GeO_3 by dehydration. Knowledge of the sequence of formation of the two compounds is not essential to our argument since, in either event, formation of GeO_2 can take place on or near the germanium surface.

The formation of a layer of GeO_2 at high HNO_3 concentrations is explained as follows. The rate of formation of GeO_2 increases as the rate of the cathodic reaction increases according to [2]. At the same time, however, the solubility and/or the dissolution rate of the oxide decreases. Thus, the germanium-liquid interface becomes saturated with respect to GeO_2 . Since diffusion of GeO_2 or H_2GeO_3 away from the interface is relatively slow, nucleation and growth of GeO_2 occurs on the germanium surface before GeO_2 precipitates out in the bulk of the solution. At very high concentrations sufficient GeO_2 precipitates out within a few seconds and in a suitable form to cover all of the germanium surface and bring about passivity.

In low concentrations, but not below 6N, GeO_2 at first forms adherent "patches" on the germanium surface. Thus, the surface exposed to the solution is decreased. If at any time sufficient germanium area were exposed for reaction [7] to proceed faster than [5], the dissolution mechanism should be the same as described for dilute HNO_3 solutions. In such a case, the rate of the cathodic reaction and hence, the average dissolution rate should not be affected by the presence of oxide patches. Thus, the attack should become localized at the bare germanium surface. Indeed, intensified local attack was observed in HNO_3 solutions with concentrations near those corresponding to the maximum dissolution rates. Above these concentrations, however, the average dissolution rate decreases with increasing HNO_3 normality. This clearly suggests that reaction [5] ceases to be rate determining. Since reaction [5] is catalyzed by metallic surfaces, the possibility exists that its average rate is a function of the

amount of the germanium surface not covered by oxide. If this were the case, the dissolution process at these concentrations should be under cathodic control and, thus, the dissolution potential should shift toward more anodic values as the dissolution rate decreased (8). Since a potential shift toward more cathodic values was observed, the system is now under anodic control and the anodic reaction [3] determines the rate of the over-all dissolution process.

The growth of thick oxide films as in the present case (of the order of microns, Fig. 12) by diffusion of oxygen inward or germanium ions outward is not plausible at room temperature and in the absence of very strong electric fields (21). On the other hand, the approximate linear growth for the first few hours in 10.3*N* and 12.0*N* can be explained on the basis of poor film adhesion, blistering, cracking or other such macroscopic defects in the film (22). Actually, in the present case, the greater the limiting thickness the more porous and the less dense the oxide film appeared under microscopic examination. In some respects the passivity of germanium resembles the passivity of metals caused by insoluble salts as described by Müller (23).

The time necessary for passivity and the limiting average oxide thickness decrease with increasing HNO_3 concentration. This trend extends to appreciably higher concentrations than those shown in Fig. 11 and 12. The experimental approach employed does not lend itself to establishing a quantitative expression of this trend. It was found, however, that in the concentration beyond 16*N* (without stirring) the time required for passivation is of the order of seconds and the oxide thickness approximately 150Å. Thus, it appears that the limiting oxide thickness is inversely related to the initial germanium dissolution rate and to the solubility (and/or the dissolution rate) of the oxide in the HNO_3 solutions. The initial dissolution rate increases and the solubility of GeO_2 decreases with increasing HNO_3 concentrations. High rates of formation of GeO_2 lead to adhering dense surface oxide film for reasons which are not clear at present. Extension of the passivating range to lower HNO_3 concentrations in the presence of HNO_2 (Fig. 5, curve IV) is readily understood in the light of the fact that, for a given HNO_3 concentration, HNO_2 increases the initial dissolution rate of germanium.

Our views that the behavior of germanium and its passivity in concentrated HNO_3 solutions are determined by the formation and presence of a GeO_2 surface film rather than by absorption of certain species from the solution onto the surface are consistent with the fact that in these solutions both n- and p-type germanium behave alike. In dilute solutions where no oxide film is present, distinct differences were observed between the two types of germanium. If adsorption played an important role in the passivity of germanium, the two types of germanium would probably exhibit measurable differences in their passivating characteristics. Passivity in HNO_3 due to adsorption and/or chemisorption was hypothesized in the case of iron (24, 25). It is not necessary that passivity in HNO_3 is established

by the same mechanism for all metals. Thus, iron passivity may and may not be comparable to germanium passivity. The Ge-HNO_3 reaction, however, as pointed out earlier, lends itself to a more direct study than the corresponding behavior of iron in nitric acid.

Summary

I. In HNO_3 solutions below ca. 6*N*.—The dissolution rate of germanium is a function of the concentration of undissociated HNO_3 and HNO_2 . Since HNO_2 is formed during the reaction of germanium with HNO_3 , the dissolution process is "autocatalytic." Consequently, stirring decreases the dissolution rate by removing reaction products from the germanium HNO_3 interface. In addition, for a given stirring rate, the dissolution rate increases with time owing to an increase in concentration of HNO_2 .

In unstirred solutions the dissolution rate reaches a maximum in approximately 6*N* HNO_3 ; the maximum occurs at a higher concentration (8-9*N*) with stirring and at a somewhat lower concentration when relatively large amounts of HNO_2 are present.

The dissolution potential of n-type germanium is more noble than that of p-type. Furthermore, for a given HNO_3 concentration the dissolution rate of the former is smaller than that of the latter.

The dissolution potential of both n- and p-type germanium becomes more noble with increasing HNO_3 concentration and, hence, with increasing dissolution rate. Thus, the dissolution process is controlled by the cathodic reaction (reduction of HNO_3) and the dissolution potential by the anodic reaction.

The presence of HF does not affect the dissolution rate unless the HF concentration becomes sufficiently high (above ca. 6*N*) to decrease the dissociation of HNO_3 .

II. In HNO_3 solutions above 6*N*.—The dissolution rate decreases with increasing HNO_3 concentration and increases with stirring. For a given HNO_3 concentration the dissolution rate decreases with time and eventually approaches zero; the higher the HNO_3 concentration, the sooner germanium acquires passivity. The time required varies from a few hours to a few seconds. A surface oxide film (very likely GeO_2) is associated with passive germanium. The average thickness of the oxide film can vary from a few microns to approximately 150Å.

The dissolution potential becomes more noble with increasing HNO_3 concentration and, hence, with decreasing dissolution rate. Thus, the reaction of germanium with concentrated solutions of HNO_3 is controlled by the anodic reaction (formation of GeO_2) and passivity is associated with pronounced anodic polarization. The decrease in solubility and/or rate of solution of GeO_2 with increasing HNO_3 concentration is of paramount importance in the passivation process.

Passivity of germanium in HNO_3 solutions is prevented or destroyed by the presence of HF since HF prevents the formation of a protective oxide film.

Acknowledgment

The authors wish to express their appreciation to L. J. Gordon for his skillful assistance with many

of the experiments and Dr. W. W. Harvey for valuable suggestions.

Manuscript received Sept. 23, 1957. This paper was prepared for delivery before the Cleveland Meeting, Sept. 30-Oct. 4, 1956. The research in this paper was supported jointly by the Army, Navy, and Air Force under contract with Massachusetts Institute of Technology.

Any discussion of this paper will appear in a Discussion Section to be published in the June 1959 JOURNAL.

REFERENCES

1. H. Newcombe, W. McBryde, J. Bartlett, and F. Beamish, *Anal. Chem.*, **23**, 1023 (1951).
2. A. Portevin, *Rev. Met.*, **26**, 617 (1929).
3. U. R. Evans, "Metallic Corrosion Passivity and Protection," p. 247, Edward Arnold and Company, London (1948).
4. *Ibid.*, p. 225.
5. E. Abel and H. Schmid, *Z. Physik. Chem.*, **132**, 55 (1928).
6. K. Vetter, *Z. Anorg. Chem.*, **260**, 244 (1949).
7. G. C. Hood, O. Redlich, and C. A. Reilly, *J. Chem. Phys.*, **22**, 2067 (1954).
8. R. B. Mears, *J. (and Trans.) Electrochem. Soc.*, **95**, 1 (1949).
9. J. O'M. Bockris, "Modern Aspects of Electrochemistry," p. 255, Academic Press Inc., New York (1954).
10. W. H. Brattain and C. G. B. Garrett, *Bell System Tech. J.*, **34**, 129 (1955).
11. J. T. Law, *J. Phys. Chem.*, **59**, 543 (1955).
12. A. C. Makrides, N. M. Komodromos, and N. Hackerman, *This Journal*, **102**, 363 (1955).
13. H. C. Gatos, *ibid.*, **103**, 286 (1956).
14. H. C. Gatos, *Corrosion*, **12**, 322 (1956).
15. D. R. Turner, *This Journal*, **103**, 252 (1956).
16. K. Vetter, *Z. Physik. Chem.*, **194**, 199 (1950).
17. R. G. Monk and J. T. Ellingham, *J. Chem. Soc.*, **1935**, 125.
18. O. H. Johnson, *Chem. Rev.*, **51**, 431 (1952).
19. W. W. Harvey and H. C. Gatos, to be submitted for publication to *J. Electrochem. Soc.*
20. W. Pugh, *J. Chem. Soc.*, **1929**, II, 1537.
21. N. F. Mott, *Trans. Faraday Soc.*, **43**, 429 (1947).
22. U. R. Evans, *Trans. Electrochem. Soc.*, **91**, 547 (1947).
23. W. J. Müller, "Die Bedeckungstheorie der Passivität der Metalle und ihre Experimentelle Begründung," Verlag Chemie (1934).
24. H. C. Gatos and H. H. Uhlig, *This Journal*, **99**, 250 (1952).
25. H. H. Uhlig and T. L. O'Connor, *ibid.*, **102**, 562 (1955).

Studies of the Anodic Behavior of Aluminum

I. The Direction of Ionic Movement

John E. Lewis and Robert C. Plumb¹

Research Laboratories, Aluminum Company of America,
New Kensington, Pennsylvania

ABSTRACT

It is demonstrated, by a series of marker experiments in which layers of nonporous anodic oxide were tagged by incorporating radioactive material in them, that nonporous anodic oxide grows at, or close to, the oxide-electrolyte interface; it is concluded that the aluminum ion is the mobile species. Similar experiments with a porous oxide may also be interpreted in terms of formation of the oxide at the oxide-electrolyte interface, but in this case the interface is at the bottom of pores filled with electrolyte.

Two distinct types of oxide films may be formed on aluminum by anodic oxidation, depending on the rate at which the oxide is dissolved by the electrolyte during the oxidation (1).

Where there is little solvent action, thin nonporous films, whose thickness is proportional to the applied voltage, are formed (2). When there is appreciable solvent action, thick porous films, whose thickness increases with the time anodized, are formed (3). It has been shown that the porous films contain a hexagonal array of pores, each of which extends from the solution inwards almost to the metal surface. The base of each pore is separated from the metal by a thin nonporous layer of oxide (4). A slight tendency toward porosity with electrolytes which do not have solvent action has been noted by Franklin (5). The classification of anodic films as "essentially nonporous" and "porous" will be retained, however.

It has not been demonstrated by experiment

whether, during formation, aluminum moves outward through the film or oxygen moves inward, or if both processes take place. Depending on which of the three possibilities is in fact realized, the oxide film will be growing at the oxide-solution interface, at the metal-oxide interface, or somewhere between the two interfaces. In the case of porous-type coatings, the electrolyte probably fills the pores, making contact with the oxide at the pore bases, and the growth of further oxide must take place somewhere between the pore bases and the metal. This has, in fact, been demonstrated in numerous experiments (6, 7) by observing the movement of layers of porous oxide which were tagged by pigments incorporated in the pores. These experiments, however, do not tell whether the new oxide is being formed at the oxide-metal or the oxide-solution interface, and hence give no information about the movement of aluminum or oxygen through the oxide layer.

The experiments to be described are similar to those in which oxide layers were tagged with pig-

¹ Present address: Department of Chemical Engineering and Chemistry, Worcester Polytechnic Institute, Worcester, Massachusetts.

ments, but in this case the complication of a pore structure was avoided by using essentially nonporous oxide films tagged by forming in a radioactive electrolyte. It will be shown in a later paper (8) that during anodizing some of the anion from the electrolyte is incorporated in the oxide as an essential component of it. The tagged layer was applied either before or after applying a rather thick (700Å) nonradioactive, nonporous oxide layer. The position of the tagged layer in the composite film was determined by dissolving the oxide slowly and measuring the remaining radioactivity of the sample.

Experimental

Sulfur-35 tagged electrolyte was prepared by adding carrier H_2SO_4 to radioactive H_2SO_4 (Oak Ridge Cat. Item S-35-P-1), fuming to remove chloride ion, and diluting to make a 0.1% electrolyte having a specific activity of 0.6 mc/mg SO_4 . Anodizing in a sulfuric acid electrolyte for an extended time gives a porous type film. However, by very brief anodizing in such an electrolyte with a suitable applied voltage, the buildup of a porous layer can be minimized and one will obtain primarily a nonporous barrier layer (4). In this work, 99.99% Al specimens were immersed for various periods of time in the bath, at a distance of 5 cm from an aluminum cathode with an applied voltage of 15 v. Where a sulfate coating was applied after the 50-v tartrate coating, a 52-v potential was used.

The 700Å thick nonradioactive coatings were obtained by anodizing at a 50-v potential in a 3% ammonium tartrate electrolyte (2).

The radiation from the oxide films was measured with an end window Geiger-Mueller counter with a precision of 2%. The 700Å thick coating would attenuate less than 2% of the sulfur-35 radiation.

The oxide was dissolved from the specimens with a 5% H_3PO_4 -2% CrO_3 solution at 50°C. This reagent does not attack the aluminum, and it should not undermine the oxide.

The activity remaining on the specimens was plotted against the total time of exposure to the oxide stripping solution.

Results

Figure 1 shows the results on three specimens treated with (a) 30-sec H_2SO_4 coating only, (b) 700Å inert layer, then 30-sec H_2SO_4 coating, (c) 30-sec H_2SO_4 coating, then 700Å inert layer. In all cases, the H_2SO_4 coating was radioactive. It is apparent from these three curves that the oxide layer which is applied first is the last layer to be removed during the stripping treatments, so the oxide must have formed at the oxide-solution interface.

It is difficult, because of the possibility of non-uniform attack on the oxide by the stripping solution, to say precisely that the oxide is being formed at the oxide-solution interface rather than at some point within the oxide layer but quite close to the oxide-solution interface. In this sense, the results are qualitative, and one can only conclude that the oxide is being formed much nearer the solution interface than the metal interface. It follows that the principal material transported through the

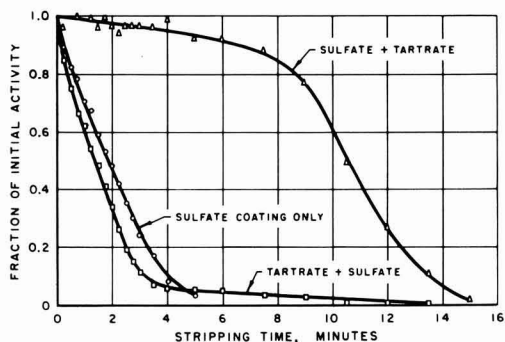


Fig. 1. Decrease in activity of sulfur-35 tagged oxide vs. time exposed to oxide stripping solution. Curves, top to bottom: 30-sec sulfate coating followed by 50-v tartrate coating; 30-sec sulfate coating only; 50-v tartrate coating followed by 30-sec sulfate coating.

oxide film during anodizing is aluminum and not oxygen. This result is consistent with work which indicates that, under forming conditions, barrier type oxides are nonstoichiometric, containing excess aluminum.

Another interesting set of curves is shown in Fig. 2. In this case, 30-sec, 3-min, and 10-min coatings were formed in the radioactive sulfuric acid. After the radioactive coatings were applied, the specimens were anodized in ammonium tartrate to give a 50-v (700Å) nonporous layer. It would be expected that the tartrate anodizing would: (a) form a uniform nonporous layer on top of the essentially nonporous 30-sec coating, (b) completely fill the pores of the 3-min coating and perhaps build a nonporous layer on top of it, and (c) tend to fill the pores of the 10-min coating, but to a lesser extent than with the 3-min coating. The curves in Fig. 2 are, in fact, just what would be expected with

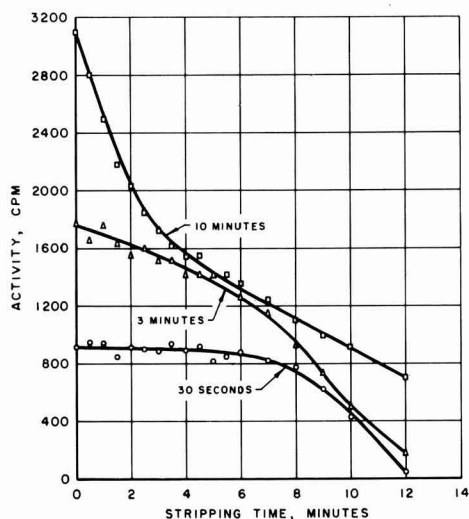


Fig. 2. Decrease in activity of sulfur-35 tagged oxide vs. time exposed to oxide stripping solution. Curves, top to bottom: 10-min sulfate coating followed by 50-v tartrate coating; 3-min sulfate coating followed by 50-v tartrate coating; 30-sec sulfate coating followed by 50-v tartrate coating.

this model. The activity of the sample which had a 10-min coating decreased rapidly, showing that the pores in the tagged oxide applied first were not filled up completely by the nonradioactive oxide. The activity of the sample which had a 3-min coating, whose pores would be completely filled by the nonradioactive oxide, decreased but at a much slower rate than the activity of the 10-min sample. The sample with the 30-sec coating of tagged oxide did not show a decrease in activity until the non-radioactive oxide on top had been dissolved away.

These marker experiments demonstrate conclusively that the aluminum ion is the mobile species in the anodic oxidation of aluminum. The result is analogous to that found in the anodic oxidation of tantalum (9).

When the electrolyte has no solvent action on the oxide, the aluminum combines with oxygen at or near the oxide-solution interface, building up the thickness of the oxide in a continuous, uniform manner. When the electrolyte has solvent action on the oxide and causes pores to be formed, the aluminum ions combine with oxygen at or near the base of the pores. This new oxide apparently fills in between the outer porous oxide layer and the metal, and must itself become a part of the porous oxide

after further oxidation takes place. The details of the process by which the porous layer is built up continuously from oxide which is formed near the bases of the pores are not clear at the present time.

Acknowledgment

The authors would like to express thanks to Mr. F. Keller and Mrs. Phyllis Towner for valuable discussions of the manuscript.

Manuscript received Jan. 20, 1958. This paper was prepared for delivery before the Ottawa Meeting, Sept. 28-Oct. 2, 1958.

Any discussion of this paper will appear in a Discussion Section to be published in the June 1959 JOURNAL.

REFERENCES

1. J. D. Edwards, *Trans. Electrochem. Soc.*, **81**, 341 (1942).
2. G. Haas, *J. Opt. Soc. Amer.*, **39**, 532 (1949).
3. J. D. Edwards and F. Keller, *Tech. Publ. No. 1710, AIMME* (1944).
4. F. Keller, M. S. Hunter, and D. L. Robinson, *This Journal*, **100**, 411 (1953).
5. R. W. Franklin, *Nature*, **180**, 1470 (1957).
6. Unpublished results, Alcoa Research Laboratories.
7. N. D. Pullen and B. A. Scott, *Trans. Inst. Met. Finishing*, **33**, 163 (1956).
8. R. C. Plumb, *This Journal*, **105**, 498 (1958).
9. D. A. Vermilyea, *Acta Met.*, **2**, 482 (1954).

Studies of the Anodic Behavior of Aluminum

II. Coulometry of Barrier Layer Production

Robert C. Plumb¹

Research Group on the Physics and Chemistry of Solids, Cambridge University, Cambridge, England

ABSTRACT

In order to avoid solvent action by the electrolyte during anodic oxidation of aluminum, the electrolyte must have a high buffering capacity. With such an electrolyte the conversion of aluminum to aluminum oxide is essentially quantitative. The film thickness is proportional to the voltage drop across the film, and the proportionality constant does not depend on the length of time which the voltage is left applied. The film contains, as an essential part of its structure, a quantity of the anion from the electrolyte. The film appears to be nonstoichiometric, having excess aluminum during formation, the amount of excess decreasing with increased length of anodizing time. The coulombic transfer during film formation is quantitatively accounted for during formation by oxidation of aluminum to the trivalent state and liberation of oxygen gas. After the film growth has ceased, the current can be only partially accounted for by oxygen evolution, but it is thought that this is because of difficulty in nucleating oxygen bubbles.

It is now well known that an oxide film whose thickness is proportional to the voltage may be formed on aluminum by anodic oxidation in an electrolyte which has no solvent action on aluminum oxide. This paper describes several experiments designed to determine to what extent a quantitative electrochemical description of the process can be made. It considers the relationship between the thickness of the film and the potential drop across it, the composition of the film, the nature of the

electrolyte, and the coulombic efficiency in forming the film. The physics of the ion transport through the film is not considered explicitly, although evidence of nonstoichiometry is presented.

Many factors may influence the coulombic efficiency in film formation. Haas (1) found by multiple beam interferometry that the film thickness per volt for anodizing aluminum in an ammonium tartrate electrolyte at a pH of 5.5 increases from 12.2Å/v in 30 sec anodizing to 13.5Å/v after 15 min anodizing and increases further at a rate of 1%/hr after that. He found that the aluminum oxide film

¹ Present address: Department of Chemical Engineering and Chemistry, Worcester Polytechnic Institute, Worcester, Massachusetts.

accounted for only 80% of the aluminum consumed, although the electrolyte itself did not attack the film. Dewald (2,3) and Young (4,5) have discussed the role of space charge, in the form of excess metal ions, during anodic oxidation. Young (5) has demonstrated that such space charge is probably "frozen into" the oxide when current is interrupted. Direct chemical observation of "frozen in" space charge has not been made. It has been proposed (6,7) that low valent aluminum is a direct product of anodic oxidation, and that its oxidation to the trivalent state results in hydrogen being liberated at the anode. Although hydrogen evolution does undoubtedly occur in some electrolytes, it is usually thought that oxygen is the gas evolved when aluminum is anodized in electrolytes which are suitable for the development of oxide films. It has been observed by many investigators that porous anodic oxide coatings (formed in electrolytes with solvent action on aluminum oxide) contain measurable amounts of the acid anion, e.g., 12-14% SO_4 from H_2SO_4 (8).

Experimental

Weighting and oxide stripping.—The average thickness of an oxide film on aluminum was determined directly by weighing a specimen, anodizing under the appropriate conditions, reweighing, dissolving the oxide off in a reagent which does not attack aluminum, and weighing again. This gives the aluminum consumed in forming the oxide film and the total weight of the film. The reagent used was 5% H_3PO_4 -2% CrO_3 at 85°C. Dissolution of ordinary anodic oxide films which have not been formed at excessively high voltages or temperatures is complete in 5 min, whereas the attack on the aluminum is less than 2A/min, as determined by radioactive tracer experiments (9) and less than 0.06 $\mu\text{g}/\text{cm}^2/\text{min}$ as determined by direct weighing measurement in preliminary work in this investigation. The inertness of the aluminum results from the formation of a 10-20Å thick mixed phosphate-chromate film on the surface by reaction with it (9). The aluminum consumed in forming an oxide film may be determined from the weight loss of a specimen when a film is formed and then stripped off.

In this investigation, a 99.9% Al foil, with 34 cm^2 area, suspended from a 0.010 in. Al wire, was used. An Oertling torsion balance, counterbalanced to accommodate the foil, which weighed about 30 mg, was used. The precision of weighing was $\pm 10 \mu\text{g}$. The calibration of the torsion scale was not affected by the counterbalancing. Samples were rinsed twice in distilled water and twice in acetone, dried by suspending in hot air over a hot plate, and weighed. Thermal equilibrium in the balance was reached within 5 min. Electrostatic charges interfered with weighing on very dry days. No loss of precision was noted as a result of the sample washing and drying procedure.

Anodizing.—Two different electrolytes were used. One was a 3% tartaric acid solution, adjusted to a pH of 5.5 with ammonia, as used by Haas. The other was a solution of 1.6 wt % H_3PO_4 , adjusted to a pH of 7.0 with KOH. The electrolytes were saturated

with oxygen gas. A platinum cathode was used. The voltages across the film were measured with a vacuum tube volt meter, using an oxygen-platinized platinum reference electrode near the sample. The reference electrode and correction for its half-cell were similar to those described in a subsequent publication (10).

Radioactive tracer experiments.—The phosphate content of anodic oxide films formed in the phosphate electrolyte was measured by using neutron irradiated KH_2PO_4 , and comparing the activity of the films with standards prepared by evaporation of aliquots of the electrolyte. Activities were measured with a 1.5 mg/cm^2 end window Geiger-Mueller detector to a precision of 1%. No self-absorption by films of the thickness employed is to be expected.

The samples in this portion of the work were 1-in. squares of 0.064-in. thick, high-purity sheet (99.99% Al), chemically polished by the Alcoa R-5 bright dip process.² Weighing of these samples was done with a Kuhlmann microbalance.

Results

The electrolyte.—The previous observation (1), that more aluminum is consumed during anodizing in a tartrate electrolyte than can be accounted for in the film, was confirmed by weight change measurements. Up to 50% excess aluminum could be consumed in forming an 1100Å coating. The excess was variable and depended on current density and other unknown factors. This author has observed in other studies that barrier-type films cannot be formed in certain other electrolytes such as K_2SO_4 , but that porous films similar to those formed in H_2SO_4 are obtained. Neither ammonium tartrate nor potassium sulfate electrolytes will dissolve Al_2O_3 by simple contact without current flow.

The behavior observed in the different electrolytes may be explained readily in terms of the buffering capacity of the electrolyte. By discharge of oxygen anions, through formation of Al_2O_3 or liberation of oxygen gas, a zone adjacent to the surface which is deficient in anions is formed. In the absence of a buffering agent this zone will be acidic. The oxide is forming at the oxide-solution interface (11), and, while in the process of forming, will not show any of the customary aging effects which are responsible for the difficulty usually encountered in oxide dissolution. Hence, it should dissolve readily if the solution adjacent to it has a pH below about 3.5 (12). Potassium sulfate has almost no buffering capacity and ammonium tartrate only little, and it is not unreasonable to expect that the pH at the oxide surface falls below 3.5 during anodizing. A suitable electrolyte for quantitative conversion of aluminum to Al_2O_3 should have, as the pH of maximum buffering capacity, a value close to that of least solubility of Al_2O_3 . Of course, anions such as chloride, which have a deleterious effect on the blocking power of the oxide, should be avoided.

The phosphate electrolyte described previously (a mixture of KH_2PO_4 and K_2HPO_4 -pH 7), with a high buffering capacity, has been used. The conversion of metallic aluminum to an oxide film is es-

² U. S. Pat. 2,650,157.

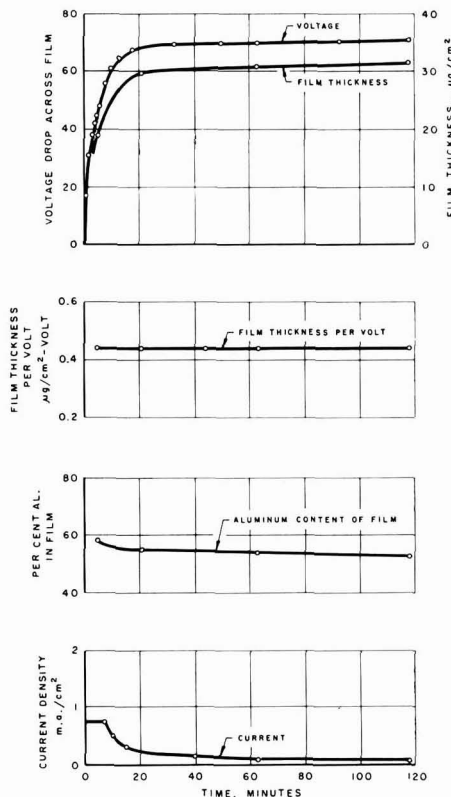


Fig. 1. Variation of voltage, film thickness, film thickness per volt, aluminum content of film, and current density with time in formation of barrier-type anodic oxide film in phosphate electrolyte.

entially quantitative with this electrolyte. During the initial stages of film formation there is an apparent excess of aluminum over that required to form the film (e.g., as seen in Fig. 1, to be discussed later), but the apparent excess decreases with increasing length of anodic treatment. Since it is unlikely that aluminum lost to the solution could re-enter the coating, the excess aluminum must be in the coating rather than lost to the solution by solvent action.

Film thickness per volt.—Figure 1 shows the potential drop across a film, the film thickness, and the density thickness per volt as a function of time when a film was formed in the phosphate electrolyte. The current was limited to $0.75 \text{ ma}/\text{cm}^2$ in the initial stages of film formation by an external variable resistance. A slight break in the voltage curve just above 30 v corresponds to the point at which gas starts to be liberated at the sample surface. The current density is also shown. It is seen that the thickness per volt is constant (within an experimental error of 1 or 2%) from the point where only 65% of the film thickness has been reached to the time when the film thickness is changing at a rate of only 1%/hr.

The linearity of the relationship between film thickness and voltage is shown in Fig. 2.

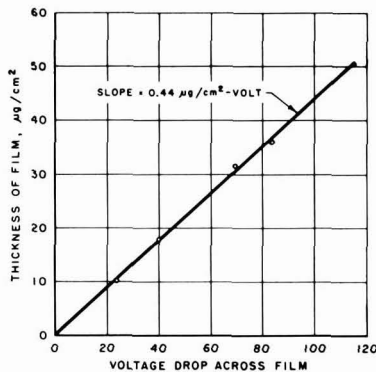


Fig. 2. Relationship between film thickness and voltage drop across barrier-type anodic oxide film formed in phosphate electrolyte.

Using a density of 3.2 for the film, which is in agreement with other investigations of anodic oxidation of aluminum, the film thickness in $\text{\AA}/\text{v}$ is 13.8 ± 0.3 which is in excellent agreement with Haas's value of $13.5 \text{ \AA}/\text{v}$ for 15 min anodizing.

Although the film thickness per volt was found to be independent of time in this work, Haas (1) did observe a dependence. Two reasons may account for this. First, cathode polarization and ohmic losses through the electrolyte were avoided in this work by measuring only the potential drop across the film by means of a reference electrode. Second, the slight tendency for the oxide to dissolve in the tartrate electrolyte may cause a previously undetected porosity in films formed in that electrolyte.

Composition of film.—By forming films in an electrolyte containing phosphorous-32, it was found that the film contains phosphorus equivalent to about 6% PO_4 , as shown in Fig. 3. The amount of phosphorus in a film varies in direct proportion with its thickness, showing that the phosphorus is in the film rather than absorbed on the surface. If it is present as AlPO_4 , then a stoichiometric film contains 8% AlPO_4 and 92% Al_2O_3 . The most likely form for the phosphorus would be P_2O_5 with the phosphorus atoms simply substituted for aluminum atoms in the

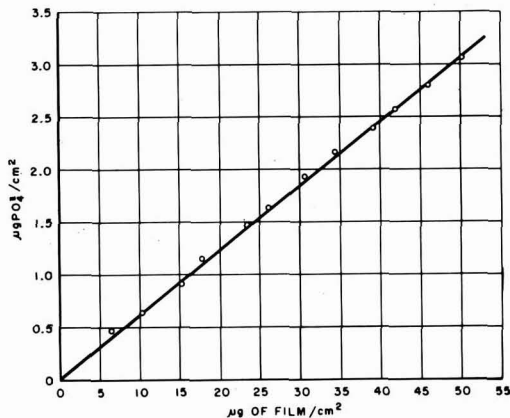


Fig. 3. Phosphate content as a function of thickness of barrier-type anodic oxide film formed in phosphate electrolyte.

oxide lattice. In this case, the composition would be 3.5% P_2O_5 and 96.5% Al_2O_3 . In either case, the stoichiometric composition of the film would be 51% Al. Figure 1 shows the measured percentage of aluminum used in forming a 70-v film, as a function of time. After 5 min forming, while a current of 0.75 ma/cm² was flowing through the film, 58% Al had been consumed. The percentage of aluminum decreased with length of forming time to only 53% Al in 2 hr. There is no evidence of hydration of the barrier-type films.

A more detailed study of the composition of anodic oxide films is being pursued and a discussion of the significance of the nonstoichiometry to the mechanism of ionic transport will be postponed until further information is available. The results presented here do support, by direct chemical methods, Young's (4) prediction of excess metal ions being "frozen into" the oxide when anodizing is stopped.

Current efficiency.—When forming oxide films by anodic oxidation in the phosphate electrolyte, the current passing through the film may be accounted for quantitatively by the oxidation of aluminum to the trivalent ion (forming an oxide film of thickness 14Å/v, density 3.2, and containing the nonstoichiometric 55% Al) and the liberation of oxygen gas at the anode surface. After the oxide film reaches its maximum thickness for a given applied voltage, only about 80% of the residual current flowing through it may be accounted for in terms of oxygen gas liberation at the anode. These effects are illustrated by an experiment summarized in Fig. 4. Specimens were polished metallographically and chemically micropolished by the procedure given by Lewis and Plumb (9). They were then anodized in the special cell described in the next paper of this series (10). The total coulombs passed through the cell, the voltage drop across the film, and the volume of gas liberated at the anode were measured at various times during the formation of a 77 v film. Using the thickness factor (13.8Å/v), density, and composition expected from previous work, and assuming oxidation of aluminum to the trivalent state, the coulombs re-

quired to form the film were calculated. Adding to this the coulombs required to generate the observed volume of gas, the curve marked "film plus oxygen" was obtained. It is seen that the agreement with the experimental curve is quantitative while the film is forming, but less good when the film formation is almost complete. The poor agreement after film formation has practically ceased does not necessarily indicate that oxygen liberation and film formation do not quantitatively account for the current under all conditions. During formation of the oxide film at the solution-oxide interface, the surface is changing continuously and would supply sites where oxygen bubbles could nucleate readily; in contrast to this, a stationary surface would not provide as many sites for nucleation, and hence would favor discharge of oxygen without nucleation of gas bubbles producing a diffusion-type current similar to that which occurs at any anode when the oxygen overvoltage is not exceeded.

The coulombic efficiency, as defined by the ratio of coulombs necessary to oxidize the proper amount of aluminum to the trivalent state, to the total coulombs passed through film, varies greatly with the thickness of the film and the length of time the voltage is applied. It is generally observed that no oxygen is evolved from the anode until there is a voltage drop of 15-20 v across the film. Until then the current efficiency is close to 100%. As the film thickens, a continuously higher percentage of the total current appears as oxygen, and the efficiency drops to 50% and lower. When the film stops growing, some current (usually called leakage current) continues to flow, and the apparent current efficiency drops still lower depending on how long the leakage current is allowed to flow.

The results obtained may be explained without postulating low valent aluminum ion production. If even 10% of the aluminum were produced as a divalent or monovalent ion, these coulometric measurements should have detected it. It is possible that the low valent aluminum ions are produced to a lower extent and were detected by Davidson's (6, 7) sensitive experiments but escaped detection in this work. Further, there are probably basic differences between the electrolytes used by Davidson and those used in this work, since his electrolytes were not generally suitable for forming protective oxide coatings. It is likely that the nature of the ionic species produced will be sensitive to this difference.

Summary

The measured potential drop across an anodic oxide film formed in a KH_2PO_4 - K_2HPO_4 electrolyte at a pH of 7 appears to be a precise measure of the thickness of the film, independent of whether the film is undergoing formation or whether growth has ceased. Using a KH_2PO_4 - K_2HPO_4 electrolyte, the conversion of aluminum to aluminum oxide is essentially quantitative and the coulombic transfer may be accounted for by conversion of the aluminum to the trivalent state and the liberation of some oxygen gas.

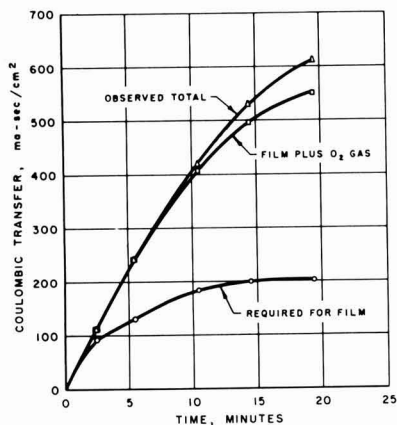


Fig. 4. Coulombic transfer in formation of 80-v barrier layer film by anodizing in phosphate electrolyte.

Acknowledgments

Work was supported by a grant from the National Science Foundation. The author wishes to thank the Aluminum Company of America for permission to include the results of the radioactive tracer measurements of the phosphate content of the anodic oxide films, performed in their research laboratories. Special thanks are expressed to Dr. F. P. Bowden for encouraging this work and providing laboratory facilities.

Manuscript received Jan. 20, 1958. This paper was prepared for delivery before the Ottawa Meeting, Sept. 28-Oct. 2, 1958.

Any discussion of this paper will appear in a Discussion Section to be published in the June 1959 JOURNAL.

REFERENCES

1. G. Haas, *J. Opt. Amer.*, **39**, 532 (1949).
2. J. F. Dewald, *Acta Met.*, **2**, 340 (1954).
3. J. F. Dewald, *J. Phys. Chem. Solids*, **2**, 55 (1957).
4. L. Young, *Acta Met.*, **4**, 100 (1956).
5. L. Young, *Trans. Faraday Soc.*, **52**, 502, 515 (1956).
6. W. E. Barnett, A. W. Davidson, and J. Kleinberg, *J. Am. Chem. Soc.*, **74**, 732 (1952).
7. E. Raijola and A. W. Davidson, *ibid.*, **78**, 556 (1956).
8. R. B. Mason, *This Journal*, **102**, 671 (1955).
9. J. E. Lewis and R. C. Plumb, *Intern. J. Appl. Radiation and Isotopes*, **1**, 33 (1956).
10. R. C. Plumb, *This Journal*, **105**, 502 (1958).
11. J. E. Lewis and R. C. Plumb, *ibid.*, **105**, 496 (1958).
12. S. P. Marion, A. W. Thomas, *J. Colloid Sci.*, **1**, 221 (1946).

Studies of the Anodic Behavior of Aluminum

III. The Specific Surface Area of Aluminum with Variable Resolution from 20Å to 1000Å

Robert C. Plumb¹

Research Group on the Physics and Chemistry of Solids, Cambridge University, Cambridge, England

ABSTRACT

A new technique for studying the surfaces of metals that can be anodically oxidized is proposed. Its development and application for a variety of aluminum surfaces is described. It gives a measure of the specific area of aluminum with what may be described as a continuously variable resolution from 40Å to 1000Å. The results agree with measurements of specific surface area by a radiochemical technique which has a resolution of about 20Å and optical measurements made at resolution greater than 1000Å. The shape of a particular surface area vs. resolution curve gives information about the topography of the surface.

If one could look at an ideally prepared cross section of a metallic surface with a continuously variable magnification from less than 1 diameter to about 10⁶ diameters, more and more detail of the surface contours would be revealed as smaller and smaller asperities, cracks, fissures, etc., were resolved, until ultimately the asperities consisting of a few atoms, together with oxide layers and adsorbed molecules, were revealed. Such a detailed direct examination of surface contours over a suitable magnification range is impossible at the present stage of development of electron microscopy and sample sectioning techniques. Special techniques for revealing surface contours such as multiple beam interferometry and reflection electron microscopy are applicable only to relatively smooth surfaces. As a result, the knowledge of surface topography of rough surfaces is very limited.

One may further consider the hypothetical examination of a surface under idealized conditions. If the surface area were measured at each magnification, one would find it continuously increasing in the manner of a geometric progression since the smaller asperities, fissures, and cracks would appear as irregularities on larger asperities which had been ob-

served at lower magnifications. The converse relationship is that, if the surface area could be measured with continuously variable resolution, the distribution of asperity sizes could be inferred from the variation of the measured surface area. Such a process is considered here.

The surface area of metals may be measured by several physical chemical techniques. Measurements by gas adsorption have recently been reviewed by O'Connor and Uhlig (1). Bowden and Rideal (2) devised the classical technique of measuring double layer capacitance of a metal in an electrolyte. This technique has been re-examined recently by Wiebe and Winkler (3). Adsorption of radioactive fatty acids from solution has been used (4). The formation of a thin radioactive barrier layer on aluminum has been used by this author (5). Each of these methods of area measurement has a characteristic resolution or resolving power corresponding to the thickness of the layer applied to the surface. Because of experimental difficulties in the measurements and the questionable validity of the results in some cases, the surface area frequently remains an unknown factor in otherwise quantitative investigations of surface phenomena.

Many metals, when anodically oxidized in a suitable electrolyte, become covered with a thin oxide

¹ Present address: Department of Chemical Engineering and Chemistry, Worcester Polytechnic Institute, Worcester, Massachusetts.

film whose thickness is in direct proportion to the voltage drop across the film. Aluminum and tantalum have been investigated in the most detail. Zirconium, uranium, silicon, chromium, niobium, and many other metals may also be anodically oxidized, although the detailed variation of film thickness with voltage has not been elucidated. With aluminum, in a suitable electrolyte (6), the film thickens until the field strength is reduced to about $0.07 \text{ v}/\text{\AA}$, and then the film stops growing. If such a film is formed on a rough surface, the film reproduces the contours of the surface only if the height or width of the asperities exceeds the thickness of the film. By measuring the amount of a film of a known thickness formed on a surface, the area of the surface would be determined with a specified resolution (the film thickness).

This technique of measuring surface area with variable resolution has been developed for aluminum. The results have been compared at each end of the resolution curve with measurements of the specific surface made by a radioactive tracer technique (5) (resolution 20\AA), and electron and optical microscopic techniques (resolution $1000\text{--}10,000\text{\AA}$).

Measurement of Specific Surface Area by Anodic Oxidation

As shown in a previous paper (6), the thickness of the oxide film formed on aluminum by anodic oxidation in a 1.6% H_3PO_4 electrolyte, adjusted to a pH of 7.0 with KOH, is $0.44 \text{ mg}/\text{cm}^2\text{-v}$ or $14\text{\AA}/\text{v}$. The film contains about 55% aluminum under forming conditions, and the coulombic transport through the film during its formation may be accounted for to within 5% by oxidation of aluminum to the trivalent ion and the liberation of some oxygen gas. The surface area should be measurable then by forming an oxide film of a known thickness, measuring the total amount of film formed from the coulombic transfer (correcting for oxygen gas evolution), and calculating the extension of the film in area units. Dividing by the geometric area gives the specific surface area or roughness factor.

Coulometer.—The coulombic transfer was measured with a hydrogen gas coulometer, which also served as the cathode for anodizing. The cathode was a $1/8$ -in. long platinized platinum wire. The gas volume in the coulometer above the liquid was kept under 0.3 ml to minimize the effects of temperature variations. Since the electrolyte was saturated with oxygen, whenever the level of the liquid was raised the coulometer was conditioned by passing current for a short time to consume any oxygen which might combine directly with the hydrogen at the platinum surface. The response of the coulometer, as determined by comparison with a good quality ammeter, was within 1% of the theoretical volume of gas/coulomb in the range of $200 \mu\text{a}$ to 50 ma. At $175 \mu\text{a}$ the response was 95% and at $100 \mu\text{a}$ it was 70%. Day-to-day barometric changes were negligible. Gas collection after passing current was complete in 2 or 3 min, and with care the volume of gas could be measured to 0.001 ml (1λ) corresponding to a sensitivity of 0.008 coulombs.

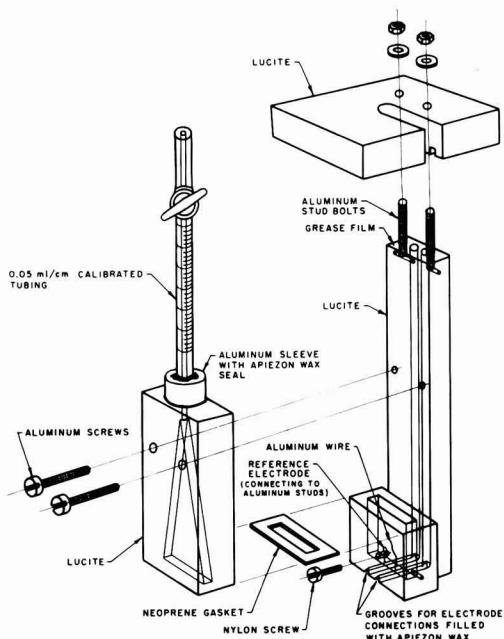


Fig. 1. Anode compartment of anodizing cell

Cell design.—The design was directed toward quantitative collection of oxygen gas. The cell is shown in Fig. 1. Gas bubbles were collected by tapping on the top of the cell. The addition of 1% amyl alcohol to the electrolyte greatly facilitated bubble collection without affecting the characteristics of the anodizing process. To minimize diffusion current, the electrolyte was kept saturated with O_2 gas that was bubbled into the electrolyte through a fine capillary at high pressure. Electrical contact with the sample was made with a 0.010 in. aluminum wire pressed into the surface of the sample by a nylon screw. Before the initial assembly of the cell, the wire was anodized to a 160-v barrier layer. In operation of the cell with a piece of plastic substituted for the sample, no detectable current was observed. A film of grease at the joint between the top and central portions of the cell prevented the accumulation of a conducting moisture film between the two electrode connections. The voltage drop across the film was measured with an O_2 reference electrode, consisting of a platinized platinum wire about 1 mm away from the sample. The reference electrode was kept saturated with O_2 from the solution and by passing current ($4 \text{ ma} \times 15 \text{ sec}$) through it before each step of anodizing. O_2 reference electrodes show instability and lack of reproducibility in the range of tens of millivolts, but since the voltages to be measured here were large, good precision was needed only on the differences between successive voltages and not on their absolute value. The O_2 electrode had the special advantage that there was no risk of introducing foreign ions, such as chloride, which can be very deleterious to anodizing.

Power supply.—Sets of 22.5-v and 1.5-v dry cells were arranged with multiple taps to give any pre-

set voltage from 0 to 160 v in 1.5-v steps. An auxiliary circuit was used to pass the conditioning current through the platinum electrodes.

Sample preparation.—To limit the area of a specimen for measurement, the desired area was masked off with apiezon wax and the rest of the specimen was anodized to a 160-v coating. The wax was then removed by a thorough benzene vapor degreasing. No other procedure tried was effective because of the tendency for anodic oxide to penetrate beneath any protective coating. The procedures for obtaining the various surfaces are given in the captions for the figures.

Measurement procedure.—After a sample had been inserted, the electrolyte saturated with O_2 , temperature equilibration reached, and the hydrogen coulometer conditioned, voltages were applied to the sample in 1.5 v and larger steps. Voltage drops across the film were measured and plotted against time. Since the recovery of O_2 did not appear to be quantitative when the film growth was very slow (6), the voltages were applied for short times (2-5 min) only, until the measured voltage across the film showed signs of leveling off. The H_2 and O_2 (if any) were collected and measured, and a new voltage step was applied. It was generally found that the first voltage at which O_2 was evolved was near 20 v.

Calculation of specific surface area and resolution.—The measured potential difference between the reference electrode and the aluminum specimen is the sum of the oxygen half-cell at the platinum (0.4 v), the potential drop across the film, and double layer and interfacial potentials which may be safely ignored because of their magnitude. The potential drop across the film is the sum of the aluminum half-cell ($Al \rightleftharpoons Al^{3+} + 3e$, 1.7 v) which will be polarized to some extent by the oxide films, and that potential derived from the external source. The sum of the potentials (2.1 v) for the aluminum half-cell and the oxygen electrode were added to the observed voltage readings to obtain the total potential drop across the film. The thickness of the oxide film was then calculated at $14\text{\AA}/v$ and this used as a measure of the resolution. Corrections are probably good to better than a volt. The resolution will then be correct to within about 10\AA . The differences between the voltages at the end of two successive steps were used as a measure of the additional thickening of the film in that step. The specific surface area was then calculated from three quantities: the thickness of the film formed in the voltage step, the amount of oxide formed as determined coulometrically, and the geometric area of the specimen. The calculated area from the voltage step where O_2 was first evolved generally disagreed with points obtained just before and after. This measurement was discarded in all work.

Measurement of the Specific Surface Area by Radioactive Phosphate-Chromate Barrier Film

This technique has been described in detail previously (5). When aluminum is treated with a solution of 5% H_3PO_4 -3% CrO_3 at $85^\circ C$, the oxide is dissolved and a phosphate-chromate film is formed on

the surface by reaction with the aluminum. This film, 10-20 \AA thick, seals the surface and prevents further reaction on the aluminum by the acid mixture. The amount of the film can be determined by using radioactive phosphoric acid (phosphorus-32), and its thickness is reproducible so that the surface area can be calculated. The resolution is thought to be 20 \AA . The measurements by this method were performed on portions of the samples used for the anodic oxidation work, but independently, and in separate laboratories.

Measurement of Specific Surface Area by Microscopic Techniques

Specimens which had been used for the anodic oxide work were mounted face down against another specimen of aluminum with Araldite adhesive, thermally cured, mounted in plastic, and a perpendicular cross section cut and polished by metallographic methods. Araldite was used because it wets the oxide surface very well, and when cured it has a hardness close to that of aluminum. The good contact between two materials of similar hardness is essential in polishing a cross section of an edge to prevent metal flow and distortion of the edge. The specimens were photographed at the desired magnification and the photographs were enlarged 10X by projection. A soft wire 1 mm thick (corresponding to 0.1 mm on the photograph) was bent to conform to the irregularities of the cross section of the surface. The specific surface area was calculated as the ratio of the length of the wire to the extension of the wire after bending to conform

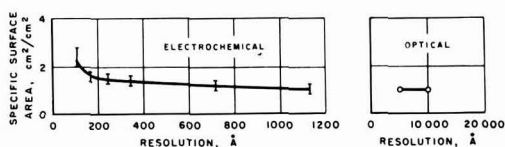


Fig. 2. Area-resolution curve for aluminum sheet chemically polished by Alcoa R-5 bright dip treatment (U. S. Pat. 2,650,157).

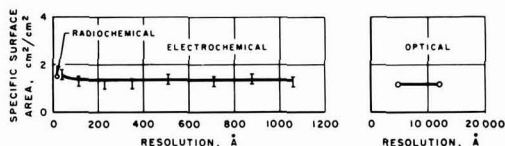


Fig. 3. Area-resolution curve for aluminum sheet specimen faced in lathe. No lubricant used but a clean cut with no tendency for stock to gall, seize, or chatter.

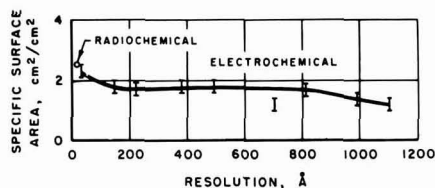


Fig. 4. Area-resolution curve for aluminum sheet specimen in "as rolled" condition.

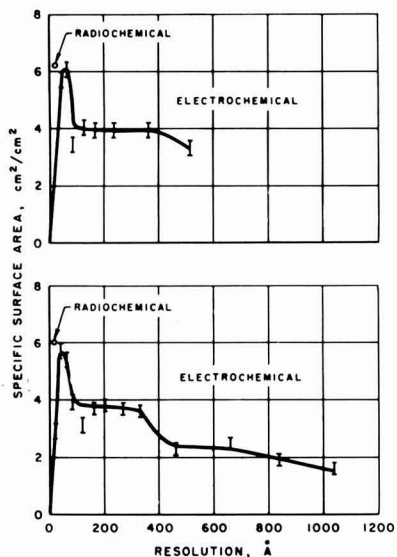


Fig. 5. Area-resolution curves for two specimens abraded separately on No. 320 "Aloxite" cloth with kerosene lubrication. Specimens were mounted in plastic. "Aloxite" cloth was mounted on metallographic polishing wheel rotating at 300 rpm light hand pressure on sample.

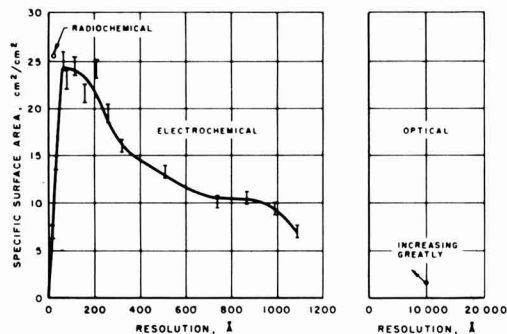


Fig. 6. Area-resolution curve for aluminum abraded successively with No. 120, No. 240, and No. 600 silicon carbide paper using kerosene lubrication but (a) using very short irregular strokes in random direction, (b) rubbing only long enough to develop scratches characteristic of the paper in use but not long enough to remove the scratches from the previous paper.

to the projected surface. The resolution was taken as the thickness of the wire divided by 10X times the magnification.

Comparison of Results of Surface Area Measurements by Three Methods

Figures 2-6 show the results of surface area measurement on a variety of aluminum surfaces. The radiochemical result is shown to the left, the anodic oxide measurements are shown in the middle, plotted as specific surface area vs. resolution, and the optical measurements are plotted to the right, again as a function of resolution. Radiochemical results are not included for the chemically polished surface in Fig. 2 because the phosphate film left by the chemical polishing treatment interfered with

the measurement. Optical measurements were made only on surfaces which were relatively smooth and which could be measured easily.

All aluminum surfaces which have been exposed to oxygen are covered with a natural oxide which is 20-30Å thick at room temperature. This natural oxide should affect the area measurements by anodic oxidation since the expected ionic current flow through the film will not occur until the measured film thickness exceeds that of the natural oxide. It is seen from Fig. 5 and 6 that the measured surface area increases as the measured film thickness (resolution) increases, until it exceeds 20 or 30Å. The surface area measured at resolutions of 30Å and lower are of course not valid, because of the natural oxide, and have been omitted from the other curves but retained on Fig. 5 and 6 for illustrative purposes. The fact that the experiments reveal the natural oxide and give an approximately correct thickness for it lends confidence to the method. The surface areas measured by anodic oxidations are absolute in the sense that they are based on the independently measured physical parameters of thickness per volt (7), density (7), and composition of the oxide (6). Most comparative surface area measurements (2, 4, 5) are based on the magnitude of a physical quantity which has been measured on a surface which is assumed to be smooth.

It is seen from Fig. 2-6 that the radiochemical measurements agree with the anodic oxide measurements within about 5% over the range of specific surface areas from 1.5 to 25. Considering the widely divergent sources of the fundamental parameters used in calculating the specific surface area from anodic oxidation, and the extreme differences between the radiochemical and the electrochemical techniques, the agreement is gratifying. Even the slight difference between two samples shown in Fig. 5, which had been prepared identically, but independently, are reproduced by the radiochemical and the electrochemical measurements. The difference in area between the two was 3.5% by the radiochemical technique and 5% by the electrochemical technique. It is thought that the area measurements at 30 to 40Å resolutions are accurate to at least 10% and possibly 5%.

Only two samples (Fig. 3 and 4) were studied in detail at resolutions greater than 1000Å by optical methods, but the agreement was good.

Distribution of Asperity Sizes on a Surface and Observations on the Nature of Surfaces Produced by Several Treatments

The curves shown in Fig. 5 are the most interesting of the surface area resolution curves from the viewpoint of the structure of the surface which is revealed. The specific area at a resolution of 1000Å is 1.5. This is increased by about 50% by irregularities which can be detected at a resolution of 600Å but not at 1000Å. Irregularities about 300Å in size cause another 60% increase in area, and irregularities less than 90Å in size increase the area by another 50%. The rather sharp breaks in the curves such as are shown in Fig. 5 were not obtained on most of the other curves. However, a few general

trends are indicated. For example, the measurements shown on the very rough surface in Fig. 6 indicate that there is little contribution to the surface area by irregularities smaller than 200Å, but the surface area is a result of a rather continuous range of irregularities varying in size from 200Å up to more than 10,000Å. From Fig. 4 it is seen that a rolled surface has irregularities smaller than 150Å, almost no irregularities in the size range from 150Å to 700 or 800Å, but a quite significant contribution to the surface area by irregularities in the range of 1000Å. One of the most interesting surfaces was that obtained by lathe turning. This surface had macro roughness visible to the unaided eye, but within an experimental error of $\pm 10\%$ no micro roughness aside from a small contribution from irregularities detectable at 50Å resolution. In terms of surface area this compares very well with the best metallographically polished surfaces which have a specific surface area of about 1.3 (5).

It is apparent that the specific surface area of aluminum surfaces may vary greatly depending on the method of sample preparation. Surfaces with roughness factors between 1.25 and 25 have been observed and results by three independent methods are in excellent agreement. Further, by measuring the specific surface area with variable resolution, the dimensions of the asperities which contribute to the surface area may be deduced. It would seem that the information about the surface area and surface topography would be of value in the quan-

titative interpretation of oxidation and corrosion rates, and would aid in interpreting lubrication, friction, and adhesion phenomena.

Acknowledgments

Work was supported by a grant from the National Science Foundation. To the Aluminum Company of America the author expresses thanks for a leave of absence and for supplying numerous samples of aluminum and performing the radiochemical measurements. To Dr. F. P. Bowden he expresses appreciation for making the facilities of his laboratory available and for providing continuous encouragement and suggestions.

Manuscript received Jan. 20, 1958. This paper was prepared for delivery before the Ottawa Meeting, Sept. 28-Oct. 2, 1958.

Any discussion of this paper will appear in a Discussion Section to be published in the June 1959 JOURNAL.

REFERENCES

1. T. L. O'Connor and H. H. Uhlig, *J. Phys. Chem.*, **61**, 402 (1957).
2. F. Bowden and E. Rideal, *Proc. Roy. Soc. (London)*, **120A**, 59 (1928).
3. A. Wiebe and C. Winkler, *Can. J. Chem.*, **31**, 306, 665, 111B (1953).
4. J. W. Shepard and J. P. Ryan, *J. Phys. Chem.*, **60**, 127 (1956).
5. J. E. Lewis and R. C. Plumb, *Intern. J. Appl. Radiation and Isotopes*, **1**, 33 (1956).
6. R. C. Plumb, *This Journal*, **105**, 498 (1958).
7. G. Haas, *J. Opt. Soc. Amer.*, **39**, 522 (1949).
8. M. S. Hunter and D. L. Robinson, *J. Metals*, **5**, 717 (1953).

Schlieren Studies of Concentration Gradients at a Cu|HCl Anode

Ralph S. Cooper¹

Department of Physics, University of Illinois, Urbana, Illinois

ABSTRACT

Schlieren optical techniques have been applied to the study of the anolyte at a Cu|HCl anode during current transients. Both the space and time dependence of the concentration gradients were quantitatively observed and correlated to the electrochemical processes occurring at the anode. The depletion of Cl⁻ ion in solution, owing to the formation of a solid CuCl anode layer, and the entrance into solution of Cu⁺⁺ ion and the CuCl₂⁻ complex were observed. The development and relative importance of diffusion and natural convection were studied under various conditions. In addition, using a Cu|CuSO₄ anode, experimental evidence was obtained, confirming the concentration distribution within the natural convection layer expected on theoretical grounds.

Detailed information concerning the concentration gradients at an electrode would be invaluable in the fields of electrodeposition, corrosion, and polarization. The purpose of this paper is to present information of this type for a Cu|HCl anode, obtained by use of the schlieren optical technique. Schlieren methods have been used previously to observe electrochemical phenomena qualitatively (1-4) and at least semiquantitatively by Stephenson (5) and Yeager and co-workers (6).

Experimental Arrangement

Design and Principles

The schlieren apparatus used in these experiments was designed by Stephenson (5) and required only slight modification to produce quantitatively accurate results. Its resolving power (10^{-2} mm) permits detailed examination of diffusion layers only 0.1 mm thick.

The schlieren apparatus produces an image in which the brightness at any point is proportional to the gradient of the refractive index at that point

¹ Present address: Los Alamos Scientific Laboratory, Los Alamos, New Mexico.

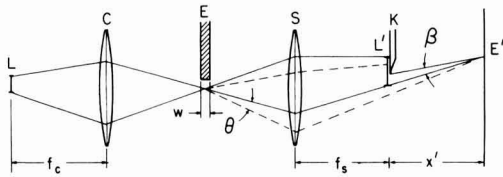


Fig. 1. The schlieren optical system

in the object space. Thus by integration one can obtain the index of refraction at any point in the solution and, consequently, obtain information concerning the ionic concentrations. The principle of the instrument is as follows (Fig. 1). A beam of light from a source (L) illuminates the solution near an electrode (E), whose image is formed on the film at E'. The lens system is arranged so that the image of the electrode (E') lies beyond the image of the light source (L'). A knife edge is placed at L' to intercept some of the rays from the electrolyte. If a concentration gradient (and, consequently, a refractive index gradient) exists in the electrolyte at some point, the bundle of rays passing through that point will be bent, e.g., as shown by the dotted lines. This will not alter the formation of the image at E' but will shift the image of the light source (S') with respect to the knife edge. Thus the amount of light reaching E' will depend upon the refractive index gradients at E. The angle θ through which the beam is bent in passing through the anolyte is given by

$$\theta = wn' \quad [1]$$

where w is the region in which the gradient lies, and this region is defined in practice by shielding the electrode with two glass cover slips. n' is the value of the gradient in the x direction which is perpendicular to the knife edge and in a plane parallel to the film plane. It is useful to know how far the image of the source will be shifted with respect to the knife edge under a particular gradient. Denoting this by Δz , the result is

$$\Delta z = wn'f_s = \theta f_s \quad [2]$$

for the lens system employed here, where f_s is the focal length of the schlieren lens. Note that this is independent of the exact position of the electrode and the position and focal length of the collimating lens and depends only on the fact that the image of the source lies at the focal point of the schlieren lens.

An exact analysis of diffraction phenomena in schlieren systems is very difficult and has not been carried out thus far, but simple considerations can give useful results. The critical phenomenon is the diffraction which occurs when the knife edge cuts off most of the light from the source. The main effect of this is to lower the resolution of the instrument, spreading the light from a single point in the anolyte over a region in the film plane. The half width of the diffraction pattern is approximately

$$h = \frac{\lambda}{\sin \beta} = \frac{\lambda x'}{z} \quad [3]$$

where λ is the wave length of light, x' is the distance from the knife edge to the film, and z is the height of that portion of the source image which is not intercepted by the knife edge. Thus the knife edge must not be allowed to cut off too much of the beam and reduce the resolving power of the instrument to below that required. For our apparatus, if $z = 0.05$ mm, then the resolving power is reduced to 0.04 mm, which is a considerable fraction of the field of view. The collimating lens has a focal length (f_c) of 48 mm, and the schlieren lens has $f_s = 24$ mm. The light source L is actually an illuminated slit, placed at the focal point of the collimating lens. Therefore, its image will be at the focal point of the schlieren lens and be half the size of the slit. The apertures in our system permit a maximum slit height of 3 mm, giving a maximum Δz of 1.5 mm. The electrode thickness (w) is of the order of 1 mm, which puts an upper bound of 0.06 riu/mm on the gradient of the refractive index. This is roughly equivalent to a concentration gradient of 6 molar/mm of NaCl or a current density of 60 ma/cm².

The recording system of the schlieren apparatus was a commercial 8 mm motion picture camera, with an appropriate lens set behind the knife edge. The direct magnification was of the order of unity while the field of view was approximately 1 cm². The film could be examined microscopically to obtain the maximum resolving power of the instrument. Photographs could be taken at rates of 16-64 frames/sec to yield the temporal development of diffusion transients. To analyze the photographic data, a metallurgical microscope was modified to project a beam of light on the film which was placed in the normal viewing position on the stage of the microscope. The beam, rectangular in cross section and only 20 μ wide at the film, passed through the film to a photomultiplier tube mounted under the stage. Thus it was possible to determine the relative density of a portion of the film only 2×10^{-5} cm² in area. The film was mounted on a movable, calibrated stage so that the density could be obtained as a function of the distance along the film which was equivalent to distance in the object space. In order to process the data automatically, the stage was driven by a constant speed motor while the output of the photomultiplier was fed through an amplifier into a Brown recording potentiometer.

Calibration

The calibration of the instrument may be carried out by two distinct methods: by placing a standard in the object space, or by adjusting the knife edge. The latter method depends on the fact that the position of the slit image relative to the knife edge determines the intensity of the film. Thus by moving the knife edge by Δz from its normal setting, one obtains the intensity corresponding to a gradient $\Delta z/wf_s$. A lens may serve as a standard schlieren or to check the other method of calibration. The angle through which a ray is bent in passing through the lens at a distance r from the center of the lens is just r/f_s for small angles. The ray through the center is undeviated. Thus a schlieren photo of a lens would show one side bright with the intensity

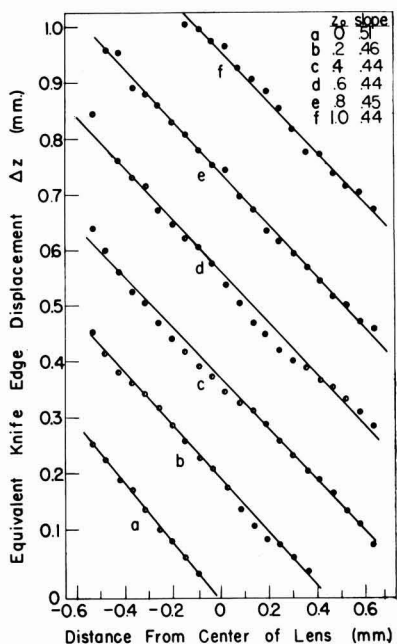


Fig. 2. Results of schlieren photographs of a lens as an object, taken with various settings of the knife edge.

decreasing linearly toward the other side. The difficulty in using a lens as a standard is that the center is not exactly known. Nevertheless, it is valuable as a check on the apparatus, including the diffraction error. Figure 2 shows the result of photographing a lens of focal length f_1 with various settings of the knife edge. Since

$$\Delta z = \theta f_1 = \frac{r}{f_1} f_1 \quad [4]$$

one expects a straight line of slope f_1/f_1 for a plot of Δz vs. distance r across the lens. For all cases where the knife edge was open 0.2 mm or more, the difference between the experimental result and that predicted on the basis of the focal lengths agree to within 3%. On the other hand, the one curve which corresponds to low values of Δz and, consequently, poor resolving power, gave a result high by 13%. In this case, the calibration was carried out by photographing the empty object space with various settings of the knife edge.

The Electrochemical System

The system chosen for study was the Cu|HCl anode which had already been investigated by standard electrochemical techniques (1, 4, 7). With a fixed applied voltage, the current transients show one or more periods (current plateaus) where the current is independent of time, followed by relatively rapid decreases. The current may go through a minimum before approaching a steady state, and even may exhibit sustained oscillations. The same experimental arrangements were used in this work, using anodes which permitted natural convection to take place. Unless otherwise noted, the bulk acid concentration was 2*N*.

An anode was constructed with a vertical rectangular surface, 1 mm wide by 2.4 mm high. Thin glass cover slips were cemented to the sides of the electrode to define the region w (Fig. 1) in which the concentration gradients lie. The presence of the cover slips did not appreciably affect the convection process.

Schlieren motion picture (8 mm) were taken of transients at 16 frames/sec, which is sufficiently rapid to give a continuous development in time of the diffusional processes, yet allows photographing a sufficient period (15 sec) to observe the motion of the fluid in the complete development of natural convection. The results were observed qualitatively with a standard 8 mm motion picture projector. The film was then examined frame by frame, and representative frames were selected for quantitative analysis. Intensity calibration was affected by the method of altering the knife edge position, and spatial calibration was made by photographing a reticle placed at the electrode.

Results and Discussion

Schlieren Studies of the Cu|HCl System

The first transient to which the schlieren technique was applied exhibited most of the phenomena of interest. The first current-time plateau ($i_1 = 3.6$ ma) was completed in 3 sec, before appreciable convection was observed. After a very brief second plateau, the current reached a minimum of 0.3 ma ($t = 5$ sec) and then rose to its steady-state value of 1.5 ma. In the steady state the reaction products include Cu^{++} ion, as the applied potential was sufficient for its formation (7). Schlieren motion pictures were taken from $t = 0$ to $t = 12$ sec, and during the steady state ($t = 4$ min). Frames at approximately 1, 2, 3, 4, and 7 sec, plus one in the steady state were selected for quantitative analysis. The results (Fig. 3 and 4) are presented as graphs of the refractive index gradient (n') vs. the distance from the electrode face (x), with the convention that a positive gradient corresponds to n increasing toward the anode. Since the refractive index is roughly proportional to the total ionic concentra-

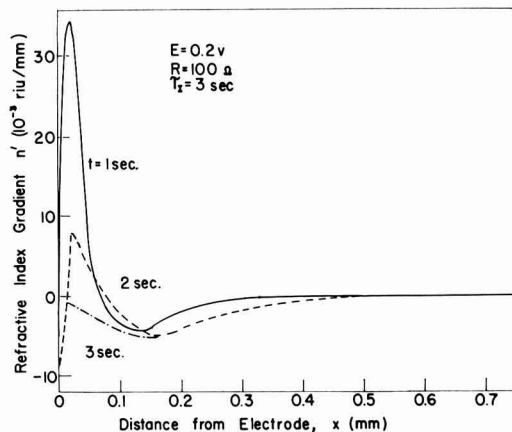


Fig. 3. Refractive index gradients near a Cu|HCl anode during the early stages of a current transient.

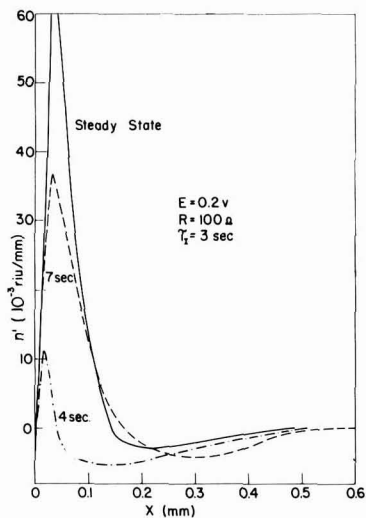


Fig. 4. Refractive index gradients near a Cu|HCl anode after the current drop, and in the steady state.

tion, the curves may also be thought of as plots of concentration and density gradients.

From Fig. 3 we see that after 1 sec a positive gradient has arisen in the region $0 < x < 0.065$ mm. (The apparent decrease in n' for $x < 0.02$ mm is due to diffraction at the edge of the anode. The curves should be extrapolated into that region to obtain values at the anode surface.) The gradient is negative from $x = 0.065$ mm to $x = 0.04$ mm, where it approaches zero. Integrating in from the bulk,² we find that the index of refraction first decreases, reaching a minimum (of $n = n_{\text{bulk}} - 0.05 \times 10^{-3}$) at 0.065 mm, and then increases to $n_{\text{bulk}} + 1.2 \times 10^{-3}$ at the anode face.

It is clear that there are at least two distinct³ concentration gradients required to produce the result observed for $t = 1$ sec. These are a large positive gradient close to the anode ($x = 0.06$ mm) and a smaller negative gradient reaching further out into the solution. Since Cu^{2+} has been shown not to occur at the potentials associated with the first plateau (7), and the anolyte becomes saturated with CuCl_2^- prior to precipitation of CuCl , the large positive gradient must be due to saturation of the anolyte by CuCl_2^- . The negative gradient corresponds to a lower total ionic concentration which can be accounted for only by depletion of chlorine ions due to the formation of the CuCl layer and the CuCl_2^- complex close to the anode face.

If the separation of the two gradients (Fig. 5) is valid, we may compare the concentrations computed from them to values obtained by independent means. From the area of the negative gradient in

² The bulk solution serves as a reference point for the refractive index and the concentration, which is 2N HCl unless noted otherwise.

³ There are at least three compounds which may appear in solution: HCl, CuCl , and CuCl_2 . In solution, these will be ionized or complexed and will exist largely as a mixture of H^+ , Cl^- , CuCl_2^- , and Cu^{2+} . To a first approximation, we may consider the contributions to the refractive index by the various components to be additive and proportional to the concentrations of the respective compounds. The partial molar refractivities are 8.6×10^{-3} for HCl, 1.44×10^{-2} for CuCl_2 , and estimated to be 1.0×10^{-2} for CuCl in HCl.

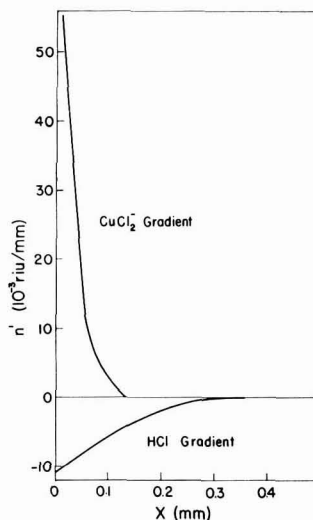


Fig. 5. A decomposition of the configuration $t = 1$ sec (Fig. 3) into two components refractive index gradients, a positive gradient owing to the entrance of Cu^+ into solution as the CuCl_2^- complex, and a negative gradient due to the depletion of the Cl^- ion used in the formation of the solid CuCl layer.

Fig. 5, we find the difference (Δc) between the bulk and anode acid concentrations to be 0.17N. We can estimate the HCl concentration at the surface using diffusion theory (7) by the equation

$$\Delta c = \frac{it_i \sqrt{4Dt}}{FSD \sqrt{\pi}} = 6.4 \times 10^{-2} i \sqrt{t} \quad [5]$$

where i is in ma, and Δc in moles/liter. D is the diffusion coefficient of the salt; F is the Faraday constant; t_i is the transference number of the H^+ ion; and S is the anode surface area. For $t = 1$ sec, this gives $c = 0.2M$, in good agreement with observation, and well within the approximations involved. Second, the presence of solid CuCl indicates that the solution at the anode face is saturated with CuCl_2^- , which is about 0.22N in 1.8N HCl. From the area of the positive gradient, we compute 0.25N, again in good agreement.

Now consider the time dependence of the gradients (Fig. 3 and 4). After 2 sec, the CuCl_2^- gradient has greater spatial extent but is smaller in magnitude, while the HCl gradient has become larger. This trend is continued throughout the duration of the first plateau (< 3 sec), the HCl gradient becoming so large compared to the other that the net refractive index gradient is negative everywhere (at $t = 3$ sec). This behavior is to be expected, because the total CuCl_2^- concentration difference cannot be greater than the concentration of the saturated solution, while the HCl concentration decreases as \sqrt{t} until its concentration has been reduced to zero at the anode face. This type of behavior is observed for all transients for which the current drop occurs before convection begins. The higher i_t is, the more pronounced is the negative gradient as is to be expected from Eq. [5]. This

region is seen (1) to convect upward, which demonstrates that it corresponds to a solution of concentration lower than the bulk. The HCl gradient does not continue to grow indefinitely but is reduced by the effect of natural convection.

After the current drop, the electrode voltage (V) rises into the range for Cu^{++} ion formation, $V \cong -0.05$ v (7). The entrance of a new salt into solution can be seen at $t = 4$ sec (Fig. 5) as a new positive gradient next to the electrode. This increases rapidly even while the current is passing through its minimum, and has submerged most of the HCl gradient. As the current rises to the steady state, the positive gradients increase, but convection limits the region in which they occur to about 0.17 mm. The negative gradient is also reduced because of the bulk transport of ions by convection. In the steady state, the HCl gradient must be small as can be seen by considering the Cl^- concentration gradient necessary to carry the steady-state current across a stagnant layer of width Δx . By Fick's law

$$\frac{i}{SF} = D \frac{\Delta c}{\Delta x} \quad [6]$$

Therefore, $\Delta c = 0.3M$. Convection effects will reduce this considerably, and the fact that Cu^{++} ions are carrying some of the current also will decrease Δc . Thus the HCl concentration difference can be expected to be small compared to its bulk concentration (2N).

The positive gradient is composed of contributions from both CuCl_2^- and CuCl_2 . We know the approximate concentration of the CuCl_2^- at the surface to be about 0.24N (saturated solution) and can subtract its effect on the index of refraction to determine the CuCl_2 concentration. From Fig. 4, for the steady state, this results in a value of 0.22M for the CuCl_2 at the anode, which value is very close to the CuCl concentration. The value of the CuCl_2 concentration computed this way is a lower limit, as some Cu^{++}

may have replaced H^+ from the HCl, an effect which would produce a smaller effect on the refractive index than the addition of CuCl_2 to the solution. However, as CuCl and CuCl_2 are found to be produced in roughly equal amounts (7) and undergo similar mass transfer processes, one would expect that their concentration profiles would be similar and thus their concentrations at the anode roughly equal. All transients with short plateaus (< 4 sec) exhibit schlieren similar to the one just discussed, differing only in intensity and time scale.

For transients with a long first plateau, i.e., when i_1 is small, the Cl^- is not depleted at a rapid rate, and thus large negative gradients never arise. The schlieren of such a transient (Fig. 6) shows a positive gradient which increases for the first few seconds and then becomes stabilized by convection. The concentration gradients are then constant until the current drop. If V remains less than -0.05 v, then no concentration changes occur during or after the current drop, as it is observed that the convection layer has already become stabilized, and no new electrode process is found to occur (7). For those cases where V increases beyond -0.05 v, an increase in the positive gradient in the convection layer is observed between the end of the first plateau and the current minimum. This increase remains until the steady state is reached (Fig. 6). It is attributed to the entrance of Cu^{++} into solution as this is the only mechanism which could increase the ionic concentration beyond that of saturated CuCl and because Cu^{++} is observed as a reaction product for $V \cong -0.05$ v. In 2N HCl, the second current-time plateau is too short to distinguish whether the increase in n' occurs during or after the plateau, but this is possible at lower concentrations. In 0.5N HCl, the maximum CuCl concentration is only 0.015N, and thus only a very small positive gradient could be due to saturation of the HCl at the anode face. The second plateau is longer than the first in 0.5N HCl, giving ample time to determine the conditions existing during the second plateau. Visual schlieren observations were made using movement of the knife edge for quantitative estimates of the gradients. A large positive gradient (with a maximum of the order of 40×10^{-3} riu/mm) appeared next to the anode as soon as the second plateau was initiated. This could be due only to Cu^{++} entering the solution for the reasons cited above.

Steady State and Oscillations

Steady-state conditions are independent of early stages of the transients, and depend only on the final electrode voltage (V_s) and current (i_s). The two types of steady-state conditions have already been discussed, the region where a CuCl layer exists and only cuprous ion is formed ($-0.27 < V_s < -0.05$) and the region where cupric ion forms part of the reaction products ($V_s \cong -0.05$ v).

The final schlieren layer in the Cu|HCl system was of the diffusion layer during current oscillations. With $E = -0.2$ v and $R = 100\Omega$, the transient displayed current oscillations as observed by Bonhoeffer (8), with a period of 26 sec (Fig. 7). This

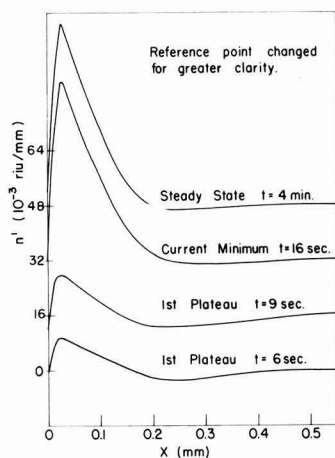


Fig. 6. Refractive index gradients near a Cu|HCl anode where convection occurs before the current drop ($\tau_1 \approx 12$ sec). A stable configuration is developed which lasts until the end of the current plateau. Afterward, a larger gradient is established and persists in the steady state.

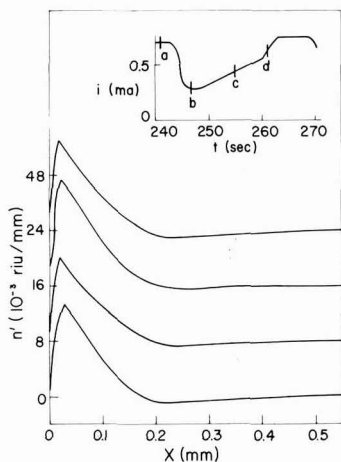


Fig. 7. The configuration of the diffusion-convection layer during current oscillations in the $\text{Cu}|\text{HCl}$ system. The reference point has been changed for greater clarity, the curves overlapping considerably. The concentrations in the layer thus appear independent of the current fluctuations.

type of oscillation was studied with more standard electrochemical techniques by Bartlett and Cooper (7) and appears to be due to fluctuations between two quasi-steady states, one with a solid anode film and the other without it, as postulated in the above paper. The first plateau lasted 90 sec with $i_t = 0.68$ ma, and the minimum current was 0.27 ma. Upon approaching the steady state (20 sec after the current minimum), the current rose suddenly to 0.65 ma and oscillations began. They lasted only eight periods and then ceased abruptly, the current immediately becoming constant at the steady-state value. Schlieren motion pictures were taken during the first 10 sec of the transient, over one complete cycle of an oscillation (the sixth) and during the steady state. The schlieren for four significant points during the oscillation were analyzed (Fig. 7). The main fact to be noted is the similarity of the four results, the concentration gradients appearing to be relatively independent of the current. Furthermore, the result for the steady state is the same as that during oscillations. This result is to be expected if the removal rate is controlled by a mass transfer process (solution of the layer as CuCl_2^- , and subsequent convection away) which is essentially physicochemical rather than electrochemical, i.e., that the removal rate is determined by physical quantities such as the rates of solution and diffusion of the salt, and specific gravity differences, rather than by the rate of some step involved in the electrode reaction. As long as the electrode has sufficient solid CuCl on it to keep the solution at the anode face saturated, the solution and convection will proceed at the same rates, and the gradients will be unaltered. This can be clearly seen experimentally in schlieren motion pictures taken when the circuit is broken with the electrode in the steady state. The concentration gradients are unaltered when the current drops abruptly to zero, and they remain unchanged for about 10 sec, finally diminishing to zero in 30 sec. The 10-sec period corresponds to the time

when the last solid CuCl is dissolved as determined by direct observation. The gradients are approximately linear as is to be expected on the basis of the theory of mass transfer (9) by natural convection, which is shown in the next section to be true for a system containing a single salt.

Natural Convection at a $\text{Cu}|\text{CuSO}_4$ Anode

The schlieren technique was applied to anodic dissolution of copper in 2N CuSO_4 , as a check on the theory of natural convection. With only one salt present, the index of refraction could be unambiguously related to the concentration. Currents in the range of 25-250 $\mu\text{a}/\text{cm}^2$ were passed and schlieren photographs taken after 30 sec, which allowed enough time for a steady state to be established. The steady-state thickness of the convection layer was found to be independent of the current density in the range investigated, in agreement with the interferometric studies of Ibl, Barrada, and Trümpler (10) on the same system.

The theory of Tobias and co-workers (9) is based on the analogy between mass transfer and heat transfer and involves the assumption that the concentration distribution in the former process is the same as the temperature distribution in the latter. This distribution is a parabolic one and thus the gradient would be linear. For CuSO_4 , the concentration is closely proportional to the increase in the index of refraction, and so the two gradients should also be proportional. Figure 8 shows that the gradient is found to be linear by direct schlieren measurement, giving direct experimental proof of this assumption.

Summary and Conclusions

The schlieren technique has been shown to be useful as a quantitative as well as qualitative tool in the study of electrode processes and has been applied to the $\text{Cu}|\text{HCl}$ anode. In this application it has given a quantitative development in time and space of the concentration gradients in the near neighborhood of the electrode. The depletion of the Cl^- ion, owing to the formation of solid CuCl , and the entrance into solution of Cu^{2+} ion have been seen and measured. By the use of cinematography, the

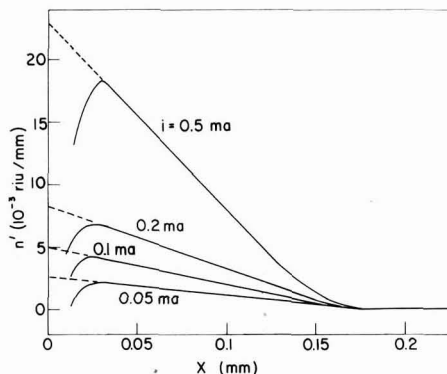


Fig. 8. Refractive index gradients near a convection controlled $\text{Cu}|\text{CuSO}_4$ anode in the steady state. For this salt, the concentration is proportional to the refractive index, and the linear relation between concentration gradient and distance from the anode is verified.

details of the convection process, including the shape and time dependence of the convection layer thickness and its relative importance under various conditions have been investigated. Finally, using the simpler system (a Cu|CuSO₄ anode), linear concentration distribution which is one of the underlying assumptions of present theories of convection has been experimentally verified.

We would like to point out the utility of the schlieren microscope as a research tool in the study of electrode phenomena. It is simple and relatively inexpensive to construct. Its adjustment for operation is not critical as are many interferometers, and thus qualitative observations are very easily obtained. Quantitative data can be obtained as close as 10⁻³ cm from an electrode without disturbing the solution in any way. Both space and time dependence of processes may be observed. By selection of the optical parameters, the sensitivity, resolving power, and field of view may be varied over wide ranges to suit various applications.

Acknowledgments

This work was supported by the Office of Ordnance Research under contract DA-11-022-ORD-939. The author is greatly indebted to Dr. L. P.

Stephenson who is primarily responsible for the design and application of this schlieren apparatus, and to Professor J. H. Bartlett for his encouragement and aid with the manuscript.

Manuscript received Dec. 11, 1957. This paper is based on a dissertation presented as partial fulfillment of the requirements for the degree of Doctor of Philosophy in Physics at the University of Illinois, Urbana, Illinois.

Any discussion of this paper will appear in a Discussion Section to be published in the June 1959 JOURNAL.

REFERENCES

1. L. Stephenson and J. H. Bartlett, *This Journal*, **101**, 571 (1954).
2. H. J. Antweiler, *Z. Elektrochem.*, **43**, 596 (1937).
3. F. H. Giles, Doctoral Dissertation, University of Illinois, Urbana, Ill. (1956).
4. R. S. Cooper, *This Journal*, **103**, 307 (1956).
5. L. P. Stephenson, Doctoral Dissertation, University of Illinois, Urbana, Ill. (1953).
6. E. Yeager, W. R. Wolfe, N. Chessin, and F. Hovorka, *This Journal*, **101**, 590 (1954).
7. J. H. Bartlett and R. S. Cooper, *ibid.*, **105**, 109 (1958).
8. K. F. Bonhoeffer and H. Gerischer, *Z. Elektrochem.*, **52**, 149 (1948).
9. C. W. Tobias, C. R. Wilke, and M. Eisenberg, *Chem. Eng. Progr.*, **49**, 663 (1953).
10. N. Abl, Y. Barrada, and G. Trümpler, *Helv. Chim. Acta*, **37**, 583 (1954).

The Electrodeposition of Iron-Molybdenum Alloys

L. O. Case and Albertine Krohn¹

Chemistry Department, University of Michigan, Ann Arbor, Michigan

ABSTRACT

A plating cell was designed to provide a method for the variable rotation of a cylindrical cathode between rubber wiper blades, since wiping the cathode greatly increased the efficiency of the process for plating iron-molybdenum alloys from a solution containing sodium molybdate, ferric chloride, and sodium pyrophosphate buffered to a pH of 8 with excess sodium bicarbonate. A complete study of the variables showed it possible to electrodeposit alloys which are bright and adherent in thicknesses of a few hundredths of a millimeter. No theoretical treatment is yet available to explain completely this type of deposition.

With increased interest in metals which have utilitarian properties at very high temperatures, molybdenum has received considerable attention because of its ready availability in this country and its valuable refractory properties (1, 2). Many attempts have been made to develop a satisfactory process for the electrodeposition of this element so that, when only surface properties were important, a coating of molybdenum could be applied. This would conserve the metal and permit one to take advantage of the structural properties of the basis metal. However, all available evidence indicates that pure molybdenum cannot be electroplated from a solvent containing oxygen in any form.

Attempts have been made by a number of investigators to plate molybdenum from aqueous solutions (3-11). None of the methods suggested pro-

duces more than a flash deposit a few microns in thickness, and there is no proof that such deposits are pure molybdenum. Organic solvents and non-aqueous systems such as liquid ammonia have failed to give molybdenum deposits (12, 13). Several moderately successful attempts to electrodeposit molybdenum from fused salt baths have been reported (14-19). The most recent of these is reported to be the first instance of the production of coherent massive electrodeposits of molybdenum (20). This process uses a melt of K₂MoCl₆ dissolved in a mixture of alkali halides, the electrolysis being carried out in an inert atmosphere.

As in the case of other metals which cannot be deposited by themselves, a number of alloys and oxides of molybdenum have been electrodeposited from aqueous solutions (21). For many years, permanent black protective and decorative coatings

¹ Present address: Chemistry Department, University of Toledo, Toledo, Ohio.

have been applied to copper, iron, and their alloys by electrodepositing hydrated molybdenum sesquioxide, $\text{Mo}_2\text{O}_5 \cdot x\text{H}_2\text{O}$, on the object and then igniting it [(22) p. 192]. Sometimes the molybdenum oxide is deposited with an alloying metal (23, 24), and colored coatings have been reported (25).

Some patents have been granted covering the electrodeposition of certain molybdenum alloys. The deposition of cobalt-molybdenum alloys (26, 27), chromium-molybdenum alloys (28), and alloys of molybdenum with cobalt, nickel, and iron (29, 30) have been patented.

A number of studies on the electrolytic production of various alloys deposited from alkaline citrate and tartrate baths have been reported (31-36). Alloys of molybdenum with iron, cobalt, nickel, copper, or zinc were obtained using a pyrophosphate bath buffered with sodium bicarbonate (37).

All of the reports mentioning iron-molybdenum alloys indicated that it is possible to electrodeposit alloys containing up to about 60% molybdenum. This is a higher molybdenum content than appears possible with other codepositing metals. However, the plating processes were inefficient and the alloys were described as being of poor quality. Because of their comparatively high molybdenum content, these alloys were selected for more intensive study. This research was undertaken in an attempt to develop an aqueous plating bath suitable for the production of these alloys, and to investigate the possibilities of increasing the efficiency of the process.

Preliminary Studies

Approximately 300 plating runs were made during the preliminary work. About 170 of the deposits were analyzed for their iron and molybdenum contents. The first experiments were carried out with a citrate solution (34), but the deposits obtained were dull, dark, and nonadherent. Attempts to modify the bath by replacing the citric acid with $\text{NaKC}_2\text{H}_3\text{O}_7$ or $\text{KHC}_2\text{H}_3\text{O}_7$ were unsatisfactory.

More promising results were obtained using a modification of the pyrophosphate bath suggested by Myers (37). The function of the sodium pyrophosphate is to form a complex with the Fe^{+++} and thus prevent the precipitation of ferric hydroxide in the alkaline solution. It has advantages over the citrates and tartrates used in other baths in that the solutions are very stable and that the pyrophosphate does not produce undesirable products during electrolysis. A commercial chelating agent, Versene Fe-3 Specific, was tried as a replacement for the pyrophosphate. The deposits obtained were about the same, but the solutions were less stable particularly at higher temperatures.

Using the pyrophosphate solution, several series of plating runs were made to determine the effects of the variables on the composition of the deposits and on the cathode current efficiency. A few runs were made using the apparatus for periodic current reversal which had been designed for another study (38). The deposits produced were of inferior quality, so the experiments were discontinued. A crude setup was used to test the effect of rotating the electrode between a pair of rubber wiper blades.

This process improved the efficiency so much that new apparatus was designed in order to permit a more thorough study with the incorporation of the wiping procedure.

Experimental

Apparatus.—The plating cell consisted of a cylindrical Lucite container with an electrolyte capacity of about 800 ml. The cell was fitted with a plastic cover to which was attached the anode holder. The cover had an opening in the center to permit insertion of the cathode and another near one side for a calomel electrode. The details of the plating cell assembly are shown in Fig. 1. For the anode, a piece of sheet platinum was rolled and slipped inside the anode holder. Several small holes were drilled near the top of the holder to permit free circulation of the plating solution.

The cathodes were cylinders of platinum or brass $1\frac{3}{4}$ in. long, $\frac{5}{8}$ in. OD, 9/16 in. ID. The plating area of such a cathode is 3.43 in.² (0.217 dm²). Plating with cylindrical anodes and cathodes results in a more symmetrical current distribution than plating on flat cathodes.

The top of the cathode holder was machined from stainless steel to give a friction fit with the cathode cylinders. The exposed portion of the holder was protected with stop-off lacquer. The lower end of the upper holder was threaded to fit the bottom holder which was made of plastic. The bottom holder was turned to precision fit the cathodes, so that, when the cylinder was slipped over the holder and the two parts tightened, the system was leak proof. An L-shaped stirrer was threaded into the bottom cathode holder.

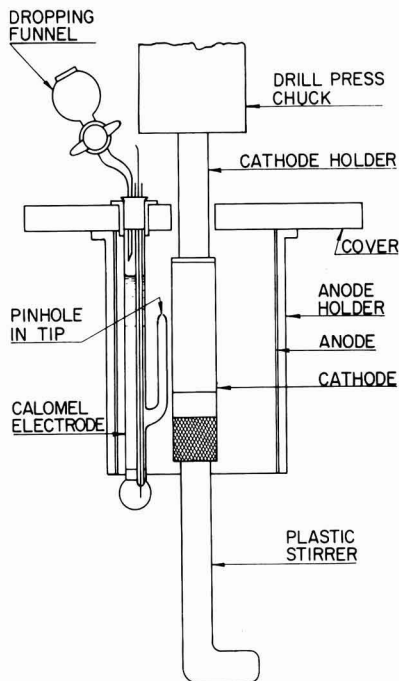


Fig. 1. Side view of plating cell assembly

A bench size drill press operated by a half-horsepower motor served as a convenient device for rotation of the cathode. Since the cathode and spindle were rotating during the plating process, a direct connection was impossible. Contact was established by means of a pool of mercury in a small hole drilled in a steel cylinder attached to the top of the spindle. A steel bar supported a piece of platinum wire which dipped into the mercury.

Provision was made for wiping the cathode during the plating run by the use of two adjustable wiper blades attached to the plating cell cover (see Fig. 2). The wiper blades were 2-in. lengths of 5 ply rubber windshield wiper which slipped into slotted plastic holders. The top of each holder was tapped to take a brass machine screw which passed through an opening in the cell cover. After adjusting the position of the wiper blades, the screws were tightened. The entire plating assembly was immersed in a constant temperature bath.

Analysis of the deposits.—Alloy deposits were washed, dried, weighed, and dissolved from the cathode in 5*N* nitric acid. They were analyzed by a colorimetric method based on the fact that both molybdenum and iron form colored compounds with mercaptoacetic acid (39-42).

Experimental Results

Unless otherwise specified, plating runs were made at 50°C with a current density of 15.6 amp/dm² (140 amp/ft²). Most plating times were 10 min. The usual composition of the bath was:

Sodium molybdate (Na ₂ MoO ₄ · 2H ₂ O)	1.0 <i>N</i>	(40 g/l)
Ferric chloride (FeCl ₃ · 6H ₂ O)	0.1 <i>N</i>	(9 g/l)
Sodium pyrophosphate (Na ₂ P ₂ O ₇ · 10H ₂ O)	0.4 <i>N</i>	(45 g/l)
Sodium bicarbonate (NaHCO ₃)	0.9 <i>N</i>	(75 g/l)

The effects of changes in the solution composition and plating conditions on the composition of the

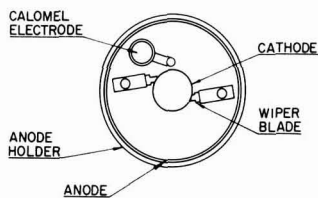


Fig. 2. Top view of plating cell

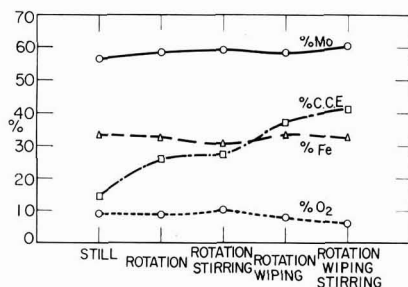


Fig. 3. Effect of rotation, stirring, and wiping

deposits and on the cathode current efficiency are summarized by the following graphs and discussion. Cathode current efficiencies were calculated on the basis of the deposition of iron from iron(III) and molybdenum from Mo(VI).

Effect of cathode rotation, stirring, and wiping.—Runs were made in a still bath; with rotation of the cathode at 1750 rpm; with rotation at the same speed with the L-shaped stirrer attached to the cathode fixture; with rotation between fixed wiper blades without the stirrer; and finally with rotation, stirring, and wiping. The efficiency of the cathode plating process is nearly tripled when rotation, stirring, and wiping are used (see Fig. 3). The wiping process aids in the removal of hydrogen bubbles and also decreases the oxide content of the deposits.

Deposits from a still bath were dull dark gray. Those made with the use of rotation without wiping had a frosty gray appearance, while those which were wiped had a bright metallic luster and did not tarnish.

Effect of the rate of cathode rotation.—Runs were made with the cathode rotating at 875, 1750, 2675, and 3500 rpm. These correspond to 143, 286, 429, and 572 ft/min. As shown in Fig. 4, the rate of cathode rotation does not affect appreciably the composition of the alloy deposits except at very high speeds when the molybdenum content increased and the oxide content decreased. At 3500 rpm the vigorous rotation threw the solution away from the top of the cathode. The deposit obtained at this rate of rotation was iridescent dark blue near the top and tended to flake off the base metal when dried. The efficiency decreased at the higher speeds also because of the tendency for the solution to be thrown away from the rotating cathode, even though the wiper blades served as baffles to some extent. The greatest efficiency was obtained at 1750 rpm, so this speed was used in all subsequent experiments.

Effect of current density.—Nine runs were made at current densities varied from 2.2 to 20.0 amp/dm² (20 to 180 amp/ft² in increments of 20 amp/ft²). The time of each plating run was adjusted so that 2100 coulombs passed during each run. At current densities below 8.9 amp/dm² (80 amp/ft²) the deposits were coarsely crystalline, the rate of growth of the nuclei exceeding the rate of nucleus formation. The molybdenum content was low and the oxide content high as shown in Fig. 5. As the current density was increased, the rate of formation of the nuclei was greater and the deposits became

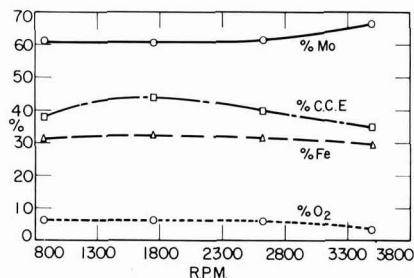


Fig. 4. Effect of the rate of cathode rotation

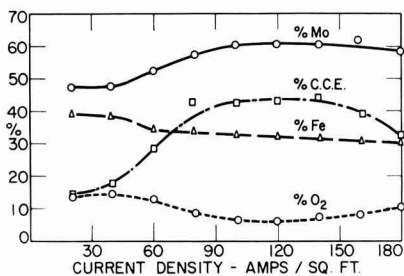


Fig. 5. Effect of current density

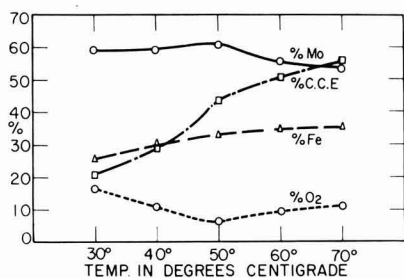


Fig. 6. Effect of temperature

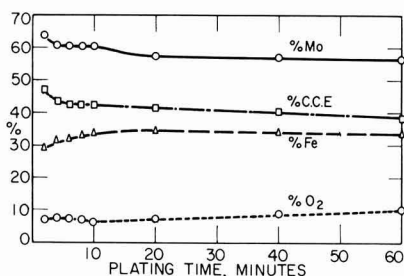


Fig. 7. Effect of length of plating time

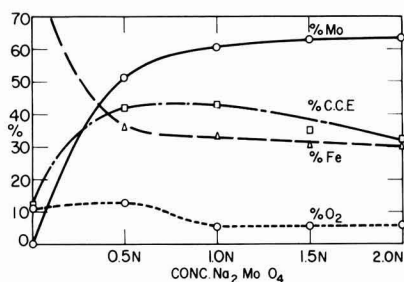


Fig. 8. Effect of Mo(VI) concentration

more fine grained. There was a decrease in the relative amount of the more noble metal (iron) since it was more rapidly depleted in the deposition zone. Current density was not critical in the range 11-20 amp/dm² (100-140 amp/ft²). The deposits were good and the process was efficient. Deposits were less bright at higher current densities and the efficiency decreased. Since the metal ions could not be discharged rapidly enough, more hydrogen was evolved instead.

Effect of temperature.—Runs were made at 30°, 40°, 50°, 60°, and 70°C. The deposits improved in appearance, becoming more smooth and bright as the deposition was carried out at higher temperatures. The efficiency of the cathode process likewise was increased. However, the percentage of iron in the alloy deposits increased at temperatures above 50°C, while the percentage of molybdenum decreased as shown in Fig. 6. In selecting an operating temperature, a choice must be made between an increase in efficiency and a decrease in the molybdenum content of the alloy. A reasonable compromise is achieved at 50°C.

Effect of the length of plating time.—Runs were made of 2- to 60-min duration. Except for very short or very long plating periods, the composition of the deposits and the current efficiency did not change significantly (Fig. 7). The deposit obtained after plating for 2 min was thin, bright, and relatively high in molybdenum content. Those obtained with 4- to 10-min plating periods were nearly identical in appearance and composition and were plated with about the same efficiency. As the length of the plating time was increased, the deposits became dull and rough and were less adherent. These experiments show that, by the present method, it is possible to electrodeposit satisfactory coatings of iron-molybdenum alloy up to about 0.01 mm in thickness.

Effect of Mo(VI) concentration.—The concentration of Mo(VI) was varied from 0.0 to 2.0N (0 to 80 g/l Na₂MoO₄·2H₂O), keeping the other bath components constant. With no Na₂MoO₄ in the plating bath, a very poor deposit was obtained. The iron plate was contaminated with considerable oxide which gave it a rough, dark appearance. Figure 8 shows that, as the concentration of Mo(VI) was increased, the molybdenum content of the deposits increased and the iron content decreased. However, the changes were not very great at concentrations above 1.0N, indicating the presence of some type of regulating mechanism which prevents the deposition of molybdenum in proportion to its concentration in the plating bath. The cathode current efficiency was greatest at 1.0N Mo(VI) and decreased at higher concentrations. All deposits were good except the one which contained no molybdenum.

Effect of Fe(III) concentration.—The concentration of Fe(III) was varied from 0.0 to 0.4N (0 to 36 g/l FeCl₃·6H₂O). To keep the iron complexed to the same extent in each solution, the amount of Na₂P₂O₇·10H₂O was correspondingly varied. The normality of Na₂P₂O₇·10H₂O used was equal to four times the normality of FeCl₃·6H₂O in each case except that without FeCl₃·6H₂O which contained the usual 0.4N pyrophosphate. Although no deposit was expected in the absence of Fe(III), a run was made in order to obtain potential measurements. Much more negative values than usual were found for the static molybdenum potentials in the solution without iron, which would seem to indicate that the Na₂P₂O₇ forms a complex with the Na₂MoO₄. This is quite likely in view of the well-known complexes of molybdate with phosphates. The compound Na(MoP₂O₇)·12H₂O has been reported (43). As the concentration of Fe(III) was increased from 0.05 to 0.4N, the iron content of the deposits increased and

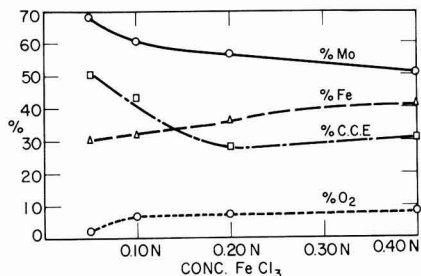


Fig. 9. Effect of Fe(III) concentration

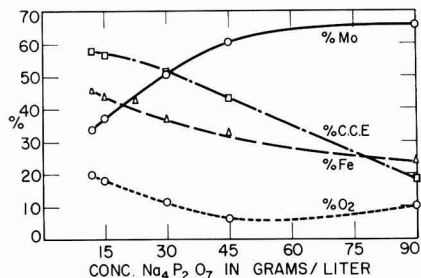


Fig. 10. Effect of sodium pyrophosphate concentration

the molybdenum content decreased (see Fig. 9). The cathode current efficiency decreased with increased Fe(III) concentration.

Effect of sodium pyrophosphate concentration.—The concentration of Na₄P₂O₇ · 10 H₂O was varied from 12 g/l to 90 g/l (approximately 0.1 to 0.8N). According to the literature, Fe(III) forms three complexes with pyrophosphate depending on their relative concentrations (44). With 4 equivalents of Fe(III) to 3 equivalents of pyrophosphate, a precipitate of Fe₃(P₂O₇)₃ is obtained. This precipitate is soluble in the presence of excess pyrophosphate to form Fe(P₂O₇)⁻ and Fe(P₂O₇)₂⁻². One run was made with just enough pyrophosphate to dissolve the precipitate Fe₃(P₂O₇)₃. The solution was dark red, indicating the probable presence of some dispersed Fe(OH)₃ since the amount of pyrophosphate present was insufficient to keep all the iron(III) in solution. The deposit obtained from this solution was low in molybdenum content and high in iron and oxygen. As the pyrophosphate content of the solutions was increased, the color changed to orange-yellow, yellow-green, and finally to blue-green. The percentage of iron in the deposits decreased as the iron was more tightly bound by the excess pyrophosphate. The efficiency of the plating process decreased markedly, as seen in Fig. 10. The static potentials of both molybdenum and iron became more negative as the concentration of pyrophosphate was increased. This supplies additional evidence to indicate that the pyrophosphate forms a complex with molybdenum as well as with iron. The alloy deposits were poor at the lower pyrophosphate concentrations.

Effect of pH.—Five runs were made over the pH range 7-10. Deposits were not obtained in acid solutions. For the first run, the NaHCO₃ was replaced by an equivalent amount of NaCl to main-

tain constant salt concentration. A few drops of dilute HCl were added to bring the pH to 7. The usual plating bath maintained a pH of 8. Higher pH values were achieved by the replacement of part or all of the NaHCO₃ by Na₂CO₃. A very poor deposit was formed from the neutral plating solution. As Fig. 11 shows, the alloy was low in molybdenum and high in iron and oxygen. The current efficiency increased up to pH 9.3. At pH 9.9 some Fe(OH)₃ was suspended colloiddally in the bath, since the pyrophosphate was unable to keep the iron completely complexed at this high pH. The deposit was exceptionally smooth and bright because of the colloid in the bath.

Reproducibility.—Four identical runs were made, keeping all factors as nearly constant as possible, in order to determine the extent to which the potential measurements and the composition of the deposits were reproducible. The composition of the deposits was found to be reproducible within 0.4%, which was about the degree of accuracy attainable with the analytical method used. The four deposits obtained were nearly identical in appearance. The static molybdenum potentials were reproducible within 3 mv. The static iron potentials and the dynamic alloy potentials were not significant either through lack of reversibility or duplicability.

Stability.—A standard 800-ml batch of plating solution was prepared and a series of 30 consecutive 10-min runs was made from the original solution. There was no evidence of solution breakdown during this series of experiments, showing that the system is very stable.

A 3200-ml batch of standard solution was prepared. One run was made using 800 ml of the freshly prepared solution, and additional runs were made on 800 ml portions of the remainder 1 day, 26 days, and 80 days later. There was no aging effect in this plating solution during the 80-day interval. The bath gave deposits of essentially constant composition with the same efficiency whether from fresh or aged solution.

Examination of the deposits.—The usual iron-molybdenum alloy deposits were bright, silvery gray and did not tarnish visibly in laboratory air during periods of four months. A typical deposit is shown in Fig. 12.

The alloys were readily soluble in 5N HNO₃, but did not dissolve in dilute H₂SO₄, H₂SO₄ plus H₃PO₄, hot 6N HCl, hot or cold dilute HClO₄, or cold concentrated HClO₄. They were slightly soluble in hot

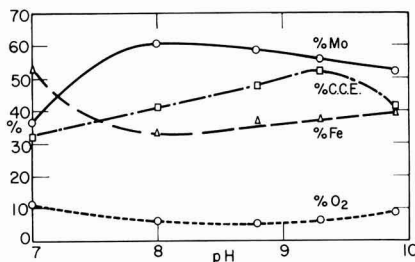


Fig. 11. Effect of pH

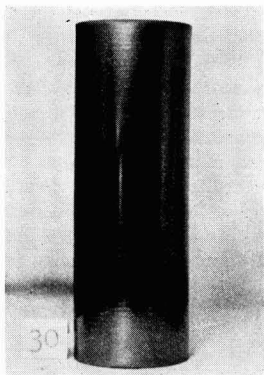


Fig. 12. A typical iron-molybdenum deposit

concentrated H_2SO_4 . The plates appear inert toward alkaline solutions.

The deposits adhere well to the cylindrical platinum cathodes as long as the thickness is not greater than a few hundredths of a millimeter. They were found to be hard and brittle.

Microscopic examination of the deposits showed that they contain numerous cracks, as shown in Fig. 13. This is a photomicrograph of a typical iron-molybdenum alloy as plated on a brass tube and then covered with copper electrodeposited from a cyanide bath. There is no evidence of a banded structure, nor are there any large occlusions in the deposits. Neither higher magnifications up to 1200 X nor the action of etching agents gave evidence of more than a single phase.

This suggests the probable formation of an intermetallic compound or a solid solution. The epsilon phase in the iron-molybdenum system (Fe_3Mo_5) is well-defined, but the composition of the deposits is more indicative of the sigma phase which has the formula $FeMo$ [(45) p. 1210]. $FeMo$ is thermally stable above $1180^\circ C$, and therefore would be metastable under the plating conditions used. The deposits were so highly strained that attempts to identify their structures by x-ray analysis resulted in bands which were too diffuse to give any definite information. The strained condition may be due to a metastable solid solution, although hydrogen absorption may well be another factor. While not a part of the present study, an investigation of the



Fig. 13. Photomicrograph of a typical iron-molybdenum deposit. Magnification 500X before reduction for publication.

possible effects of heat treatment in relieving these strains would be desirable. The place of oxygen in this system is not known.

Discussion

It is now realized that even single metal deposition is a complicated process for which no complete kinetic theory is yet available (46-48). However, molybdenum alloy deposition presents additional problems in any attempt to explain the mechanism of the cathodic process. The formation of these alloys is one example of a more general phenomenon whereby certain elements which cannot be deposited by themselves from aqueous solutions can be co-deposited with any one of a number of other metals. Iron, cobalt, and nickel are most effective in this respect, although copper, zinc, and sometimes manganese, tin, or chromium can be the codepositing metal.

In general, metals cannot be deposited from aqueous solutions if the equilibrium of the deposition reaction lies so far on the ionic side that the electrode potential is more negative than the hydrogen discharge potential. According to Lyons (49) this occurs in the case of molybdenum because the molybdate ion is stabilized by inner orbital hybridization; that is, the $4d$ orbitals are hybridized with $5s$ and p orbitals. Apparently the energy required to break such hybridization exceeds that required for the cathodic discharge of hydrogen.

There is then, superimposed on the complex mechanism of direct metal deposition by cathodic reduction, a different problem in molybdenum alloy deposition, namely, that of induced codeposition. These questions then arise: (a) if molybdenum cannot be electrodeposited by itself from aqueous solutions, why does it deposit with certain alloying metals; (b) why is the molybdenum content of the alloys limited; and (c) why do the deposits always contain oxygen? Following are some of the theories proposed to answer these questions.

Proposed Mechanisms for Molybdenum Alloy Plating

Alternate layer theory.—A mechanism proposed for the electrolytic reduction of aqueous tungstate solutions (50) might apply to the case of aqueous molybdate solutions also. According to this theory, the deposition of the alloying metal (iron) proceeds until the cathode is covered with a thin layer of iron which then reduces the activation energy for the deposition of molybdenum to occur. This reaction proceeds until the cathode surface is covered with a layer of molybdenum. Then the deposition of molybdenum ceases and the cycle is repeated.

This hypothesis fails to explain why the molybdenum alloy deposits contain oxygen, nor does it necessarily account for the laminar structure frequently encountered. Laminations also occur in single metal deposition and are not necessarily indicative of the deposition of alternate layers of two metals. Also, there is no apparent reason why only molybdenum should deposit on the initial iron layer.

Oxide film theory.—The oxide film theory (51) has been postulated as a mechanism for tungsten

alloy plating, but could include the similar phenomenon involving molybdenum. This theory proposes the deposition of a film of partly reduced tungstate (or molybdate) on the cathode and subsequent catalytic reduction of this film by hydrogen in the presence of freshly deposited iron, cobalt, or nickel.

This hypothesis explains the presence of oxides in the deposits on the basis of incomplete reduction and points out that the reason the iron-group metals are so effective in this type of deposition is because they are good hydrogenation catalysts. It does not explain why the molybdenum content of the alloys is limited.

Hydroxide film theory.—Myers (37) proposes that a mixed film of the hydrated oxides of molybdenum (III) and the carrier metal forms at the cathode during electrolysis. The presence of the carrier metal hydroxide is necessary to alter the permeability of the film so that the molybdate ions are able to penetrate it and to be discharged on the cathode surface. At the same time, the film insulates the nascent molybdenum atoms from reoxidation by the chemical action of the bath. A similar film is proposed for the reduction of hexavalent chromium at a rotated platinum cathode (52).

There is considerable experimental evidence to support this theory. First, it is important to note that no molybdenum alloy plate forms unless hydrogen is evolved. This is the same as saying that no plate forms until hydroxide ions are generated in the cathode film. (This also could be used as evidence for catalytic reduction by previously deposited hydrogen atoms.) If the solution is made acid, or if sufficient sodium cyanide is added to the bath so that the precipitation of the carrier metal hydroxide is prevented, then no alloy is deposited. By using extreme operating conditions of high temperature and very high current density, it is possible to form visible coatings of $\text{Fe}(\text{OH})_3$ and $\text{Mo}(\text{OH})_3$ around the cathode [(37), (53), pp. 160-165]. The presence of oxides of molybdenum and the carrier metal in the deposits is said to result from the occlusion of dehydrated portions of the diaphragm.

If such a film is present, it evidently is very thin and adherent since it is not destroyed by cathode wiping. The wiping process appears to be simply a means for the removal of accumulated hydrogen bubbles from the cathode surface, thus facilitating contact of the solution with the film.

This theory is capable of supplying explanations for many of the experimental results previously described. Figure 5 shows that the molybdenum content of the deposits increased initially with increased current density. The pH of the cathode film would be increased with an increase in current density, permitting the formation of a more effective hydroxide film, and an increase in efficiency and the relative amount of molybdenum deposited.

The solubility of such a film would increase at higher temperatures, which would result in a decrease in the molybdenum content of the deposits. This is borne out by the results given in Fig. 6.

The film apparently operates best when it is freshly formed (see Fig. 7). When the plating process is carried on for long periods of time, some

film breakdown is suggested by the decreased molybdenum content and increased oxide content of the deposits.

As was pointed out in the discussion of Fig. 9, the molybdenum content of the deposits did not increase in proportion to the increase in concentration of molybdenum salts in the bath. This can be explained by assuming that too great an amount of $\text{Mo}(\text{OH})_3$ in the film makes it less permeable to molybdate ions. Thus, the depositing ratio of molybdenum to carrier metal reaches a limiting value.

Changes in the sodium pyrophosphate concentration would be expected to affect the ease of film formation because of changes in the degree of complex formation with $\text{Fe}(\text{III})$. Figure 10 shows that the efficiency of the deposition process decreased with increased pyrophosphate concentration, which could be attributed to the increased difficulty of film formation. As the $\text{Fe}(\text{OH})_3$ concentration in the film decreased, the iron content of the deposits decreased and the molybdenum content increased. However, the proportion of molybdenum in the deposits again seems to approach a limiting value.

The pH of the plating solution is also an important factor in film formation, but it should be pointed out that, because of the hydrogen discharge, the pH in the vicinity of the cathode will be higher than that in the body of the solution. When deposition was carried out from a neutral solution, the hydroxide film was less readily formed, because the only source of OH^- was that resulting from hydrogen evolution. As the pH of the solution was increased, the film was formed more readily and the efficiency of the plating process was increased (Fig. 11). However, the molybdenum content of the deposits decreased and the iron content increased as the pH was increased above 8. This may be attributed to changes in the stability of the pyrophosphate complexes with increased pH. As was previously mentioned, $\text{Fe}(\text{P}_2\text{O}_7)_2^{4-}$ is not sufficiently stable to prevent the precipitation of $\text{Fe}(\text{OH})_3$ at a pH of 9.9.

Although, as has been shown in the preceding paragraphs, the hydroxide film theory can be used to explain many of the experimental data, it does not explain why the iron-group metals are the most effective in giving the film the necessary permeability.

One objection to the theory is that, if molybdenum deposition is prevented by the formation of a film containing only hydrated molybdenum oxide, then deposition at a dropping mercury electrode would be expected because such a film could not form. However, it has been reported that, while it is possible to form small amounts of molybdenum amalgam by electrolysis of an acidic molybdate solution, alkaline solutions of molybdate are not reduced at a dropping mercury electrode (54-56).

Induced codeposition theory.—A new theory has been proposed by Brenner (57) in which he refers to the phenomenon of molybdenum alloy deposition as an example of "induced codeposition." He refers to metals which cannot be deposited by themselves as "reluctant" metals, and the metals which aid in bringing about codeposition as "inducing" metals.

This theory proposes that the reluctant metals are actually more noble than the inducing metals and that their inability to deposit individually is due not to a highly negative electrode potential, but to a lack of electrochemical reactivity of their ions with electrons at the cathode. This is somewhat difficult to prove since the reversible potentials of the reluctant metals cannot be measured because these metals do not establish electrochemical equilibrium with solutions of their salts. If it is true that molybdenum is inherently more noble than iron, then the potential of the electrodeposited alloy would be expected to be more noble than that of iron. This was not the case, since the static potential of iron in the bath was about -0.2 v, while that of the alloys was -0.5 v.

To explain induced codeposition, Brenner postulates that the deposition of the inducing metal brings about an activation of the potentially depositable reluctant ion. He suggests that this is the result of an interaction whereby the energy of polarization of the inducing metal at the moment of deposition is transferred to the ions of the reluctant metal instead of being liberated as heat. If the reluctant ion is thus activated, it takes on its "normal" electrode potential and becomes capable of taking on electrons from the cathode, and the transferred energy then appears as heat.

It is further postulated that the energy of polarization is transferred as a unit and can aid in the acceptance of only one electron by the reluctant ion. This postulate explains the limitation of the reluctant metal content of the deposits by reasoning that the maximum content of reluctant metal in the deposit should approach a limit of one equivalent to each equivalent of inducing metal. If such calculations are made on the basis of Mo(VI) and Fe(III), then the theoretical limit of molybdenum in the electrodeposited alloys should be 46% by weight. This is considerably less than the percentage of molybdenum actually found in most of the deposits. The theoretical limit calculated on the basis of Mo(III) and Fe(III) gives a more reasonable limit of 63% molybdenum. Therefore, one might assume hydrogen reduction of Mo(VI) to Mo(III) followed by electrochemical reduction to the metal. An alternate assumption would be that hydrogen also acts as an inducing element. Still another point to consider is that if oxygen is essentially tied up with the molybdenum, then all of the molybdenum is not in the metallic state and thus has not been deposited. Calculations show that each per cent of oxygen ties

up approximately 4% of molybdenum. Thus a deposit containing 60% Mo, 34% Fe, and 6% O₂ would contain only 36% metallic molybdenum assuming that all the oxygen is combined with molybdenum.

This theory fails to explain why the iron-group metals are most effective in bringing about induced codeposition and why deposition occurs more efficiently at elevated temperatures under which condition polarization is lowest. It does not account for the oxide content of the deposits.

Summary and Conclusions

This summary of the experimental results is based on the fact that the primary objective of this research was to plate good quality iron-molybdenum alloys containing the highest possible percentage of molybdenum with the greatest possible current efficiency. Unfortunately, the conditions for attaining these objectives are not always the same, as shown by Table I. The first set of values for the variables lists those which favor the deposition of alloys which are high in molybdenum content, and the second set gives those which favor high efficiency. The third set of values lists those selected for practical operation of the plating system.

Deposits on a 21.7 cm² electrode using the solution composition and conditions indicated in the last column of Table I weigh about 0.17 g, contain about 61% Mo, 33% Fe, and 6% O₂, and are plated with an efficiency of about 44%. They are smooth, bright, and adhere well to the basis metal.

Of the several mechanisms proposed for the electrodeposition of iron-molybdenum alloys, the hydroxide film theory provides reasonable explanations for most of the experimental data. None of the postulated mechanisms is capable of a complete explanation of all the phenomena connected with this and other examples of induced codeposition. The final explanation must account for the presence in the deposits of substantial amounts of nonmetallic material, presumably oxygen.

The bridge complex mechanism for electrodeposition suggested by Lyons (49) might be extended to include this type of deposition, but to date there is insufficient knowledge of the structural nature of molybdenum ions in aqueous media to permit postulation of such a mechanism.

Acknowledgments

The preliminary part of this investigation was supported by the Gerity-Michigan Corporation through the Research Foundation of the University

Table I. Optimum solution composition and plating conditions using cathode stirring and wiping

Variable	Value for highest % Mo	Value for greatest % C.C.E.	Value for practical operation
Rate of rotation	3500 rpm	1750 rpm	1750 rpm
Current density	160 amp/ft ²	140 amp/ft ²	140 amp/ft ²
Temperature	50°C	70°C	50°C
Length of plating time	2 min	2 min	10 min
Mo(VI) Conc.	2.0N (80 g/l)	1.0N (40 g/l)	1.0N (40 g/l)
Fe(III) Conc.	0.05N (4.5 g/l)	0.05N (4.5 g/l)	0.1N (9 g/l)
Sodium pyrophosphate conc.	0.8N (90 g/l)	0.1N (12 g/l)	0.4N (45 g/l)
pH	8.0	9.3	8.0

of Toledo, with Dr. Nelson W. Hovey as project director. The authors wish to thank Dr. M. J. Sinnott of the Department of Chemical and Metallurgical Engineering of the University of Michigan for his assistance in the metallographic examination of the deposits, and the Climax Molybdenum Company for furnishing information on molybdenum and samples of molybdenum and molybdenum compounds.

Manuscript received June 20, 1957. This paper was prepared for delivery at the Washington Meeting, May 12-16, 1957. It is abstracted from a thesis presented by Albertine Krohn to the University of Michigan in partial fulfillment of the requirements for the degree of Doctor of Philosophy.

Any discussion of this paper will appear in a Discussion Section to be published in the June 1959 JOURNAL.

REFERENCES

- C. A. Hampel, Editor, "Rare Metals Handbook," Reinhold Publishing Co., New York (1954).
- J. J. Harwood, *Prod. Eng.*, **23**, 121 (1952).
- P. P. Belyaev and A. I. Lipovetskaya, *Korroziya i Bor'ba s Nei*, **6**, No. 2, 47 (1940).
- C. G. Fink and C. H. Eldridge, Canadian Pat. 274,429, Oct. 4, 1927.
- H. Krause, *Feinmech. u. Präzision*, **41**, 106 (1933).
- M. J. Ksycki and L. F. Yntema, *J. (and Trans.) Electrochem. Soc.*, **96**, 48 (1949).
- A. S. Minin, Russian Pat. 59,863, April 30, 1941.
- K. A. Paul, Russian Pat. 53,756, Aug. 31, 1938.
- E. Pokorný and K. Schneider (to I. G. Farbinend), German Pat. 582,528, May 22, 1934.
- W. P. Price and O. W. Brown, *Trans. Electrochem. Soc.*, **70**, 423 (1936).
- L. F. Yntema, *J. Am. Chem. Soc.*, **54**, 3775 (1932).
- H. S. Booth and M. Merlub-Sobel, *J. Phys. Chem.*, **35**, 3303 (1931).
- A. Brenner, *Record Chem. Progr. (Kresge-Hooker Sci. Lib.)*, **16**, 241 (1955).
- L. Andrieux, *Compt. rend.*, **184**, 91 (1927).
- J. W. Beckman, U. S. Pat. 973,336, Oct. 18, 1910.
- T. R. Forlund, U. S. Pat. 1,305,350, June 3, 1919.
- G. Gin, *Trans. Electrochem. Soc.*, **12**, 411 (1907).
- H. Hartmann and U. Conrad, *Z. anorg. u. allgem. Chem.*, **233**, 313 (1937).
- A. Kratky and W. Bruckner, German Pat. 263,301, April 19, 1911.
- S. Senderoff and A. Brenner, *This Journal*, **101**, 16 (1954); U. S. Pat. 2,715,093, Aug. 9, 1955.
- F. W. Salt, *Murex, Ltd., Rev.*, **1** (9), 201 (1951).
- D. H. Killeffer and A. Linz, "Molybdenum Compounds," Interscience Publishers, New York (1952).
- R. A. Hoffman and R. O. Hull, *Proc. Am. Electroplaters' Soc.*, June 1939, 45.
- R. A. Hoffman (to du Pont), U. S. Pat. 2,380,044, July 10, 1945.
- E. W. Schweikher (to du Pont), U. S. Pat. 2,351,639, June 20, 1944.
- A. Brenner and P. S. Burkhead, U. S. Pat. 2,653,127, Sept. 22, 1953.
- L. F. Yntema, U. S. Pat. 2,428,404, Oct. 7, 1947.
- C. C. Ma (to Westinghouse Electric Corp.), U. S. Pat. 2,516,227, July 25, 1950.
- M. L. Holt and H. J. Seim, U. S. Pat. 2,599,178, June 3, 1952.
- L. F. Yntema and M. J. Ksycki, U. S. Pat. 2,499,807, March 7, 1950.
- I. N. Frantsevich, T. F. Frantsevich-Zabludovskaya, and E. H. Zhelvis, *J. Appl. Chem. U.S.S.R.*, **25**, 387 (1952) (Engl. Trans.); *Zhur. Priklad. Khim.*, **25**, 350 (1952).
- T. F. Frantsevich-Zabludovskaya, *J. Appl. Chem. U.S.S.R.*, **25**, 1369 (1952) (Engl. Trans.); *Zhur. Priklad. Khim.*, **25**, 1314 (1952).
- T. F. Frantsevich-Zabludovskaya, I. N. Frantsevich, and K. D. Modylevskaya, *Zhur. Priklad. Khim.*, **27**, 413 (1954).
- H. J. Seim and M. L. Holt, *J. (and Trans.) Electrochem. Soc.*, **96**, 205 (1949).
- R. F. McElwee and M. L. Holt, *This Journal*, **99**, 48 (1952).
- D. W. Ernst, R. F. Amlie, and M. L. Holt, *ibid.*, **102**, 461 (1955).
- H. S. Myers, "The Electrodeposition of Molybdenum," unpublished Ph.D. thesis, Columbia University (1941).
- N. W. Hovey, J. L. Griffin, and A. Krohn, *This Journal*, **102**, 470 (1955).
- E. Lyons, *J. Am. Chem. Soc.*, **49**, 1916 (1927).
- H. W. Swank and M. G. Mellon, *Ind. Eng. Chem., Anal. Ed.*, **10**, 7 (1938).
- J. H. Hamence, *Analyst*, **65**, 152 (1940).
- F. Will, III, and J. H. Yoe, *Anal. Chem.*, **25**, 1363 (1953).
- J. W. Mellor, "A Comprehensive Treatise on Inorganic and Theoretical Chemistry," Vol. XI, 671, Longman's Green & Co., London (1930).
- L. B. Rogers and C. A. Reynolds, *J. Am. Chem. Soc.*, **71**, 2081 (1949).
- T. Lyman, Editor, "Metals Handbook," American Society for Metals, Cleveland (1948).
- J. O. Bockris, Editor, "Modern Aspects of Electrochemistry," Butterworth Scientific Publications, London (1954).
- H. Fischer, "Elektrolytische Abscheidung und Elektrokristallisation von Metallen," Springer-Verlag, Berlin (1954).
- A. G. Gray, Editor, "Modern Electroplating," John Wiley & Sons, Inc., New York (1953).
- E. H. Lyons, Jr., *This Journal*, **101**, 363 (1954).
- M. L. Holt and L. E. Vaaler, *ibid.*, **94**, 50 (1948).
- W. E. Clark and M. H. Lietzke, *ibid.*, **99**, 245 (1952).
- I. M. Kolthoff and A. M. Shams El Din, *J. Phys. Chem.*, **60**, 1564 (1956).
- E. F. Smith, "Electro-analysis," 5th ed., Blakiston, Philadelphia (1911).
- L. J. Merrill and A. S. Russell, *J. Chem. Soc.*, **1929**, 2389.
- R. Holtje and R. Geyer, *Z. anorg. u. allgem. Chem.*, **246**, 258 (1941).
- Y. P. Hokhshtein, *J. Gen. Chem. U.S.S.R.*, **10**, 1752 (1940).
- A. Brenner, "A Theory of the Induced Codeposition of Metals," Private communication (1955).

Isolation of the Diffusion Layer at an Electrode and the Determination of Concentration Polarization

Theodore Yannakopoulos¹ and Abner Brenner

National Bureau of Standards, Washington, D. C.

ABSTRACT

A method has been developed for sampling the electrolyte (concentration C_1) that exists during electrolysis at the interface of electrode electrolyte. Copper was electrodeposited from sulfate baths (concentration C_2) on to the outside surface of a hollow, microporous metal cylinder, and electrolyte was slowly drawn into the interior which contained an organic liquid immiscible with water. The electrolyte being less dense rose to the surface of the organic liquid and was collected.

The difference, $C_2 - C_1 = \Delta C_u$, was somewhat greater than theoretical. Also, ΔC_u was larger for baths of higher copper content.

From the values of C_1 , the Nernst concentration polarization was calculated and shown to be about 10 mv in ordinary plating operations and hence is not significant.

A knowledge of the concentrations of ions in the vicinity of an electrode is necessary for a clear understanding of the mechanism of electrochemical processes. The concentrations of metal-containing ions affect various phenomena, such as polarization, the structure of electrodeposits, and the composition of electrodeposited alloys. The authors were particularly interested in the relation between polarization and the concentrations existing at the interface of cathode and electrolyte. There has been a considerable amount of speculation about the magnitude of concentration polarization. It has not been measured with certainty, because the methods that have been used were indirect and involved unproved assumptions.

The most direct method for determining concentration polarization would be to measure the metal ion concentration existing at the interface of the electrode and the solution and apply Nernst's formula to the data. Although several methods have been proposed for measuring concentrations at the interface, each one has certain disadvantages. A new method for isolating the interfacial solution has been developed and was applied to the study of the concentration polarization that occurs during electrolysis of copper sulfate solutions.

Methods of Measuring the Concentrations at the Electrode-Solution Interface

Two general methods have been used for determining the concentrations that exist at the electrode-solution interface: optical and sampling techniques. The optical method was first applied to the measurement of the composition of the cathode diffusion layer by Samarcev (1) who used schlieren interferometry to determine the concentration profile of copper ion in a diffusion layer formed during electrolysis of a copper sulfate solution streaming between horizontal electrodes. The same general

method was later used by Ibl and co-workers (2) and by Lin and co-workers (3). Ibl determined the concentration profile and the thickness of the diffusion layer on vertical cathodes under conditions of natural convection.

The optical method has the advantages over sampling techniques of being very sensitive and of not disturbing the diffusion layer. It has the disadvantage of being nonspecific, since it depends on a shift in the index of refraction. Hence, the optical method cannot be used to determine the concentrations of several different solutes present in one solution. Another difficulty with the method is that at high current densities large differences in the density of the diffusion layer occur and cause the diffraction bands to become diffuse. Also, the optical method cannot be used readily with deeply colored solutions such as a chromium plating bath.

Sampling techniques include the drainage, pinhole, and freezing methods. The drainage method consists of the quick removal of the electrode from the bath while the current is still flowing. The solution is allowed to drain from the vertical electrode for several seconds, and the remaining solution is removed with a squeegee and collected. It is a crude method, but gives a fair indication of the concentrations existing at the electrode solution interface. This method has been used by Brenner (4) for determining the concentrations at the cathode in several solutions and by Brenner and Wranglen (5) for measuring the pH at the cathode-solution interface of nickel baths.

In the pinhole method developed by Graham, Heiman, and Read (6) the diffusion layer is sampled by withdrawing it through a capillary tube cemented on the back-side of the cathode over a hole. The sampling rate was about 7 ml/hr through a capillary having an inside diameter of 1 mm. This corresponds to a rate of flow of about 12 cm/min

¹ Present address: University of Athens, Athens, Greece.

normal to the electrode. Since the diffusion layer in a conventional plating bath is only about 0.3 mm thick and requires about 1 min to reach equilibrium with respect to concentration, it is evident that this rate of sampling is too great. The concentration changes observed by Graham, Heiman, and Read were only about one-tenth of those observed by Brenner (4). This indicates that a large proportion of the sample of Graham, Heiman, and Read probably came from the body of the bath.

The freezing method developed by Brenner (4) involves deposition on the outer surface of a hollow cylindrical electrode. At the moment that the current is cut off, a slurry of partially frozen isopentane is poured into the cylinder causing the diffusion layer to be frozen on the cylinder. This layer is turned off in increments on a lathe and each one analyzed. The freezing method permits the measurement of both the concentration profile and the thickness of the diffusion layer. Difficulties with the method are the collection of frost during the turning operation, the occasional poor adhesion of the frozen layer to the cylinder, and the low eutectic temperature of some solutions.

Experimental

A new method of sampling the diffusion layer has been developed which involves the use of a sheet of microporous metal to form part or the entire wall of a hollow electrode. The method will be referred to as the porous-electrode method. The electrochemical reaction takes place on the outer surface of the microporous metal, and the solution existing at the interface of the electrode and the bath is slowly withdrawn into the interior of the hollow electrode and collected. The pores of the microporous metal were about 5μ in diameter and the voids amounted to about one-half the volume of the metal.

The use of a hollow, porous electrode for separating the reaction product of an electrolysis from the bulk of the solution is not new. It was mentioned by Knobel (7). Also some patents (8, 9) have been issued on the subject. The most important work was that carried out for the National Carbon Company by Heise (10), Janes (11), and Winslow (12). All of these prior studies of porous electrodes have dealt with the use of porous graphite. In the studies of the National Carbon Company, the aim was to obtain a high yield of product, and therefore the solution at the interface was withdrawn into the interior of the cell rapidly enough to accomplish this purpose.

The technique described in this paper is an improvement over the use of graphite electrodes for the study of diffusion layers in that microporous metal has a much finer porosity than graphite and, because of its greater strength, permits it to be fashioned into vessels with much thinner walls. Some further improvements in the technique are described in a later paragraph. The rate of sampling used in our experiments was about one-tenth of that used in the experiments of the National Carbon Company. A low rate of flow was necessary to prevent inclusion of solution from the body of the bath.

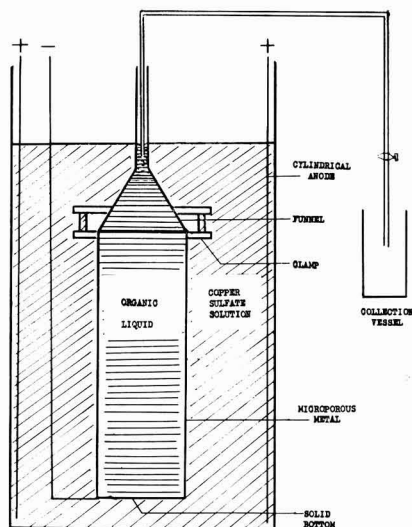


Fig. 1. Schematic diagram of hollow cylindrical cathode of microporous stainless steel and auxiliary equipment used for sampling the diffusion layer formed in the electrolysis of copper sulfate solution.

The hollow electrode vessel may take several shapes. For example, it may consist of a plane sheet of microporous metal attached to the mouth of a funnel. In the experiments described here, the electrode consisted of a vertical cylinder of microporous stainless steel, with a solid bottom, shown schematically in Fig. 1. The cylinder was 15 cm in length and 5 cm in diameter. The wall thickness was 0.07 cm. An inverted glass funnel was clamped to the top of the cylinder by two rings, the lower one of which was rigidly attached to the cylinder by a resin cement. The purpose of the funnel was to facilitate the collection of the sample which was drawn into the interior of the vessel at the rate of about 0.25 ml/min.

Two problems were encountered in the use of the vertical cylinder: (a) attaining a uniform hydrostatic pressure along the height of the cylinder, and (b) holding the solution inside the cylinder to a small volume so that a sample would not be mixed with part of a preceding one.

Since the hydrostatic pressure varied along the length of the vertical, cylindrical electrode and was greatest at the bottom, the tendency was for solution from the bath to be withdrawn into the cylinder more rapidly through the bottom walls. Various means were tried for obtaining a uniform hydrostatic pressure along the vertical length of the wall. The problem was solved by filling the interior of the cell with an organic liquid, immiscible with water, which had the same density as the body of the bath. In this manner the hydrostatic pressure was made equal on the inside and outside of the cylinder along its entire length, and a uniform flow of solution through the walls of the cylinder was obtained by reducing the pressure on the interior.

The use of the immiscible liquid had a further advantage in that it caused the less dense solution

collected at the cathode-solution interface to rise rapidly to the surface where it could be collected. Since the interior of the electrode was completely filled with the organic solvent at the start of the electrolysis, it also solved the problem of lessening the dilution of the sample with extraneous solution.

Porosity and Wall Thickness of the Electrode

In preliminary experiments, electrodes of different porosity were tried. The electrode with the smallest pores was the easiest to manipulate and seemed to give a more accurate sampling of the diffusion layer.

The porosity of the electrode was not uniform along its length. However, the uniformity of flow through the wall was considerably improved by pumping a suspension of alumina through the cylinder. Resistance to flow was increased about tenfold. This was desirable, since the effect of small differences in the hydrostatic pressure between the inside and outside of the electrode was diminished.

A thin electrode wall was desirable. The interstices of the wall were filled with plating bath at the beginning of the experiment, and the plating solution in the wall mixed with the sample of the diffusion layer as it passed through the wall. Consequently, the sampling had to be continued until all the bath initially in the wall had been drawn through. The thicker the wall, the longer was the time required for obtaining a representative sample of the diffusion layer. The thinnest wall commercially available was slightly less than 1 mm in thickness. Still thinner walls would be desirable.

Procedure

The first step in an experiment consisted in filling the pores of the cylinder with a suspension of alumina as mentioned previously. The excess was removed from the surface of the electrode by washing with a stream of water. The electrode was then immersed in a vessel of the plating solution in order to fill the pores. The interior of the electrode was next filled with a mixture of chloroform and paraffin oil having the same density as that of the bath. The organic liquid was slowly poured into the cylinder while the latter was slowly lowered into the bath at such a rate that the height of the liquids on the inside and outside of the cylinder were about the same. The siphon, also filled with organic liquid, was next attached to the inverted funnel.

After the electrolysis was started, the flow through the siphon was regulated with a stopcock to the desired rate, usually about 0.25 ml/min. At first a few milliliters of organic liquid was delivered, but soon the siphon which was of small diameter became filled with the aqueous solution and delivery of the latter began. A sampling rate of 0.25 ml/min was equivalent to a displacement of the interface layer of about 4×10^{-3} cm/sec. This calculation is based on an area of pores of about 1 dm². It is believed that this rate of movement is too low to affect significantly the steady-state concentrations in the diffusion layer.

The electrolysis usually lasted about 1.5 to 2 hr, during which time 15 to 30 ml of solution was obtained, depending on the sampling rate. The first

solution delivered contained some of the solution which was initially in the porous walls of the electrode. Consequently, the concentration of each succeeding sample of solution diminished and approached either a constant value or a flat minimum which was taken as the concentration of the solute existing at the cathode-solution interface.

Copper sulfate solutions ranging in concentration from 0.25 to 0.94M were used. No additions, such as sulfuric acid, were made to the solution, as it was desired to keep the composition of the bath simple so that the data could be more easily compared with diffusion theory. The plating was done at about 25°C without stirring. The samples were analyzed for copper by the iodide method.

Results

Variation of copper content of successive samples.

—The decrease in the copper content of successive samples mentioned in the previous section is illustrated in Fig. 2. This datum was taken before the technique of plugging the pores of the cylinder walls with alumina was developed. With the latter technique the upturn of the curve at the right was not pronounced. The cause of the increase in the copper content of successive samples with period of plating is not definitely known, but it is believed to be caused by the covering over of the small pores on the outer surface of the cylinder with the copper deposit. This caused a larger proportion of the sample to be drawn into the cylinder through a relatively small number of larger pores, with the result that the velocity of flow of the diffusion layer at these points was greatly increased. The upturn was less pronounced with a plugged cylinder wall probably because the large pores were eliminated.

We believe that the copper content of the sample approximates the composition of the solution at the cathode-solution interface. The latter actually has no thickness and, strictly speaking, cannot be sampled. The decrease in copper content below that of the body of the bath is not caused, as has been suggested, by deposition of copper in the interstices of

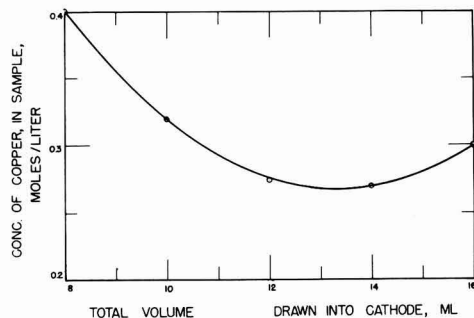


Fig. 2. Relation between the copper content of a sample drawn into the cylinder and the total volume of solution passing through the cylinder. The abscissa is the total volume of solution collected up to and including the volume of the sample used for analysis. The ordinate is the concentration of copper in a 1-ml sample individually collected. Rate of flow of liquid into cylinder, 0.25 ml/min; copper concentration in the body of bath, 0.94M; current density, 2.86 amp/dm²; room temperature; apparatus as shown in Fig. 1.

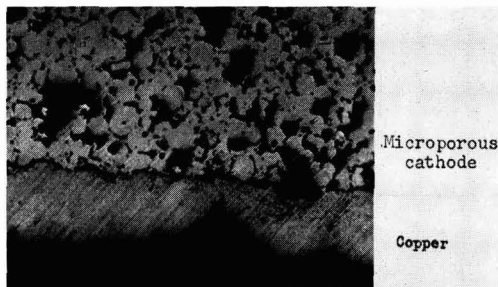


Fig. 3. Photomicrograph of a cross section of copper deposited on microporous stainless steel.

the cell wall. Deposition of copper within the interstices is improbable because of the minute current that flows into deep recesses having a cross section of the order of 5μ . Definite evidence that deposition does not occur in the pores of the cylinder is given in Fig. 3, which shows that the copper coating lies only on the outside surface of the microporous cathode.

Since the internal surface of the electrode walls is very large, the possibility exists that an appreciable amount of copper would deposit within the walls without attaining a thickness sufficient to be observed microscopically. This possibility was explored by determining the amount of copper leached out of the cell walls with nitric acid. The walls of this cell were twice the thickness of those of the cell used for obtaining the values of ΔCu reported in this paper. In a blank experiment, the thick-walled cell was immersed in copper sulfate solution for 2 hr to determine if copper deposited by immersion. The copper extracted from the cell walls with nitric acid amounted to only a few milligrams and hence was negligible. In another experiment, copper was deposited at 4 amp/dm^2 from a 1M bath over the cylinder as in an ordinary experiment. The copper coating was then peeled from the exterior of the cylinder and any residual copper nodules were removed with a polishing wheel. The copper obtained

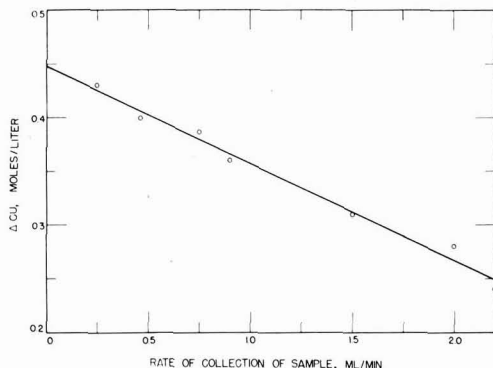


Fig. 4. Variation of ΔCu with rate of sampling. $\Delta\text{Cu} = C_b - C_1$ where C_b is the concentration of copper in the body of the bath and C_1 is the concentration of copper in the sample of the diffusion layer. $C_b = 1\text{M}$; current density, 1.5 amp/dm^2 ; temperature, 28°C ; microporous cathode, 0.15 cm thick; apparatus as in Fig. 1.

by a nitric acid extraction amounted to only 12 mg. This copper was probably not deposited on the interior of the wall but probably existed in surface cracks too deep to be reached by the polishing wheel. This amount of copper would affect the value of ΔCu only about 1%, which is less than the experimental reproducibility.

Rate of withdrawing samples.—The rate of withdrawing samples was an important variable. At a high sampling rate, some of the bulk solution was drawn into the cell along with the diffusion layer. Figure 4 shows the relation between the decrease in the copper content in the collected sample and the rate of collection of the sample. At a rate of 0.25 ml/min the decrease in the copper concentration, ΔCu , differed by only 3% from the value of ΔCu obtained by extrapolating the straight line of the figure to zero rate of sampling. Each point of Fig. 4 was obtained by the method illustrated in Fig. 1.

Relation between Current Density and ΔCu

The relation between ΔCu and current density is shown in Fig. 5 for copper sulfate solutions of three different concentrations. The current densities are based on the apparent area of the cylinder, considered as a continuous surface. Some observations were made at higher current densities than those recorded in Fig. 5. At the highest current density, which was above the limiting current density of metal deposition, the samples withdrawn from the electrode were virtually colorless indicating almost complete removal of copper.

One interesting aspect of Fig. 5 is that ΔCu at a given current density is larger the more concentrated the plating bath. A similar trend of metal depletion in the cathode diffusion layer was observed by Brenner (4) with nickel solutions and by Samarcev (1) with copper sulfate solutions. The explanation given by Samarcev, as well as by Brenner, was that in the dilute solution, and particularly in the still more dilute diffusion layer, the rate of diffusion of the metallic ions was greater than in

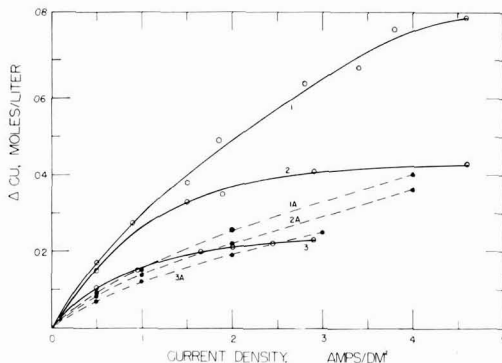


Fig. 5. Relation between ΔCu and current density in the electrolysis of copper sulfate solutions of three different concentrations. Rate of collection of sample, 0.25 ml/min . Curve 1. 0.94M copper sulfate; Curve 2. 0.49M copper sulfate; Curve 3. 0.24M copper sulfate; Curves 1A, 2A, and 3A are calculated curves based on diffusion theory (see Table I) according to Keulegan (13), for the same bath concentrations as curves 1, 2, and 3.

the concentrated solutions. This would result in a smaller value of ΔCu for the more dilute baths. However, the variation of the diffusion constant of copper sulfate with concentration seems inadequate to explain the differences of more than twofold in the values of ΔCu obtained at a given current density for the different baths.

Comparison of Data with Theory

Within recent years a considerable amount of theoretical and experimental investigation has been made of the hydrodynamics of electrode diffusion layers by Ibl and co-workers (2, 21, 22), Wagner (17, 18), and Tobias, Eisenberg, and Wilke (19, 20). The various approaches lead to similar numerical results for ΔCu (23) even though they involve some different assumptions.

The values of ΔCu obtained with the porous electrode were compared with those theoretically expected. The theory of the diffusion layer developed by Keulegan (13) was used in making the calculations. This theory was used because the authors were more familiar with it, and its use does not imply that it is more correct than the other theories. Actually it involves two assumptions that did not obtain in our experiments, namely, that the depletion of metal ion was uniform over the cathode and that the hydrodynamic boundary layer coincided with the diffusion layer.

Theory based on hydrodynamics and diffusion does not predict widely separated curves, as shown in Fig. 5, for solutions of different initial concentrations. Keulegan's theory leads to the following equation for ΔC . This ΔC , like the ΔCu obtained with the porous electrode, is the value of the reduction in metal ion concentration *averaged* over the cathode surface.

$$\Delta C = \left(\frac{It_a}{0.63F} \right)^{4/5} \cdot \frac{(\rho_1 \nu x m)^{1/5}}{g^{1/5} D^{3/5}}$$

where I = current density, amp/dm²; t_a = transference number of anion; F = 96,500 coulombs; ρ_1 = density of the bulk of the bath; ν = kinematic viscosity, poises; x = length of cylinder, (13.2 cm);

$m = \frac{dc}{d\rho} = 0.0132$ g equiv/g, c is the concentration

of the copper sulfate solution in gram equiv/ml, and ρ is the density of the copper sulfate solution; $g = 981$ cm/sec²; D = diffusion constant of copper sulfate, cm²/sec. This equation is based on equations 89 and 118 of Keulegan's paper. For the present experiments, the above equation simplifies to the following:

$$\Delta C = 2.5 \times 10^{-5} (It_a)^{4/5} \cdot \frac{(\rho_1 \nu)^{1/5}}{D^{3/5}}$$

In using this equation, the values of the variables are those of the solution at the interface of the cathode and the solution, except for ρ_1 which refers to the density of the bulk of the bath.

Calculations were made using the above equation. The values of the different variables are given in Table I. The results are represented in Fig. 5 as

dotted curves. The three curves based on Keulegan's equation lie close together, indicating that the effects of the variations of transference number, viscosity, and diffusion constant with concentration were not sufficient to explain the large difference in ΔCu experimentally obtained with the three different solutions at a given current density. The agreement of experiment with diffusion theory was best for the 0.24M copper sulfate solution.

We do not have a satisfactory explanation for the large difference between the three curves of Fig. 5 and the difference between curve 1 and the theoretical curve. It is possible that the roughness of the cathode surface or some other experimental detail may be responsible. Also, electrical migration may directly affect the thickness of the diffusion layer.

This latter suggestion is based on the behavior of liquid junctions in the moving boundary method of determining transference numbers. With suitably chosen solutions, the junctions remain sharp while current is passing. However, it is also possible for the current to dissipate a junction, depending on the relative mobilities of the ions involved. A similar phenomenon occurs at the junction of two solutions of different concentration. Thus, the electrical migration may have an effect on the establishment, the thickness, and the sharpness of the diffusion layer in addition to the factors of hydrodynamics.

Concentration Polarization

The polarization that occurs during an electrochemical reaction has been considered by electrochemists to be of two types: activation polarization and concentration polarization. The division is somewhat arbitrary since there are no direct experimental measurements for distinguishing between them. Very roughly, concentration polarization is considered to be caused by the change in concentration of the reactive ions at the electrode surface (24). The remainder of the polarization is considered to be of the other type. Various means for discriminating between them have involved different assumptions. It is assumed that stirring eliminates concentration polarization but does not affect activation polarization. Also, it is assumed that the latter type disappears more rapidly than the former when the circuit is broken. However, since nothing is known definitely about the activation type of polarization, one cannot, a priori, assume that concentration polarization is affected by a certain variable, such as stirring and the other one is not.

Concentration polarization, P_c , at a cathode is usually defined by the Nernst expression:

$$P_c = \frac{RT}{nF} \log \frac{A_o}{A_i}$$

where A_o is the activity of the metal ion in the body of the bath and A_i is the activity of the metal ion at the cathode-solution interface. That is, the concentration polarization is equivalent to the potential of a concentration cell with negligible liquid junction. In actual measurements of polarization with a capillary, a variable liquid junction potential exists between the solution of the reference electrode and

Table I

Calculations of ΔCu from the formula,

$$\Delta\text{Cu} = 2.5 \times 10^{-5} \cdot (It_a)^{4/5} \cdot \frac{(\rho_1\nu)^{1/5}}{D^{3/5}}$$

 ΔCu is given by the formula in units of $\frac{\text{g-equiv}}{\text{cm}^3}$

I , current density, amp/cm²; t_c , transference number of cation; t_a , transference number of anion; ρ_1 , density of body of bath; ν , kinematic viscosity, poises; D , diffusion constant, cm²/sec; C_b , concentration of copper in the body of the bath, g-equiv/cm³; C_i , concentration of copper at the cathode-solution interface, g-equiv/cm³.

C_i g-equiv/cm ³ $\times 10^4$	t_c	t_a	I amp/cm ²	$(It_a)^{4/5}$ $\times 10^4$	ν $\times 10^2$	$(\rho_1\nu)^{1/5}$	D $\times 10^6$	$D^{3/5}$ $\times 10^4$	ΔCu g-equiv/cm ³	
									Calc.	Exp.
		$C_b = 0.94\text{M}$		$\rho_1 = 1.130$						
15.4	0.275	0.725	0.005	111	1.27	0.428	5.05	6.6	1.8	3.4
12.8	0.285	0.715	0.01	192	1.22	0.425	5.1	6.68	3.0	6.0
8.6	0.300	0.700	0.02	329	1.10	0.416	5.2	6.76	5.1	10.2
3.8	0.34	0.66	0.04	546	0.98	0.406	5.4	6.9	8.0	15.0
		$C_b = 0.490$ moles		$\rho_1 = 1.075$						
6.4	0.307	0.693	0.005	108	1.05	0.408	5.25	6.80	1.6	3.4
4.6	0.325	0.675	0.01	183	1.00	0.404	5.30	6.84	2.7	5.2
2.6	0.370	0.630	0.02	302	0.96	0.400	5.56	6.98	4.3	7.2
1.2	0.390	0.610	0.04	512	0.93	0.398	5.6	7.06	7.2	8.6
		$C_b = 0.240\text{M}$		$\rho_1 = 1.035$						
2.7	0.370	0.630	0.005	99.7	0.96	0.397	5.5	6.98	1.4	2.1
1.8	0.390	0.610	0.01	169	0.94	0.396	5.65	7.10	2.4	3.0
0.6	0.395	0.605	0.02	293	0.91	0.393	6.2	7.51	3.8	4.2
0.2	0.395	0.605	0.03	405	0.90	0.392	6.9	8.00	5.0	4.6

Data for D taken from Eversole, Kindsvater, and Peterson (15) for concentration of copper sulfate up to 0.35M. Other values of D were obtained by extrapolation.

Data for t_c is that for Zn^{++} in zinc sulfate, as given by Conway (14B), as the transference number of Cu^{++} should be about the same.

that of the bath, because with no current flowing the capillary is immersed in a solution having an ion activity A_b , and with the current flowing the activity of the ion is A_i . However, this junction potential is too small to be of consequence.

Concentration polarization as defined by the Nernst equation will be referred to in the following discussion as Nernst concentration polarization. It has a definite meaning, because it depends only on the activities of a particular species of ion. From a knowledge of the concentrations of solute, C_i , at the interface of the electrode and solution, and C_b , the concentration in the body of the bath the Nernst concentration polarization can be calculated; or it can be measured by setting up a concentration cell, with metal concentrations C_i and C_b , provided the metal has a reversible static potential.

At a given current density, Nernst concentration polarization is a more definite and reproducible quantity than activation polarization. For example, the latter may increase greatly in the presence of a small amount of an addition agent in a solution although the basic electrode reaction has not changed. In contrast, the concentration of metal ions which determine concentration polarization is largely a function of current density and is fairly reproducible from one experiment to another.

Only one prior study has been made to calculate Nernst concentration polarization from measurements of concentration. This work was done by Samarcev (1) with a copper sulfate solution. He showed that the polarization was greater than that which could be accounted for on the basis of Nernst concentration polarization. Prior to his work many electrochemists had considered the polarization involved in the deposition of copper from a sulfate bath to be entirely concentration polarization. This work of Samarcev stands out as being the first determination of concentration polarization based on measurements of concentration.

Concentration polarization corresponding to curves 1, 2, and 3 of Fig. 5 were calculated by means of the Nernst equation using the activities for copper ion given by Conway (14A). The results of these calculations are shown in Fig. 6. To compare the magnitude of concentration polarization with the total polarization of copper deposition, curve 4 is included. This is for the deposition of copper from a 1M solution containing 0.05M sulfuric acid. A comparison of curve 1 with 4 shows that the contribution of concentration polarization to the total polarization is rather small.

Shreir and Smith (16) attempted to measure the concentration polarization of copper sulfate solu-

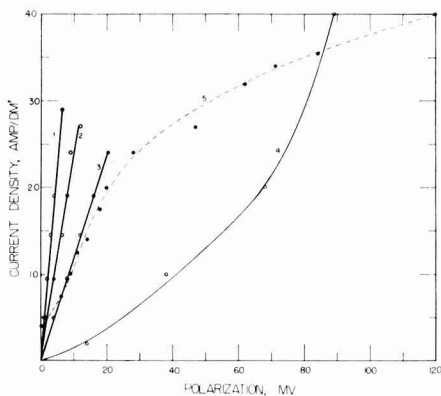


Fig. 6. Nernst concentration polarization calculated from the copper concentration, C_1 , at the electrode interface. Curves 1, 2, and 3 refer to the like-numbered curves of Fig. 5. Curve 4 is the total polarization for a solution 1.0M in copper sulfate and 0.05M in sulfuric acid measured with a Luggin capillary. Curve 5 is the concentration polarization of a solution 0.5M in copper and 0.5M in sulfuric acid obtained by the stirring method. Data of Shreir and Smith (16). [Calculations for curves 1, 2, and 3 are based on the activities of copper ions given by Conway (14)].

tions by measuring the difference in potential of the electrode in a still and in a stirred bath. Their data for a bath 0.5M in copper sulfate and 0.5M in sulfuric acid is reproduced in Fig. 6 as a broken line. Their data indicates a considerably larger concentration polarization than was obtained by the present method. A comparison between our data and theirs is valid even though their bath contained sulfuric acid. The maximum effect of the acid would be to decrease the transport number of copper ions. If the transport number were reduced to zero, this would result in only about a 30% increase over our values of concentration polarization given in Fig. 6.

The probable reason that our values are smaller than those of Shreir and Smith is that the latter's values include some contributions due to activation polarization. Activation polarization is a function of concentration, as well as of current density, as is shown by the data of Shreir and Smith (16). Since the concentration of metal ion at the electrode surface in the still solution must have differed from that in a stirred solution, the activation polarization must also have varied under these two conditions. Thus the procedure of measuring the Nernst concentration polarization by the difference in potential between a stirred and unstirred bath is not accurate because it also includes the effect of concentration on activation polarization.

The relation between activation polarization and concentration of the solution could be determined in the following way. A series of solutions of different concentrations could be electrolyzed at the same current density and the concentration of metal at the electrode-solution interface and the total electrode polarization determined. The Nernst concentration polarization can be calculated and subtracted from the total polarization to yield the activation polarization. The latter could be related to either the metal concentration of the body of the

bath or to the concentration at the interface of the electrode and the solution.

Discussion

The porous electrode method of sampling the diffusion layer has the advantage over the freezing method of being simpler to set up and operate. Also the diffusion layer can be continuously sampled. However, it does not yield the concentration profile of the diffusion layer as does the freezing method and cannot be used to study the rate of attainment of the steady state in the diffusion layer. The drainage method is simpler than the porous electrode method but is a less precise way of isolating the solution at the electrode interface. In carrying out the drainage method, some mixing of the bulk of the bath with the diffusion layer probably occurs.

The porous electrode method yielded larger values for ΔCu than either the freezing method or the optical method. The value of ΔCu given in Fig. 5 for the 0.94M solution at 4 amp/dm² was twice as large as that obtained by Brenner (4) with the freezing method. The value of ΔCu for the 0.49M solution at 0.5 amp/dm² was about three times larger than that obtained by Ibl and co-workers (2) with the interferometric method. The comparison of our results with those of the latter workers may not be strictly valid, because they measured a local ΔCu , not an average value, and the length of their electrode was only about one-fourth the length of ours.

The fact that the porous electrode method yielded larger values of ΔCu than other methods may be evidence that it comes closer than the other methods to giving the true concentration of metal ion at the electrode interface. Experimental difficulties, such as mixing of the cathode diffusion layer with the bulk of the bath, would have led to smaller values of ΔCu . The fact that the values of ΔCu in Fig. 5 were larger for the more concentrated solutions is further evidence that no large amount of mixing took place between the diffusion layer and the bulk of the bath.

The concentration polarizations shown in Fig. 6 are rather small compared with the total polarization. These results can be applied to electrodeposition in general, since the experiments with the copper sulfate solutions covered the usual range of concentration of metallic salts and of current density employed in conventional electroplating. The current densities used in electroplating are usually not over half of the limiting current density for metal deposition, that is, the concentration of metal ions at the cathode interface usually would not be reduced below about half that in the body of the bath. Consequently, on the basis of the results given in Fig. 6, it may be concluded that in ordinary electrodeposition the Nernst concentration polarization is small. In particular, Fig. 6 shows that the concentration polarization in the 0.49M and 0.94M solutions was less than 10 mv at a current density of 2 amp/dm², which is a current density commonly employed in plating. Since the precision of measuring electrode polarization is usually of the order of 5 mv to 10 mv, the concentration polarization

should be barely detectable at the current densities used in conventional electroplating. The directly observed polarizations, such as curve 4 in Fig. 6, must be attributed to other causes than the Nernst explanation.

Summary

1. A method for isolating the solution at the interface of an electrode and the bath has been developed.

2. The Nernst concentration polarization has been calculated for copper sulfate solutions.

3. It is concluded that the Nernst concentration polarization probably is not significant in plating baths operated at conventional current densities.

Acknowledgment

Theodore Yannakopoulos expresses his appreciation to the National Academy of Sciences under whose auspices he was a guest research worker at the National Bureau of Standards during 1954-1955.

Manuscript received Sept. 20, 1957. This paper was prepared for delivery before the Pittsburgh Meeting, Oct. 9-13, 1955.

Any discussion of this paper will appear in a Discussion Section to be published in the June 1959 JOURNAL.

REFERENCES

1. A. G. Samarcov, *Z. Physik. Chem.*, **A168**, 45 (1934).
2. N. Ibl, Y. Barrada, and G. Trümpler, *Helv. Chim. Acta*, **37**, 583 (1954).
3. C. S. Lin, R. W. Moulton, and G. L. Putnam, *Ind. Eng. Chem.*, **45**, 636 (1953); *ibid.*, 640.
4. A. Brenner, *Proc. Am. Electroplaters' Soc.*, **1940**, 95; *ibid.*, **1941**, 28.
5. A. Brenner and E. G. Wranglen, *Särtryck ur Svensk Kemisk Tidskrift*, **67**, 81 (1955).
6. (a) A. K. Graham, S. Heiman, and H. J. Read, *Proc. Am. Electroplaters' Soc.*, **1939**, 95; (b) H. J. Read and A. K. Graham, *Trans. Electrochem. Soc.*, **78**, 279 (1940).
7. M. Knobel, *Ind. Eng. Chem.*, **17**, 826 (1925).
8. Boehringer and Sons and Messinger, German Pat. 109,051, Oct. 1898.
9. E. Schlumberger, U. S. Pat. 1,598,018, Aug. 31, 1926.
10. G. W. Heise, *Trans. Electrochem. Soc.*, **75**, 147 (1939).
11. M. Janes, *ibid.*, **77**, 411 (1940).
12. N. M. Winslow, *ibid.*, **80**, 121 (1941).
13. G. H. Keulegan, *J. Research Nat. Bur. Standards*, **47**, 156 (1951).
14. B. E. Conway, "Electrochemical Data," Elsevier Publishing Co., New York (1952), A.p.79; B.p.166.
15. W. G. Eversole, H. M. Kindsvater, and J. D. Peterson, *J. Phys. Chem.*, **46**, 370 (1942).
16. L. L. Shreir and J. W. Smith, *This Journal*, **99**, 64 (1952).
17. C. Wagner, *J. (and Trans.) Electrochem. Soc.*, **95**, 161 (1949).
18. C. Wagner, *This Journal*, **104**, 129 (1957).
19. C. W. Tobias, M. Eisenberg, and C. R. Wilke, *ibid.*, **99**, 359C (1952).
20. C. R. Wilke, M. Eisenberg, and C. W. Tobias, *ibid.*, **100**, 513 (1953).
21. N. Ibl and R. Müller, *Z. Elektrochem.*, **59**, 671 (1955).
22. N. Ibl and R. Müller, Paper delivered at the Fall Meeting of the Electrochemical Society, 1956.
23. N. Ibl, Private communication, February 1958.
24. J. V. Petrocelli, *This Journal*, **98**, 187 (1951).

Phase Equilibria and Fluorescence in a Portion of the System $\text{ZnO-MnO-P}_2\text{O}_5$

F. A. Hummel and Fred L. Katnack

*Department of Ceramic Technology, College of Mineral Industries,
The Pennsylvania State University, University Park, Pennsylvania*

ABSTRACT

Phase equilibrium data have been obtained for compositions in the ternary system lying near the $\text{Zn}_3(\text{PO}_4)_2$ compound, particularly those on the orthophosphate join. It was found that "gamma zinc orthophosphate" is a ternary solid solution which has a region of stability on the orthophosphate join ranging from about 5 to about 25 mole % $\text{Mn}_3(\text{PO}_4)_2$. A definitive x-ray pattern characteristic of the ternary solid solution series is given.

$\beta\text{-Zn}_3(\text{PO}_4)_2$ forms an extended series of solid solutions with $\text{Mn}_3(\text{PO}_4)_2$ at temperatures above 940°C. The melting behavior of the $\beta\text{-Zn}_3(\text{PO}_4)_2$ solid solution is difficult to determine in air due to the usual change in oxidation state of manganese at temperatures above 1000°C.

Emission curves for cathode ray excitation are presented for α and β zinc orthophosphate, the so-called "gamma-zinc phosphate," $\text{Zn}_3\text{P}_2\text{O}_7$, and the two forms of $\text{Zn}(\text{PO}_3)_2$.

In a recent paper by Katnack and Hummel (1), the equilibrium relationships for the system $\text{ZnO-P}_2\text{O}_5$ were established, and it was shown that low- and high-temperature forms of ortho-, pyro-, and metaphosphate compounds existed.

The primary purpose of this paper was to establish the equilibrium relationships in the ternary system $\text{ZnO-MnO-P}_2\text{O}_5$ in the neighborhood of

$\text{Zn}_3(\text{PO}_4)_2$ and to relate these data to the fluorescence of the α , β , and "gamma" forms of the orthophosphate. A second purpose was to obtain luminescence data on $\text{Zn}_3\text{P}_2\text{O}_7$, and the two forms of the metaphosphate.

Compositions and Procedure

General.—The raw materials and experimental techniques were the same as those described in the

Table I. ZnO-MnO-P₂O₅ compositions on the Zn₃(PO₄)₂-Mn₃(PO₄)₂ join

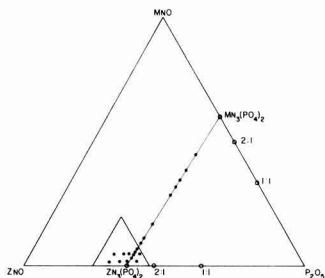
No.	Composition (Mole %)		Mole ratio	Equivalent ternary composition (wt %)			Initial heat treatment	
	Zn ₃ (PO ₄) ₂	Mn ₃ (PO ₄) ₂		ZnO	MnO	P ₂ O ₅	Time, hr	Temp, °C
1	99	1		62.64	0.55	36.81	24	826
2	98	2		62.08	1.11	36.81	3	700
3	96	4		60.88	2.22	36.90	3	700
4	95	5		60.32	2.76	36.92	12	828
5	94	6		59.72	3.33	36.95	3	700
6	91.67	8.33	11:1:4	58.35	4.62	37.03	3	700
7	90	10		57.36	5.52	37.12	12	828
8	88.89	11.11	8:1:3	56.71	6.18	37.11	3	700
9	85	15		54.40	8.36	37.24	12	826
10	83.33	16.67	5:1:2	53.39	9.32	37.29	24	500
11	80	20		51.42	11.20	37.38	12	826
12	70	30		45.36	16.95	37.69	12	818
13	50	50		32.96	28.73	38.31	12	818
14	44.44	55.56	4:5:3	29.42	32.06	38.52	12	800
15	40	60	6:9:5	26.58	34.75	38.66	12	800
16	33.33	66.67	1:2:1	22.28	38.84	38.89	12	800
17	25	75	3:9:4	16.83	44.01	39.17	12	800

previous paper (1). C.P. MnCO₃ was the source of MnO. Spectral distribution curves were obtained with a demountable cathode ray tube operating at 16 kv anode potential, 0.5 μa/cm² beam current density on a standard scan T.V. raster of 65 cm² area. Brightness under the above conditions was measured using an eye-corrected Weston foot-lambert meter.

ZnO-MnO-P₂O₅ compositions lying on the Zn₃(PO₄)₂-Mn₃(PO₄)₂ join.—Since the β-Zn₃(PO₄)₂:Mn phosphor was thought to be of primary interest, the ZnO-MnO-P₂O₅ ternary system was first studied along the zinc orthophosphate-manganese orthophosphate join. The compositions on this join were made either directly from previously prepared end members, Zn₃(PO₄)₂ and Mn₃(PO₄)₂, or from a mixture of Mn₃(PO₄)₂, ZnO, and H₃PO₄.

Seventeen compositions were made on this join by substituting Mn₃(PO₄)₂ for Zn₃(PO₄)₂ on a molar basis. These compositions are given in Table I. The equivalent ternary compositions on a weight per cent basis are listed beside the molar compositions. Compositions 5-17 are presented graphically in Fig. 1. Compositions 1-4 are not included because of limited space.

ZnO-MnO-P₂O₅ compositions not on the Zn₃(P₂O₅)₂-Mn₃(PO₄)₂ join.—Eight ZnO-MnO-P₂O₅ compositions were made in the vicinity of pure Zn₃(PO₄)₂ but not lying on the Zn₃(PO₄)₂-Mn₃(PO₄)₂ join. These compositions were made at 2 and 5 wt % levels of MnO with varying amounts of ZnO and P₂O₅.

Fig. 1. Compositions studied in the system ZnO-MnO-P₂O₅.

The raw materials used for these compositions were ZnO, MnC₂O₄·2H₂O, and H₃PO₄. The batches were mixed at room temperature and dried at 110°C. No preliminary heat treatment was given to this group of compositions. These eight compositions are listed in Table II and shown graphically in Fig. 1.

Experimental Results and Discussion

Phase Relationships on the Zn₃(PO₄)₂-Mn₃(PO₄)₂ join.—Compositions on the Zn₃(PO₄)₂-Mn₃(PO₄)₂ join were heat treated only in quench furnaces. The results of the quenching data are listed in Table III. In general, longer heat treatments were used in this system than in the ZnO-P₂O₅ binary system as crystalline batches were used as starting materials throughout the study.

A not-impossible phase diagram was drawn from these quench data and is presented in Fig. 2. This diagram reveals the existence of four different phases. The phase listed as α-Zn₃(PO₄)₂ gave an x-ray pattern corresponding to the low (α) form of pure zinc orthophosphate. The β-Zn₃(PO₄)₂ solid solutions gave x-ray patterns corresponding to the high (β) form of the zinc orthophosphate end member. The form listed as "γ-zinc phosphate" gave an x-ray pattern which in no way resembled the low or high form of Zn₃(PO₄)₂. The major peaks of this x-ray pattern generally corresponded to the x-ray pattern presented by Smith (2) for the so-called

Table II. ZnO-MnO-P₂O₅ compositions not on the Zn₃(PO₄)₂-Mn₃(PO₄)₂ join

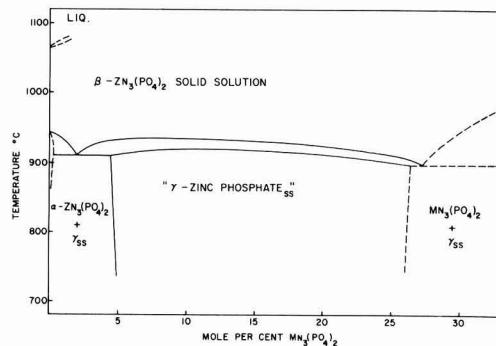
Sample No.	ZnO	Composition (wt %) MnO	P ₂ O ₅
18	65	5	30
19	62	5	33
20	60	5	35
21	56	5	39
22	68	2	30
23	65	2	33
24	62	2	36
25	59	2	39

Table III. Quench data for the system $Zn_3(PO_4)_2$ - $Mn_3(PO_4)_2$

Composition No.	Composition (Mole %)		Mole ratio	Heat treatment		Crystal-line phases present
	$Zn_3(PO_4)_2$	$Mn_3(PO_4)_2$		Time, hr	Temp, °C	
1	99	1	—	24	937	β
				24	912	α, β
				24	884	α, γ
				24	843	α, γ
				24	826	α, γ
2	98	2	—	23	936	β
				24	918	β
				24	874	α, γ
				20	858	α, γ
				23	938	β
3	96	4	—	24	926	β, γ
				23	907	α, γ
				24	874	α, γ
				20	858	α, γ
				24	938	β
4	95	5	—	8	923	β, γ
				24	892	γ
				22	867	γ
				12	828	γ
				22	937	β
6	91.67	8.33	11:1:4	24	920	β, γ
				10	901	γ
				12	894	γ
				12	845	γ
				24	925	β, γ
7	90	10	—	9	900	γ
				21	852	γ
				12	828	γ
				23	943	β
				24	935	β
8	88.89	11.11	8:1:3	22	918	γ
				24	884	γ
				24	941	β
				23	922	β, γ
				11	905	γ
9	85	15	—	21	866	γ
				12	826	γ
				10	936	β
				17	950	β
				20	932	β
10	83.33	16.67	5:1:2	20	915	β, γ
				24	895	γ
				24	887	γ
				24	883	γ
				9	862	γ
11	80	20	—	12	826	γ
				5	953	β
				22	932	β, M
				24	911	β, M
				22	893	γ, M
12	70	30	—	24	859	γ, M
				22	832	γ, M
				22	806	γ, M
				17	952	M
				12	818	γ, M
13	50	50	—	17	952	M
				12	818	γ, M

α = α - $Zn_3(PO_4)_2$
 β = β - $Zn_3(PO_4)_2$ solid solution
 γ = γ -zinc phosphate
 M = $Mn_3(PO_4)_2$

"gamma form of zinc orthophosphate." The fourth phase found in this system appeared to be the end member $Mn_3(PO_4)_2$. $Mn_3(PO_4)_2$ gave a very poorly defined x-ray diffraction pattern in comparison to the patterns of the forms of $Zn_3(PO_4)_2$ when using $CuK\alpha$ radiation. Consequently, the use of x-ray analysis as a method of identification was difficult above 30 mole % $Mn_3(PO_4)_2$. Therefore, this portion of the diagram was not investigated as thoroughly as the $Zn_3(PO_4)_2$ end, and the boundaries in this area are presented as dashed lines.

Fig. 2. Probable equilibrium relationships on the join $Zn_3(PO_4)_2$ - $Mn_3(PO_4)_2$.

At the outset of the work it was postulated that γ -zinc phosphate was a ZnO - MnO - P_2O_5 ternary compound whose composition was on the $Zn_3(PO_4)_2$ - $Mn_3(PO_4)_2$ join. In particular, a mole ratio of $8ZnO \cdot MnO \cdot 3P_2O_5$ or 88.89 mole % $Zn_3(PO_4)_2$ and 11.11 mole % $Mn_3(PO_4)_2$ was thought to be the compound. It appeared from preliminary work that this composition changed directly from γ -zinc phosphate to a β - $Zn_3(PO_4)_2$ solid solution without going through a temperature range in which both γ -zinc phosphate and β - $Zn_3(PO_4)_2$ solid solutions were in equilibrium. However, more precise work showed that the narrow band containing these two phases in equilibrium probably exists continuously from 5 to 25 mole % $Mn_3(PO_4)_2$ and does not "close up" at 11.11 mole % $Mn_3(PO_4)_2$, the $8ZnO \cdot MnO \cdot 3P_2O_5$ composition. With no other evidence supporting the existence of $8ZnO \cdot MnO \cdot 3P_2O_5$ as a compound, the identification of γ -zinc phosphate remains inconclusive and the series must simply be described as ternary solid solutions. The x-ray data for γ -zinc phosphate presented in Table IV were recorded from a sample

Table IV. X-ray diffraction data for the ternary solid solution phase (γ -zinc phosphate)

2θ	d	I/I_0	2θ	d	I/I_0
15.9°	5.57	10	45.3°	2.00	—
20.5°	4.33	90	46.6°	1.95	5
21.1°	4.21	5	46.9°	1.94	5
22.3°	3.99	40	47.8°	1.90	5
23.0°	3.87	25	48.7°	1.87	5
24.2°	3.68	5	49.3°	1.85	10
26.1°	3.41	100	50.5°	1.81	5
27.6°	3.23	20	51.0°	1.79	5
29.5°	3.03	20	51.6°	1.77	10
30.8°	2.90	10	52.1°	1.76	5
31.9°	2.81	25	53.9°	1.70	5
32.9°	2.72	15	55.0°	1.67	10
34.0°	2.64	10	55.3°	1.66	15
35.6°	2.52	35	55.7°	1.65	5
35.8°	2.51	35	56.3°	1.63	5
36.6°	2.46	55	59.6°	1.55	15
37.5°	2.40	25	Other reflections		
37.8°	2.38	10			
39.1°	2.30	10			
40.3°	2.24	10			
41.9°	2.16	5			
42.8°	2.11	10			
43.2°	2.09	25			
44.6°	2.03	20			

containing 94 mole % Zn₃(PO₄)₂ and 6 mole % Mn₃(PO₄)₂, fired to 840°C for 70 hr.

The phase diagram shows that γ -zinc phosphate is probably only soluble in α -Zn₃(PO₄)₂ to a very limited extent, less than could be measured experimentally by petrographic or x-ray analysis. Gamma-zinc phosphate coexists with α -Zn₃(PO₄)₂ at very small concentrations of Mn₃(PO₄)₂. This indicates that a pure α -Zn₃(PO₄)₂:Mn phosphor would be difficult to produce without some γ -zinc phosphate contamination. This is evident from the x-ray data presented by Smith (2) for pure α -Zn₃(PO₄)₂. The major differences between his x-ray diffraction data and those presented in Table IV can be attributed to the presence of γ -zinc phosphate in his sample of "pure" α -Zn₃(PO₄)₂. It would appear that Smith obtained his x-ray data on α -Zn₃(PO₄)₂:Mn rather than on pure α -Zn₃(PO₄)₂.

This work indicates that the β -Zn₃(PO₄)₂:Mn phosphor can be produced free from α -Zn₃(PO₄)₂ or γ -zinc phosphate by firing the phosphor batches to a temperature above 942°C, the α - β inversion temperature in the pure zinc orthophosphate end member. However, an appreciable amount of sintering takes place at this high firing temperature, and the resultant hardening and increase in particle size would probably require a grinding operation to produce a usable β -Zn₃(PO₄)₂ phosphor. A pure β -Zn₃(PO₄)₂:Mn phosphor can be made at temperatures as low as 915°C if the eutectoid composition of 98 mole % Zn₃(PO₄)₂, 2 mole % Mn₃(PO₄)₂ is utilized.

Phase relationships in ternary compositions surrounding Zn₃(PO₄)₂.—To investigate the phase relationships in the system ZnO-MnO-P₂O₅ around the binary compound Zn₃(PO₄)₂, the eight compositions listed in Table II were heat treated in a Globar furnace in platinum crucibles at three different temperature levels. Since quench furnaces were not used, a temperature variation of $\pm 10^\circ\text{C}$ is introduced. The fired batches were air quenched and the crystalline phases identified by x-ray analysis.

The results of these analyses are listed in Table V and presented graphically in Fig. 3, 4, and 5.

The results indicate that compositions to the left of the Zn₃(PO₄)₂-Mn₃(PO₄)₂ join show ZnO and γ -zinc phosphate in equilibrium at 865°C, and ZnO and β -Zn₃(PO₄)₂ in equilibrium at higher temperatures. Compositions to the right of the Zn₃(PO₄)₂-Mn₃(PO₄)₂ join generally showed Zn₂P₂O₇ in equilibrium with β -Zn₃(PO₄)₂ and γ -zinc phosphate. While

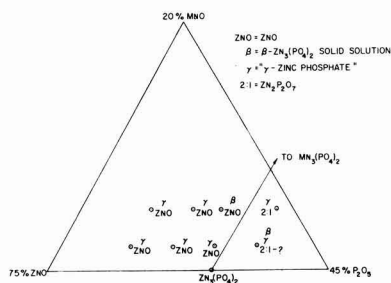


Fig. 3. Isothermal plane at $865^\circ \pm 10^\circ\text{C}$

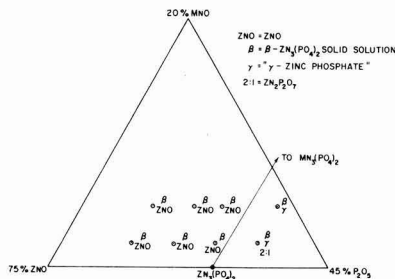


Fig. 4. Isothermal plane at $892^\circ \pm 10^\circ\text{C}$

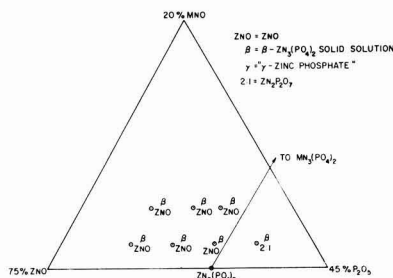


Fig. 5. Isothermal plane at $941^\circ \pm 10^\circ\text{C}$

free ZnO appeared in compositions to the left of the join and Zn₃P₂O₇ in compositions to the right of the join, these two phases were not detected in compositions on the join. The low (α) form of Zn₃(PO₄)₂ did not appear in any of these compositions after the above heat treatments.

Luminescence of the compounds and intermediate compositions in the ZnO-MnO-P₂O₅ system.—The

Table V. Phase analysis of ZnO-MnO-P₂O₅ compositions not on the Zn₃(PO₄)₂-Mn₃(PO₄)₂ join

No.	ZnO	Composition (wt %) MnO	P ₂ O ₅	Heat treatment (24 hr)	Crystalline phases present
18a	65	5	30	865	ZnO, γ
18b	65	5	30	892	ZnO, β
18c	65	5	30	941	ZnO, β
19a	62	5	33	865	ZnO, γ
19b	62	5	33	892	ZnO, β
19c	62	5	33	941	ZnO, β
20a	60	5	35	865	ZnO-?, β , γ
20b	60	5	35	892	ZnO, β
20c	60	5	35	941	ZnO, β
21a	56	5	39	865	2:1, γ
21b	56	5	39	892	γ , β
22a	68	2	30	865	ZnO, γ
22b	68	2	30	892	ZnO, β
22c	68	2	30	941	ZnO, β
23a	65	2	33	865	ZnO, γ
23b	65	2	33	892	ZnO, β
23c	65	2	33	941	ZnO, β
24a	62	2	36	865	ZnO, γ
24b	62	2	36	892	ZnO, β
24c	62	2	36	941	ZnO, β
25a	59	2	39	865	2:1-?, β , γ
25b	59	2	39	892	2:1, β , γ
25c	59	2	39	941	2:1, β

ZnO = ZnO
 β = β -Zn₃(PO₄)₂
 γ = γ -zinc phosphate
 2:1 = Zn₂P₂O₇

Table VI. Characteristic luminescence of the zinc phosphate compounds activated with manganese

Compound	Heat treatment		Luminescence	
	Time, hr	Temp, °C	Brightness (ft-L)	Peak wave length (m μ)
Low (α) Zn ₃ (PO ₄) ₂	5	805	8.7	551
High (β) Zn ₃ (PO ₄) ₂	12	960	12.0	638
Zn ₃ (PO ₄) ₂ N.B.S. Std. 1025			15.3	638
Low (α) Zn ₂ P ₂ O ₇	5	866	3.4	690
Low (α) Zn(PO ₃) ₂	72	600	0.8	626
High (β) Zn(PO ₃) ₂	12	800	4.8	570

investigation of the ZnO-P₂O₅ system indicated that five forms of zinc phosphate could be obtained at room temperature. These consisted of the low temperature stable forms of Zn₃(PO₄)₂, Zn₂P₂O₇, and Zn(PO₃)₂, and the high temperature metastable (at room temperature) forms of Zn₃(PO₄)₂ and Zn(PO₃)₂. One weight per cent MnO was added to these compounds and the batches were fired to the proper temperature to produce the five forms as shown in Table VI. The normalized emission curves for cathode ray excitation are shown in Fig. 6.

The compounds listed in Table VI were examined by x-rays to assure that only one phase was present in each case. As was to be expected, the low (α) Zn₃(PO₄)₂ contained some γ -zinc phosphate. Concentrations of MnO lower than 1.0 wt % would diminish the amount of γ -zinc phosphate formation in this phosphor. However, a 1.0% MnO level was used to maintain equal amounts of activator in all of the phosphors.

Luminescence in the ZnO-MnO-P₂O₅ system was also examined along the Zn₃(PO₄)₂-Mn₃(PO₄)₂ join. It is apparent from the phase diagram of this join that two series of solid solutions exist. The first series, labeled γ -zinc phosphate, exists from about 5 to 25 mole % Mn₃(PO₄)₂ and is stable below 900°C. The second series, labeled β -Zn₃(PO₄)₂ solid solution, extends from the pure Zn₃(PO₄)₂ end member to about 25 mole % Mn₃(PO₄)₂ and is stable above 942°C.

Seven Zn₃(PO₄)₂-Mn₃(PO₄)₂ mixtures were made to investigate the luminescence of these solid solutions. Four were in the γ -zinc phosphate solid solution series while the other three were in the β -Zn₃(PO₄)₂ solid solution series. These compositions and their heat treatments are listed in Table VII; the emission curves are presented in Fig. 7 and 8.

Table VII. Luminescence of β -Zn₃(PO₄)₂ and γ -zinc phosphate solid solutions

Composition (Mole %)		Heat Treatment		Luminescence		\bar{y}
Zn ₃ (PO ₄) ₂	Mn ₃ (PO ₄) ₂	Time, hr	Temp, °C	Brightness (ft-L)	Peak wave length (m μ)	
96	4	70	840	13.8	630	0.2650
94	6	70	840	9.7	630	
91.7	8.3	70	840	5.7	630	
88.9	11.1	70	840	2.7	630	
99	1	12	960	12.0	638	0.1911
95	5	12	960	11.5	638	
88.9	11.1	12	960	3.2	638	

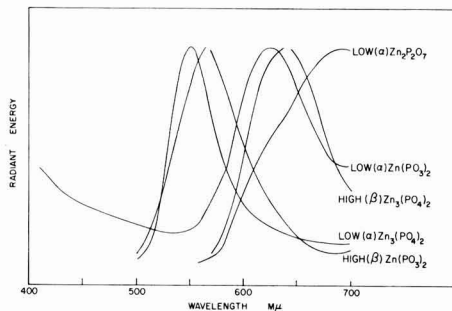


Fig. 6. Emission curves for zinc phosphate compounds under cathode ray excitation.

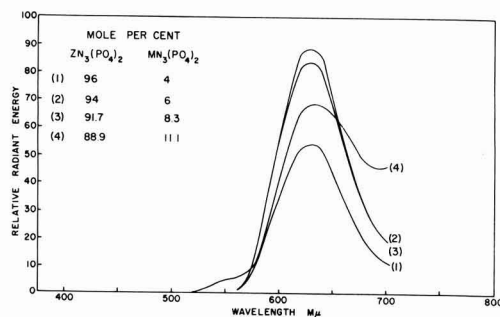


Fig. 7. Emission curves for γ -zinc phosphate solid solutions under cathode ray excitation.

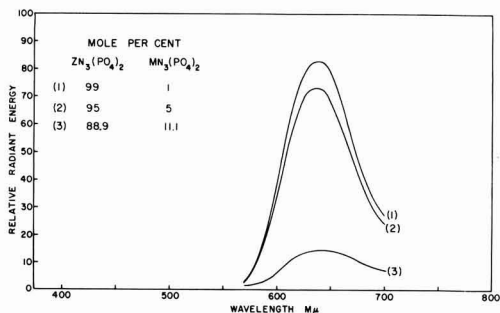


Fig. 8. Emission curves for β -zinc orthophosphate solid solutions under cathode ray excitation.

It is observed from these emission curves that the γ -zinc phosphate solid solutions have a slightly more yellow color than the β -Zn₃(PO₄)₂ phosphors. However, their intensities are less than those of the phosphors in the β -Zn₃(PO₄)₂ series. The 24-hr heat treatments used in the quench work were sufficient to produce all γ -zinc phosphate with the small quantities of material used in the quench packet. However, when larger quantities of the γ -zinc phosphate solid solutions were made for the luminescence studies, some α -Zn₃(PO₄)₂ appeared with the γ -zinc phosphate when batches were fired for 24 hr. Consequently, a 70-hr firing time was used to assure the presence of all γ -zinc phosphate.

It is observed from the emission curves of the β -Zn₃(PO₄)₂ phosphors that the brightness falls off rapidly with greater than 5 mole % Mn₃(PO₄)₂.

while the intensities of the phosphors with 1 and 5 mole % Mn₃(PO₄)₂ were quite similar. The eutectoid composition of 2 mole % Mn₃(PO₄)₂ can therefore be used to produce β-Zn₃(PO₄)₂ at the lowest possible firing temperature without suffering a significant loss in efficiency due to the presence of too much activator.

Conclusions

1. The γ-zinc orthophosphate previously reported is not a polymorphic form of Zn₃(PO₄)₂. It is a ternary solid solution series which has not as yet been identified with a ternary compound of ZnO, MnO, and P₂O₅.

2. The γ-zinc orthophosphate ternary solid solution series will yield red phosphors which are not generally comparable in brightness with the β series under cathode ray excitation. The compositions must be fired for relatively long times (70 hr) in order to assure equilibrium.

3. The β-Zn₃(PO₄)₂:Mn solid solutions yield bright red phosphors under cathode ray excitation up to 5 mole % Mn₃(PO₄)₂.

4. α-Zn₃P₂O₇:Mn is red under cathode ray excitation, as is well known.

5. High (β)Zn(PO₃)₂ is green under cathode ray excitation, while low (α)Zn(PO₃)₂ is orange.

Acknowledgment

The authors wish to thank the Chemical Products Plant of the General Electric Company for financial support during the course of this work. The assistance of various members of the Chemical Products laboratory in obtaining emission curves is gratefully acknowledged, as is the permission of Mr. R. S. Mackie to publish this paper.

Manuscript received March 14, 1958. This paper was prepared for delivery before the New York Meeting, April 27-May 1, 1958. Contribution No. 57-51 from the College of Mineral Industries, The Pennsylvania State University.

Any discussion of this paper will appear in a Discussion Section to be published in the June 1959 JOURNAL.

REFERENCES

1. F. L. Katnack and F. A. Hummel, *This Journal*, **105**, 125 (1958).
2. A. L. Smith, *ibid.*, **98**, 363 (1951).

Preparation and Properties of Aluminum Antimonide

A. Herczog,¹ R. R. Haberecht, and A. E. Middleton²

P. R. Mallory & Co. Inc., Indianapolis, Indiana

ABSTRACT

The high-energy gap intermetallic compound semiconductors, AlSb, GaAs, and InP, are considered as potential materials for devices operating at temperatures in excess of the limit for silicon. A comparative evaluation of these semiconductors is given which reveals some of the advantages and disadvantages of AlSb.

Aluminum and antimony of high purity were prepared by zone refining, and single crystals of AlSb were grown by the Czochralski technique. Effects of various impurities in the starting materials and crucibles on the electrical properties are discussed, and equipment for crystal growing under equilibrium vapor pressure of Sb is described. The resistivity of as-grown-P-type crystals can be decreased substantially by doping with carbon and increased by small quantities of Se and Te. A larger quantity of Te will change the crystals to N-type. P-N junctions were made by controlled doping during crystal growing. Effects of various surface treatments on the electrical properties of AlSb are discussed, and some data on point contact and P-N junction diodes are presented.

This work has been conducted in the interest of developing high-purity and preferentially doped aluminum antimonide crystals from high-purity metals using the Czochralski technique, and evaluating this intermetallic compound as a semiconductor to be used in place of germanium and silicon in devices capable of operating up to near 500°C.

This paper reports on purification, crystal growth, doping, P-N junction fabrication, electrical measurements and analysis, surface studies, device feasibility studies, and evaluation of the potential of aluminum antimonide for high-temperature semiconductor devices. In order to compare the relative potential of aluminum antimonide for high-tem-

perature devices with that of other high-energy gap semiconductors, a comparative evaluation of important known properties of these semiconductors is given below.

Evaluation of Potential of AlSb for Semiconductor Devices Operable at 500°C; Comparison with Other High-Energy Gap Semiconductors

Table I shows the pertinent properties of aluminum antimonide, as compared to other high-energy gap semiconductors, and assembled according to source (1-7). It can be noted in the table that, for aluminum antimonide, mobility ratios μ_n/μ_p , varying from 1/5 to 6/1, are reported. The only conclusion that one can draw is that these data were obtained on highly impure or polycrystalline material and, therefore, they are a poor indication of the true

¹ Present address: Corning Glass Works, Corning, N. Y.

² Present address: Lamp Division, General Electric Company, Cleveland, Ohio.

Table I. Summary of data on properties of high-energy gap semiconductors

Compound	Source of data	Thermal energy gap, ev	Optical energy gap, ev	μ_n	μ_p	M.P., °C
AlSb	Burstein and Egli (1)	1.6	1.5	1200	200	1060
	Dunlap (2)	1.65		35	150	1060
	Willardson, Beer, and Middleton (3)	1.55		100	100	1060
	Welker (4)	1.65	1.65	200	200	1060
	Jenny (5)	1.6		400		
GaAs	Burstein and Egli (1)		1.1	4000	200	1240
	Welker (4)	1.38	1.35	3400	200	1238
	Jenny (5)	1.35		4500		
InP	Burstein and Egli (1)		1.25	3400	650	1070
	Welker (4)	1.34	1.26	3400	50	1070
	Jenny (5)	1.25				
SiC (hex.)	Hall (7)	3.1				2200
	Jenny (5)	2.8		100		decomp
	Dunlap (2)			40-60	5-10	

mobilities and of the device potential of aluminum antimonide. This conclusion is supported by the data and analyses reported in this paper.

In evaluating the device potential of aluminum antimonide, an appraisal of the upper temperature and frequency limits of operation is of interest. The upper temperature limit is prescribed by the highest resistivity region adjacent to the P-N junction, since this region reaches the intrinsic region first with an increase in temperature. A conservative temperature limit for a transistor, made from germanium, is 50°C or more below the intersection of the extrinsic resistivity curve, characterizing the highest resistivity region of the device, with the intrinsic range curve. The available data for the intrinsic range resistivities of germanium, silicon, indium phosphide,

Table II. Maximum temperature limits for p-n junction action for high-energy gap semiconductors

Semiconductor	Extrinsic resistivity, ohm-cm	Temp. at intersection of intrinsic & extrinsic resistivity curves, °C	Temp. obtained by subtraction of Hunter's (10) correction (50°C), °C	Energy gap, ev
Ge	2	110	60	0.7
	5	80	30	
Si	2	390	340	1.1
	5	350	300	
InP	2	340	290	1.25
	5	300	250	
GaAs	2	490	440	1.35
	5	450	400	
AlSb	2	600	550	1.6
	5	540	490	

gallium arsenide, and aluminum antimonide are plotted as a function of temperature in Fig. 1 (2, 3, 6, 8, 9).

Table II shows the theoretical temperature limits of device operation for the cases of germanium, silicon, and the high energy gap semiconductors, for both 2 and 5 ohm-cm resistivity material. With due consideration to the limitations of the applicability of these data, it is apparent that aluminum antimonide is the most suitable material, among those given in Table II, for further development in attempting to achieve devices operable at 500°C.

A calculation of the reverse current flowing through a P-N junction, according to the equations of Shockley, yields for aluminum antimonide a theoretical leakage current of 10^{-10} amp/cm². In the case of silicon, a leakage current of 10^{-9} to 10^{-10} amp/cm² is obtained at room temperature, which approaches the 10^{-12} amp/cm² theoretical value. The theoretical leakage currents for gallium arsenide and indium phosphide are between 10^{-10} and 10^{-12} amp/cm². It can be concluded that, if surface control and structural perfection are achieved in the case of aluminum antimonide to an extent comparable to the case of silicon, the high-temperature leakage current of aluminum antimonide will be comparable with the room temperature leakage currents in silicon or germanium.

The frequency limit in transistors is controlled basically by charge carrier mobility and lifetime. Since the absolute minimum width of the base region is limited by voltage breakdown and by the accuracy of available methods of dimensional control, an approximate lower limit is imposed on the mobility of charge carriers for use in the two-junction type of transistor. This lower limit of mobility is estimated to be 1000 cm²/v sec for a material of 1 μ sec lifetime. Unipolar transistors, such as the field effect transistor, function by means of majority charge carriers and are not dependent in the same manner on mobility and lifetime. Jenny (5) has made a theoretical comparison of the relative frequency limits of high-energy gap semiconductors with those of germanium and silicon for unipolar transistor action using mobility values available in the literature. For the case of aluminum antimonide, his calculation is based on a mobility of 400 cm²/v sec. This is a median value considering that the data

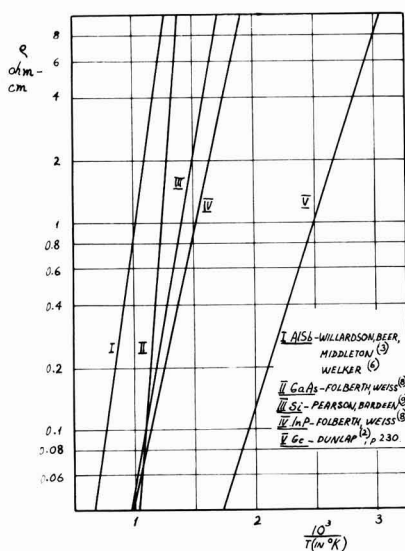


Fig. 1. Comparison of intrinsic range resistivities for Ge, InP, Si, GaAs, and AlSb vs. $10^3/T$ (in °K).

in the literature range from 1200 to 35 cm²/v sec. For this value the frequency response of aluminum antimonide has been calculated by Jenny (5) to be very similar to that of silicon.

In general, charge carrier mobilities are expected to decrease with increasing energy gap and melting point of the semiconductor. Furthermore, it has been proven by Welker and by other investigators that the group III-V intermetallic compounds generally have higher mobilities than the group IV elements for the same energy gaps and melting points. Another characteristic of group III-V compounds is that for the same energy gap the melting point is lower than is common in the group IV elements. Based on these general observations, data in the literature, calculations and analyses, the ultimate potential of high-energy gap semiconductors for high temperature rectifiers and transistors is expected to be as shown in Table III. From Table III, it appears that aluminum antimonide has potential applicability in high-temperature rectifiers and all types of high-temperature transistors, with the possible exception of the two-junction type of transistor.

Considering the expected trend of mobility with both melting point and energy gap, it appears that the electron mobility of aluminum antimonide as given by various investigators (see Table III) is anomalously low relative to expected values. This partially justifies the expectation of realizing considerably higher mobility with improved aluminum antimonide material.

Purification of Aluminum and Antimony

Antimony of 99.99% purity was purified by zone refining in aluminum oxide boats. The portion of the ingot used for crystal growing experiments contained of the order of 1 ppm spectroscopically detectable impurities. The major impurity contained in the antimony was arsenic. Arsenic was eliminated by zone refining antimony to which was added a small amount of aluminum.

The segregation of arsenic in antimony by zone refining in the presence of added or contained aluminum is quite remarkable and justifies comment here, although a detailed discussion of the mechanism of segregation involved will be deferred to a

later publication on this subject. Previous papers by Tanenbaum, Gross, and Pfann (11) and by Goering, *et al.* (12) indicate that the concentration of arsenic in a zone refined antimony ingot is practically constant over the whole length of the ingot. This implies that the segregation coefficient of arsenic in antimony is close to unity. The antimony metal used by these investigators did not contain any spectroscopically detectable amount of aluminum. In the present experiments, a segregation of arsenic was observed in all cases when aluminum was present. In attempting to obtain more conclusive evidence about the effect of aluminum on the segregation of arsenic, known amounts of aluminum were added to the front end of the antimony ingot before the zone refining was started. The results of these experiments showed that a strong segregation of arsenic occurs.

Aluminum of 99.99% purity was refined in aluminum oxide boats. The total impurity content of the zone refined aluminum used for crystal growing experiments was about 3 ppm, with iron as the major impurity. Since the weight of aluminum used for growing aluminum antimonide crystals was about one fourth that of antimony, the total amount of impurities in both metals (based on AlSb) was slightly above 1 ppm. In some cases, aluminum and antimony were also purified by zone refining in graphite boats.

AlSb Crystal Preparation and Doping

The metals were reduced to a suitable size and etched to clean the fragment surfaces. The weighed quantities of the metals were placed in an aluminum oxide crucible for crystal growing. The crucibles consisted of 99.7% pure aluminum oxide made by the Morganite Co., Long Island, New York. The crystal growing was done in an atmosphere of purified helium. Helium purification was accomplished by passing the gas through magnesium perchlorate, turnings of a titanium-zirconium alloy heated to 800°C, and finally a liquid air trap.

Before growing crystals, the equipment was heated up slowly over a period of 2-3 hr. During this time a flow of dry helium gas was maintained for the purpose of eliminating traces of water vapor

Table III. Comparison of high-temperature device potential of high-energy gap semiconductors showing trends of mobilities with melting point and energy gap

	SiC	GaP	AlAs	AlSb	GaAs	InP	Si	Ge
Energy gap in eV	~3	2.4	2.2	1.6	1.35	1.25	1.1	0.7
Melting point, °C	2200	1350	>1500	1060	1240	1070	1500	960
Electron mobility at 250°C, cm ² /v sec	decomp. 40-60	—	—	35-1200	3400-4500	3400	1900	3900
Hole mobility at 250°C, cm ² /v sec	5-10	17	—	100-200	>200	50	450	1900
Est. max. temp. for p-n junction action, °C	1000	—	—	550	440	325	350	100
Rectifying action	+	0	0	+	+	+	+	+
Transistor (2 junction) action	—	—	—	?	+	+	+	+
Unijunction transistor	×	×	×	0	0	0	+	+
Unipolar transistor	×	×	×	0	+	+	+	+

+ observed; 0 not observed but expected; — not believed possible; ? doubtful; × not observed, possible at high temperature but perhaps not at low temperature.

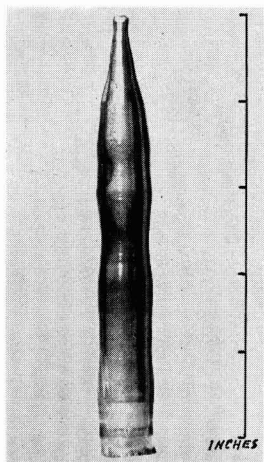


Fig. 2. AlSb crystal

and oxygen from the system. As a result of these pretreatments of the gas and the crystal growing equipment, the formation of oxide particles on the surface of the aluminum antimonide melt was minimized. Any floating particles which did appear on the melt surface were easily eliminated with a probe. The melt surface, in this mechanically cleaned state, remained clean throughout crystal growing. In the most recent work, the crucible was not rotated during crystal growing, but the seed crystal was rotated at a rate of 4 rpm.

The grown crystals have a clean metallic surface as shown in Fig. 2. Some crystals were obtained which were 80% single. Other crystals showed varying amounts of twin lines. Spectrographic data are given in Table IV for the top portion of a crystal. For comparison, the same table shows the amount of impurities contained in the zone refined metals used in growing the crystal. The amounts of copper and iron in the crystal are reduced because of segregation during crystal growing. The amount of magnesium and silicon is slightly increased because of contamination of the melt by the crucible.

Weighing was done in several cases to determine the loss of antimony by evaporation. Between 0.6 and 1.1 g was lost from approximately 122 g of antimony contained in the melt. This loss of antimony was reduced practically to zero by introducing a heated bell jar above the melt as shown in Fig. 3. The crystals grown with the heated bell jar in place were not different, however, from the crystals grown in open crucibles. As a matter of fact, they were less single in character because of difficulties encountered in skimming the surface of the melt under the bell jar.

A series of crystal growing experiments was performed under nearly identical conditions to compare the influence of small excesses of antimony or of aluminum in the melt on crystal characteristics. The data are reported in Table V. All crystals were P-type and had the same range of resistivity independent of the melt composition. It was noted that the crystals were more frequently twinned and also contained grain boundaries in the case of additions

Table IV. Analysis of aluminum antimonide crystals

Impurities, ppm	Cu	Fe	Mg	Si	As	Ca
Al + Sb metals	1.2	1.1	0.7	0.4		0.2
AlSb crystal	0.1	0.15	2.3	1.4	×	0.5
× = trace.						

Table V. Results of crystal growing experiments

Crystal No.	Addition to Sb 121.76 g Al 26.98 g	Top part of crystal		Remarks
		Resistivity ohm-cm	Type of conductivity	
26	0.5% Sb	0.8	P	Mostly single
30	2.9% Sb	0.8	P	Mostly single
29	4.0% Al	0.4	P	Polycrystalline
28	0.5% Sb	0.14	P	Sb refined in graphite boat
46	0.5% Sb	0.23	P	Al refined in graphite boat
38	10 mg C	0.013	P	Frequently twinned
27	15 mg C	0.01	P	Frequently twinned
22	10 mg Te	10.8	P-N	Large single portions
23	51 mg Te	3.6	N	Large single portions
24	75 mg Te	1.7	N	Large single portions
31	6 mg Se	9.7	P-N	Large single portions
25	61 mg Se	32.6	N	Large single portions

of an excess of aluminum. The resistivity of these crystals was also somewhat lower than normal. It is possible that the effects of excesses of aluminum and antimony on grown crystals might be explained by a nonstoichiometric composition of the crystal at the maximum melting point, as discussed theoretically by Hodgkinson (13).

In Table V, results of other crystal growing experiments are also reported for which either the aluminum or the antimony was purified in graphite boats. In both cases, and especially in the case of antimony refined in the graphite boat, the resistivity is considerably lower than normal. The indication that carbon contamination may cause a decrease in

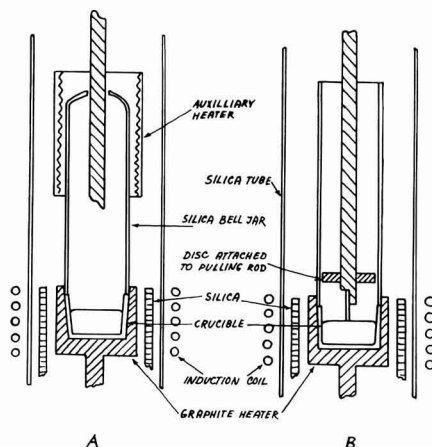


Fig. 3. Equipment to prevent evaporation from the melt during crystal growing.

resistivity is further confirmed in the case of crystals No. 38 and No. 27 where known amounts of carbon, 10 and 15 mg, respectively, were added to the metals before crystal growing. The amount of carbon actually dissolved in the melt is not known because a large portion of it was eliminated by skimming of the surface. However, the remaining quantity of carbon, which might be of the order of a few milligrams for an approximately 150-g melt, caused a great decrease in resistivity as shown in Table V.

The results of various experiments on the effect of carbon are shown in Fig. 4. Recently an analysis was made on the carbon content of antimony and of aluminum. The carbon content of aluminum was reduced by 50% by refining in an oxide boat; it was increased by 10% by refining in graphite boats. However, determinations revealed carbon contents in the range of the sensitivity of the analytical method, which was of the order of 50 ppm of carbon, and therefore cannot be considered as quantitative. Somewhat larger quantities of carbon were found in the as-received antimony. The carbon content of antimony was not appreciably reduced by zone refining.

Doping experiments were performed with various metals to gather information about type of conductivity and value of resistivity of the doped material and to evaluate their usefulness for alloyed ohmic contacts, or for rectifying junctions of any type. The impurity was added to the melt either before or during crystal growing for making P- or N-type material or P-N junctions. Figure 5 summarizes the effects of various doping agents on resistivity and type of conductivity for the available AISb.

Of special interest are the results of doping with tellurium and selenium, both of which give N-type material. A threshold seems to exist in the quantity of the added impurity which has to be exceeded in order to obtain N-type material. The quantity below the threshold is used up in compensating existing P-type centers in the crystal. It will be noted that

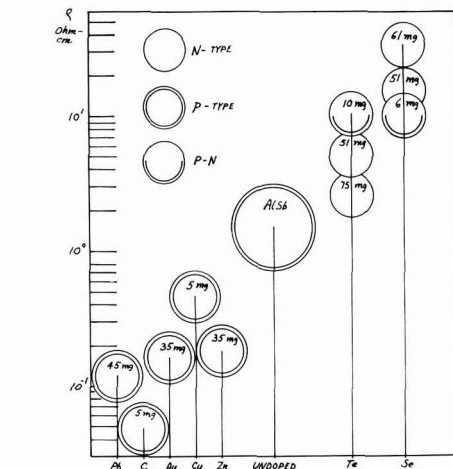


Fig. 5. Effect of various impurities on resistivity and conduction type of AISb.

a large amount of N-type addition is required, namely about 10 mg Te or 6 mg Se, to compensate for P-type centers. The chief detectable P-type impurity in the crystal is magnesium, dissolved by the melt from the crucible. The quantity of magnesium in the crystal has been determined by spectrographic analysis to be about 2 ppm. This is almost a factor of 10 lower than the amount of Se or Te used for compensation. It is concluded, therefore, that the compensation effect is due either to another impurity of unknown quantity, possibly carbon, or to antimony vacancies. Further identification will be discussed later in connection with the interpretation of Hall effect measurements.

In the case of tellurium additions, the resistivity of the crystal increases at first until the threshold quantity for compensation and conversion to N-type is reached and then decreases with any further addition of Te. In the case of selenium addition, there is a different behavior; the resistivity increases with further additions of the impurity above the threshold value for compensation.

P-N junctions were made from P-type material by doping with tellurium or selenium. Junctions can also be made by starting from selenium containing N-type material and doping with zinc to produce the junction. A lowering of resistivity for P-type material is obtained by doping with zinc and with carbon; a smaller change is obtained for lead, copper, and gold.

Hall Effect, Resistivity, and Tentative Identification of Extrinsic Charge Carrier Sources

Hall effect and resistivity measurements were made on an undoped P-type single-crystal section of 0.4 ohm-cm resistivity. The size of the sample was 1.6 x 0.62 x 0.13 cm. The current leads, Hall probes, and a thermocouple were soldered to the sample. The sample was kept under a vacuum of about 0.5 μ during the measurements. The magnetic field was calibrated against a 6 ohm-cm germanium sample by comparing its intrinsic range with pub-

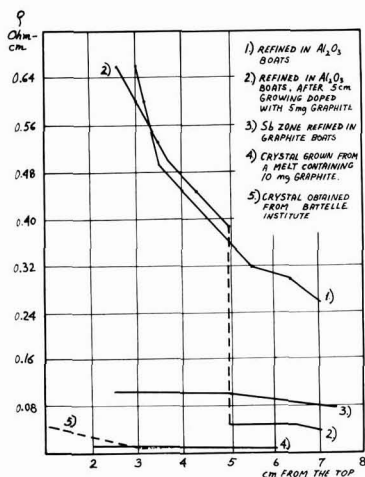


Fig. 4. Effect of carbon on the resistivity profile of AISb crystals.

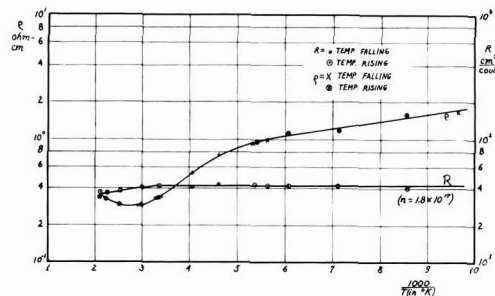


Fig. 6. Log resistivity and log Hall constant for AlSb vs. $10^3/T$ (in $^{\circ}K$).

lished intrinsic range curves. A primary current of 1 ma was passed through the sample in a magnetic field of 7000 gauss. Measurements were made between liquid air temperature and $200^{\circ}C$ for both rising and falling temperatures. Results are shown in Fig. 6. Although final interpretation of these results must await high-temperature data and similar runs on variously doped samples, some valuable conclusions can be drawn at this time.

Since the conduction is by extrinsic holes and the Hall constant is invariant with temperature over a long temperature range down to the lowest temperature investigated, the impurity levels controlling conduction are assumed to be exhausted. Using the relation $N = n = 7.37 \times 10^{-18}/R$, the number, N , of electronically active impurity centers and n , the total number of extrinsic holes, is found to be $1.8 \times 10^{17}/cc$. The constancy of the Hall constant over the entire low-temperature range suggests that acceptor centers due to impurities or lattice vacancies are present in the sample and that they lie very close to the valence band.

Since this sample has large positive hole extrinsic conduction, the relation $\mu p = R/\rho$ can be used to calculate the hole mobility. Figure 7 shows the resulting temperature dependence of mobility. It will be noted that the peak value of hole mobility is at $60^{\circ}C$ and is $105 \text{ cm}^2/v\text{-sec}$. These data on aluminum antimonide indicate that a high concentration of

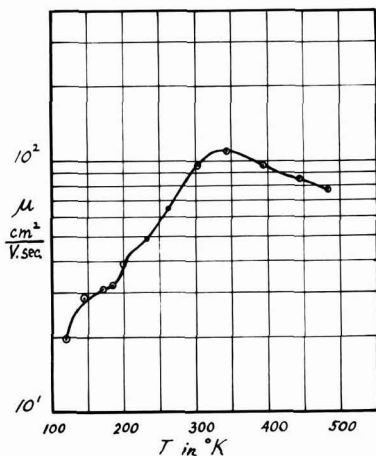


Fig. 7. Hole mobility of AlSb

centers, causing strong impurity scattering, is present in the aluminum antimonide sample. Further, it appears reasonable to conclude that the mobility of the holes in the aluminum antimonide is suppressed by the large amount of impurity scattering present.

From these data and with reference to the interpretations by Blunt and co-workers (14) of optical absorption characteristics of aluminum antimonide, some information on whether impurities or lattice defects are chiefly responsible for the observed electrical properties of aluminum antimonide can be obtained. Blunt found a deep lying level 0.75 eV above the valence band and attributed this to antimony vacancies. If Blunt and co-workers are correct in this assignment, the present Hall effect results are not easily explained on the basis of antimony vacancies, since they suggest a near-zero impurity activation energy.

With regard to the impurity which controls the electrical properties of the available aluminum antimonide, the following evidence suggests carbon as the major impurity:

1. $1.8 \times 10^{17}/cc$ P-type impurity centers in undoped material are indicated by the Hall constant vs. temperature data.
2. Carbon has been shown by doping experiments to make AlSb P-type.
3. Carbon additions in small quantities produce large reductions in AlSb crystal resistivity.
4. Tellurium doping experiments indicate that large amounts of N-type doping material must be added to compensate for the P-type centers. The Te additions cause an increase in resistivity up to the compensation concentration and then the resistivity decreases as the AlSb becomes predominantly N-type. The quantitative amount of Se and Te used for obtaining compensation was about 30-40 ppm. Since $1.8 \times 10^{17}/cc$ corresponds approximately to 10-50 ppm, the doping experiment observations are in agreement with the Hall effect determination of the number of acceptor impurity centers.

5. Justification of the spectroscopic analyses, considering the large quantity of impurity centers indicated by the Hall constant, is given by the fact that spectroscopic analysis is highly insensitive to carbon. Recently, however, carbon has been found by chemical analysis in the aluminum and antimony used for crystal growing at an indicated concentration of the order of 50 ppm.

Sample Processing and Surface Treatments

Considering the well-known tendency of aluminum antimonide to oxidize in the presence of water vapor, the problem of proper surface treatments is of utmost importance. Oxidation or hydrolysis leads to the formation of a black powder, and with passage of time all the material can be converted to this state. However, the rate of this process depends to a large extent on the existing surface properties and the structural characteristics of the specific sample of material.

The highest rate of decomposition is observed for surfaces obtained by cutting with a diamond saw using water cooling. In this case the surface is not only damaged mechanically but it is also saturated

with water. The initial damage is so deep that it can hardly be improved by further treatments unless a large quantity of material is removed from the surface in a uniform manner.

If AISb samples are cut with an oil-cooled diamond saw, the surfaces are stable enough to be kept in a desiccator, and the samples can be utilized without excessive removal of the surface layer. The surface obtained by cutting under oil can be slightly improved by lapping or by sandblasting. The material with lapped, sandblasted, or oil cut surface can be kept in a desiccator for some time without serious oxidation.

The best mechanical treatment is polishing with a fine abrasive to achieve a mirrorlike surface. Polished surfaces can be kept in open air, the only change being a development of a slight brownish color. Cleaved surfaces and the as-grown crystal behave in a manner similar to polished surfaces. This is only true for a crystal of good quality without grain-boundaries and without foreign particles such as oxide on the surface.

The best sample preparation prior to etching is either cleaving or polishing of the surface cut under oil immersion. Etching on lapped, sandblasted, or as-cut surfaces produces large etch pits and, in general, emphasizes any surface imperfections.

Various etching solutions were tried. Because of the different chemical reactivities of aluminum and antimony, it is possible to obtain surfaces with very different characteristics. Some of these surfaces show an excellent stability, not only with respect to air and water vapor, but also in contact with boiling water. It is probable that this protection is due to the presence of a slightly aluminum rich surface on which is formed an aluminum oxide layer. Surface properties were investigated by point contact rectification experiments and by four- and two-point probe resistivity measurements in order to evaluate the usefulness of various treatments for devices. The etching procedures giving best results are reported below.

A solution of HF (48%) and H₂O₂ (30%) in a ratio of 1:2 produces a mirrorlike surface of very high resistivity. The reaction is rather violent and is quenched by the addition of diluted H₂O₂ (3%) to the etch. After etching, the surface has a thin whitish layer which can be eliminated by boiling the sample in distilled water. This method has been abandoned, however, because it is not suitable for microetch or junction etch techniques. Any exposure of the sample to air after the acid treatment and before dilution of the acid causes the formation of a black deposit. The solution is unstable. It must be freshly made and used without delay.

A solution of hydrofluoric and nitric acid yields a very high resistivity surface of metallic appearance.

The best results were obtained with a solution containing hydrofluoric, nitric, and acetic acids in the ratio 2:3:0.5. The surface is bright metallic in appearance and stable in air. The same etch with a higher concentration of acetic acid is also quite satisfactory if a slower etch rate is desired.

Hydrochloric acid and potassium hydroxide, both in aqueous and alcoholic solutions, were also tried

as etches. Hydrochloric acid, in the gas phase, was investigated. The resulting surface resistivity of samples treated in these ways is somewhat low and the surfaces obtained have a rather dull metallic appearance.

It is noteworthy that four-point probe resistivity measurements give much higher values on etched surfaces than on lapped or sandblasted surfaces. The large ratio of about 10 between surface and bulk resistivity is a remarkable characteristic of aluminum antimonide.

Device Feasibility Studies

Experiments have been performed on the rectification properties of point contacts on AISb and grown junctions in AISb. The rectifying properties were found to depend strongly on the condition of the semiconductor surface. Owing to the near-degenerate nature of the AISb samples, high reverse voltages were not expected nor obtained.

Rectification experiments were carried out on cleaved, polished, and variously etched surfaces. In all cases, the sample, in the form of a cut wafer or cleavage fragment, was soldered to a metal support for external contact. Thin sheets of lead solder were used.

For producing fused junctions or ohmic contacts capable of operating at high temperatures, it is of importance to know the thermal expansion coefficient of AISb. A determination was made of the thermal expansion coefficient and the average coefficient of linear thermal expansion between room temperature and 700°C was found to be 4.9×10^{-6} .

Point contact rectifiers were made by using a small tungsten wire, 0.007 in. in diameter. This wire was bent into an S shape to provide mechanical stability. The end of it was etched electrolytically to reduce the contact area. The tungsten was welded to an external electrode. A typical unit assembly used for both point and grown junction rectifiers is illustrated in Fig. 8. The inside of the cartridge was filled with argon.

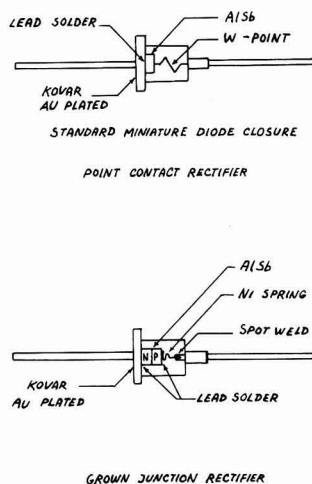


Fig. 8. Construction of point contact rectifier and junction rectifier.

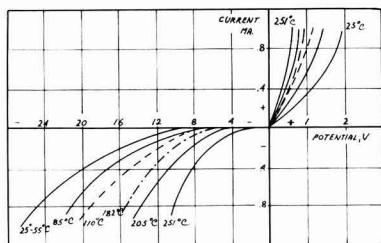


Fig. 9. Point contact rectification characteristics of AlSb as a function of temperature.

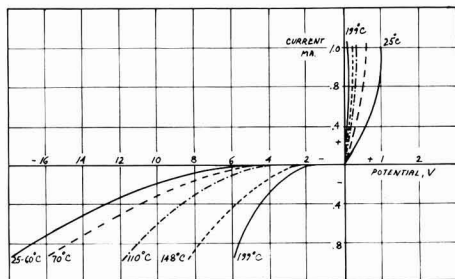


Fig. 10. Grown junction rectifier characteristics of AlSb as a function of temperature.

In the experiments, P-type material was used with 0.2-1.0 ohm-cm resistivity. Various etches were tried to improve rectification properties. Reverse voltages up to 85 v were obtained in the case of cleaved samples etched with HF-HNO₃ (1:9) using a dynamic reverse bias tester and 60 cycle pulsed D. C. Better reproducibility and good forward characteristics were obtained using cut wafers and HF-HNO₃-CH₃COOH (2:3:0.5) etch.

Figure 9 shows point contact rectification curves at various sample temperatures for a P-type AlSb, etched with HF-HNO₃-CH₃COOH. Electrical tests were made up to 250°C. Failure of the units occurred at this temperature. This may have been due either to softening of the solder, to formation of a low melting point lead-antimony eutectic, or possibly to the increase with temperature of the P-N junction leakage current, characteristic of the low resistivity material.

Grown junction rectifiers were made by doping the melt with selenium during crystal growing. Selenium pellets weighing between 10 and 60 mg were dropped into the melt without exposure of the melt to the air. The sections of the crystal containing the P-N junction were encapsulated as shown previously. Figure 10 shows the rectification characteristic of a grown P-N junction rectifier as a function

of temperature. Failure above 200°C is believed to be due to an increase of the leakage current of the P-N junction in the low resistivity AlSb with increasing temperature.

The AlSb material was also tested for transistor action using a soldered base connection and point contact emitter and collector. With the collector and emitter points in an almost shorted position (emitter floating potential about equal to the voltage applied between the collector and base), it was possible to modulate the collector current with the emitter current but not to the extent that any power gain could be developed.

Acknowledgment

The authors are deeply indebted to Mr. William Hall for his services in growing the AlSb crystals.

The work was performed under Air Force Contract 33(616)-3481 which was sponsored by Wright Air Development Center, Air Research and Development Command, Wright-Patterson Air Force Base, Ohio.

Manuscript received Oct. 6, 1957. This paper was prepared for delivery before the Buffalo Meeting, Oct. 6-10, 1957.

Any discussion of this paper will appear in a Discussion Section to be published in the June 1959 JOURNAL.

REFERENCES

1. E. Burstein and P. Egli, "The Physics of Semiconductor Materials" excerpt from "Advances in Electronics and Electron Physics," Vol. VII, Academic Press, New York (1955).
2. W. C. Dunlap, "An Introduction to Semiconductors," John Wiley & Sons, Inc., New York (1957).
3. R. K. Willardson, A. C. Beer, and A. E. Middleton, *Phys. Rev.*, **91**, 243 (1953); *This Journal*, **101**, 354 (1954).
4. H. Welker, "Intermetallic Compound Semiconductors," *Techn. Rundschau* Nr 50, 30. Nov. 1956, Bern, Switzerland.
5. D. A. Jenny, Biennial Electronic Materials Conference, Philadelphia, June 1957; IRE Device Conference, Boulder, Colo., July 1957.
6. H. Welker, *J. Electronics* (London), **1**, 181 (1955).
7. R. N. Hall, "SiC Rectifiers," Semiconductor Device Research Conference, Boulder, Colo., July 1957.
8. O. G. Folberth and H. Weiss, *Z. Naturforsch.*, **8**, 615 (1955).
9. G. Pearson and T. Bardeen, *Phys. Rev.*, **75**, 865 (1949).
10. L. P. Hunter, "Handbook of Semiconductor Electronics," Chap. 10, p. 9; McGraw-Hill Book Co., New York (1956).
11. M. Tanenbaum, A. J. Gross, and W. G. Pfann, *J. Metals*, **6**, 762 (1954).
12. H. A. Goering, *et al.*, Battelle Mem. Inst. Scientific Contract AF 33(616)-2338 Reports 1 & 2.
13. R. I. Hodgkinson, *J. Electronics* (London), **2**, 201 (1956).
14. R. F. Blunt, H. P. R. Frederickse, and J. H. Becker, *Phys. Rev.*, **94**, 1431 (1954).

Anodic Polarography with a Rotating Platinum Microelectrode

II. Oxidation of Various Indole Alkaloids

M. J. Allen and V. J. Powell

Research Department, CIBA Pharmaceutical Products Inc., Summit, New Jersey

ABSTRACT

The results obtained by anodic oxidation of some indole alkaloids indicate that in an acidic medium a one electron change occurs with probable hydroxyl introduction into the aromatic portion of the molecule. This reaction appears to be specific for those alkaloids containing a 6-methoxyindole nucleus. In a neutral medium a two electron change occurs with resultant N-oxide formation in those alkaloids in which the nitrogen has available an unshared pair of electrons.

In a previous report (1), a reproducible-type electrode system was described and applied to an investigation of the oxidation of the leuco base of crystal violet. Since the indole alkaloids are subject to oxidative changes of one form or another and since no previous study has been reported on the anodic oxidation of these alkaloids, it was felt that it would be of interest to determine if definite half-wave potentials could be obtained for one or more of these reactions and attempt, if possible, to correlate the results with the site of oxidative attack on the molecule. Due to possible hydrolysis of the ester groups present in many of the alkaloids investigated it was decided to use only acidic or neutral media for the study in order to avoid introduction of a competitive chemical reaction.

Experimental

Reagents and solutions.—All solutions were prepared with reagent grade chemicals. The alkaloids used were of maximum purity as indicated by elementary analysis and infrared spectra.

Apparatus.—An H-type polarographic cell containing a centrally fused sintered disk was used in conjunction with a Leeds and Northrup Type E Electro-Chemograph. One side of the cell had its disk face covered with an agar plug and served for the standard calomel electrode. The other half of the cell was used for the sample solution. The platinum anode was identical to that described in the previous communication (1).

Procedure.—The cell containing a 10 ml sample was immersed in a constant temperature maintained at $30 \pm 0.1^\circ\text{C}$ and de-aerated for 10 min with nitrogen previously saturated with either methanol or aqueous-methanol depending on the medium used.

Results

For comparison purposes the results obtained are given in Table I.

Coulometric analysis indicated that those alkaloids which gave a wave in the acid medium underwent a one electron change, whereas those compounds which gave a wave in the neutral medium underwent a two electron change.

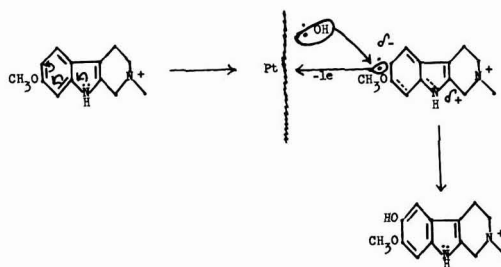
Since a wave was obtained with reserpine in an acidic medium, it was possible to estimate the

amount of this material in the presence of deserpidine which did not give a wave under these conditions. In Table II the *id* values are given for various concentrations of reserpine and reserpidine-deserpidine mixtures, and it can be seen that the values obtained for the mixtures do not differ significantly from those obtained for the various concentrations of pure reserpine.

Discussion

In order to obtain a wave in the acidic medium, the presence of the 6-methoxy group in the indole nucleus is essential under our experimental conditions, and the apparent one electron change obtained with the alkaloids containing this substituent can probably be attributed to the introduction of a hydroxyl group into the aromatic portion of the molecule. The assumption that the one electron change represents the introduction of a hydroxyl group is based on the experiences of various investigators who demonstrated that generally the initial step in the anodic oxidation of an aromatic system is the introduction of a hydroxyl group (2).

Based on the aforementioned observations the authors would like to propose the following mechanism for the introduction of a hydroxyl group in the alkaloids containing the 6-methoxy substituent.



This mechanism proposes a p-quinoid intermediate due to the activating influence of the 6-methoxy substituent which is strong enough to overcome the possible deactivating effect of the positively charged nitrogen in the ring adjacent to the indole nucleus. It is possible that this form is stabilized by adsorption on the electrode surface where an electron is removed and the radical combines with a hy-

Table I

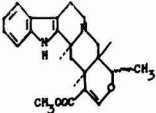
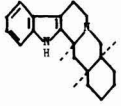
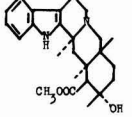
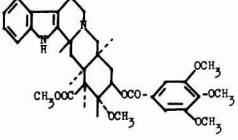
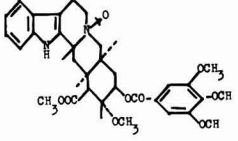
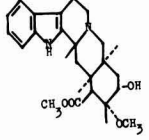
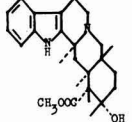
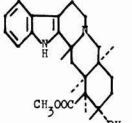
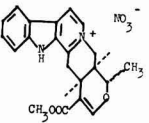
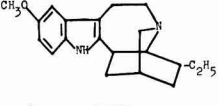

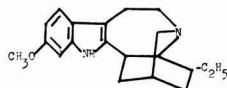
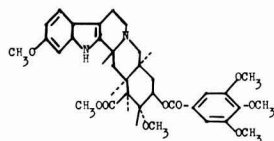
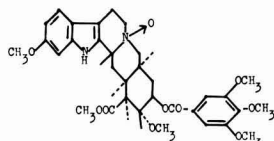
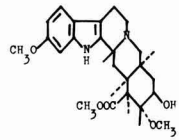
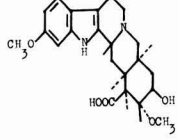
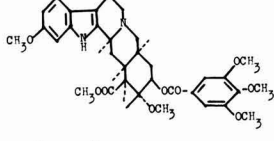
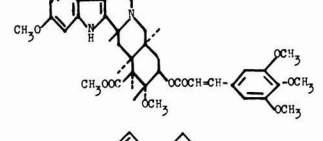
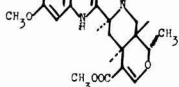
Aklaloid	Structure	Conc. in 0.2M LiCl (Abs. MeOH)	Conc. in 0.1N HCl (50% aq. MeOH)
Ajmalicine		$1.08-2.16 \times 10^{-4}M$ $E_{1/2} = +0.852$	No wave
Alloyohimbane		$1.50-3.00 \times 10^{-4}M$ $E_{1/2} = +0.805$	No wave
Corynanthine		$1.13-2.26 \times 10^{-4}M$ $E_{1/2} = +0.874$	No wave
Deserpidine		$0.692-3.462 \times 10^{-4}M$ $E_{1/2} = +0.849$	No wave
Deserpidine N-Oxide		No wave	No wave
Methyl Deserpidate		$1.41-1.88 \times 10^{-4}M$ $E_{1/2} = +0.781$	No wave
Yohimbine		$1.52-5.92 \times 10^{-4}M$ $E_{1/2} = +0.838$	No wave
3-epi- α -Yohimbine		$1.61-5.92 \times 10^{-4}M$ $E_{1/2} = +0.859$	No wave
Serpentine Nitrate		No wave	No wave
Ibogaine		$1.10-3.30 \times 10^{-4}M$ $E_{1/2} = +0.547$	No wave
Ibogamine		$1.11-3.33 \times 10^{-4}M$ $E_{1/2} = +0.577$	No wave

Table I (continued)

Tabernanthine		$1.84-6.12 \times 10^{-4}M$ $E_{1/2} = +0.460$	$1.84-6.12 \times 10^{-4}M$ $E_{1/2} = +0.720$
Reserpine		$1.36-1.78 \times 10^{-4}M$ $E_{1/2} = +0.618$	$1.46 \times 10^{-4}M$ $E_{1/2} = +0.738$
Reserpine N-Oxide		No wave	$1.20-1.28 \times 10^{-4}M$ $E_{1/2} = +0.714$
Methyl Reserpate		$1.21-6.27 \times 10^{-4}M$ $E_{1/2} = +0.650$	$1.25-6.27 \times 10^{-4}M$ $E_{1/2} = +0.832$
Reserpig Acid		$1.20-2.40 \times 10^{-4}M$ $E_{1/2} = +0.853$	$1.20-5.99 \times 10^{-4}M$ $E_{1/2} = +0.848$
Iso-Reserpine		$3.29 \times 10^{-4}M$ $E_{1/2} = +0.631$	$2.95 \times 10^{-4}M$ $E_{1/2} = +0.730$
Rescinnamine		$1.23-5.83 \times 10^{-4}M$ $E_{1/2} = +0.611$	$1.23-5.83 \times 10^{-4}M$ $E_{1/2} = +0.854$
Reserpinine		$0.749-3.746 \times 10^{-4}M$ $E_{1/2} = +0.655$	$0.644-2.576 \times 10^{-4}M$ $E_{1/2} = +0.848$

droxyl radical at the electrode with simultaneous expulsion of a proton to yield the 5-hydroxy substituted indole. That we do not detect the one electron change in going from :OH to ·OH tends to indicate that the loss of the one electron from the indole nucleus is the rate-determining step in the

reaction. The possibility of the formation of a less stable o-quinoid structure must not be overlooked. If this were to occur then substitution might very well take place in position 7. As no wave is observed under our experimental conditions with the methoxy group in position 5, the indications are that the p-quinoid structure predominates, and hydroxylation in position 5 is blocked by the substituent already present in this position. The fact that we do not observe this to occur in the unsubstituted indole nucleus can possibly be attributed to the deactivating influence of the positively charged nitrogen in the adjacent ring. Removal of this possible deactivating influence, as in indole itself, resulted in a wave at $E_{1/2} = +0.796$ v in an acidic medium.

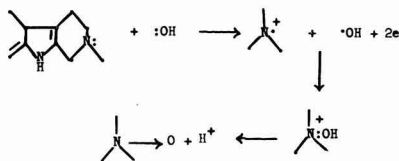
Table II. Reserpine and deserpidine in 0.1N HCl (50% aq. MeOH)

Reserpine conc. (moles/l)	id (μA)	Deserpidine conc. (moles/l)	Mixture of deserpidine and reserpine-id (μA)
0.644×10^{-4}	5.1	2.765×10^{-4}	5.2
1.288×10^{-4}	8.4	2.074×10^{-4}	8.6
1.932×10^{-4}	11.9	1.382×10^{-4}	11.9
2.576×10^{-4}	15.1	0.691×10^{-4}	14.9

It might be of interest to point to the analogous reactivity of 6-methoxy indole alkaloids with nitrous acid as compared to the resistivity of the unsubstituted and 5-methoxy indole alkaloids to reaction with this reagent (3).

The two electron change observed in a neutral medium can be attributed to the formation of N-oxides which have also been prepared by chemical means (4). Thus, as expected, reserpine N-oxide, deserpidine N-oxide, and serpentine nitrate, the latter being a quaternary salt, do not give a wave in the neutral medium because of the unavailability of the required pair of unshared electrons on the nitrogen atom. For the same reason a two electron wave is not observed in an acidic medium with those alkaloids which do show this in a neutral medium.

The mechanism proposed as a possible explanation for the observed 2 electron change is one which is analogous to that for the formation of hydrogen peroxide, i.e., $2 : \text{OH} \rightarrow 2 \cdot \text{OH} + 2e \rightarrow \text{H}_2\text{O}_2$, except



in this instance we would have at the electrode surface due to adsorption of the alkaloid molecule:

Manuscript received April 8, 1958.

Any discussion of this paper will appear in a Discussion Section to be published in the June 1959 JOURNAL.

REFERENCES

1. M. J. Allen and V. J. Powell, *Trans. Faraday Soc.*, **50**, 1244 (1954).
2. M. J. Allen, "Organic Electrode Processes," Reinhold Publishing Corp., New York (1958).
3. R. Haycock and W. J. Mader, *J. Am. Pharm. Assoc., Sci. Ed.*, **46**, 744 (1957).
4. M. Polonovski, *Bull. Soc. Chem. Belges.*, **39**, 1 (1930); C. C. J. Culvenor, *Revs. Pure Appl. Chem. (Australia)*, **3**, 83 (1953); W. I. Taylor, U. S. Pat. 2,789,112, 2,789,113, April 16, 1957.

The Preparation of Cadmium Niobate by an Anodic Spark Reaction

William McNeill

Pitman-Dunn Laboratories, Frankford Arsenal, Philadelphia, Pennsylvania

ABSTRACT

A new method of preparing cadmium niobate was demonstrated. This method involved the anodic spark reaction of cadmium in a niobate solution and crystallization of the anode product by heating at 650°C.

The crystallized anode product was made into a solid wafer by pressing it at 350,000 psi, and electrical measurements were made. Even though there was some evidence of impurity or porosity in the sample, a dielectric constant of about 600 was found at room temperature.

It is believed that anodic spark reactions might be employed to prepare a wide variety of complex oxides and possibly other compounds.

There are a number of metals, such as aluminum, magnesium, and tantalum, which exhibit high electrical resistances when made anodic in suitable solutions (1). This is due to the formation of an electrical barrier layer on the surface of the anode. The thickness of this layer is controlled by the voltage at which it is formed and is characteristic of the metal and solution used (2). For each such metal-electrolyte system there is a maximum voltage above which normal coating growth cannot occur. If this voltage is exceeded, electrical breakdown follows and, in many cases, sparking is observed on the anode surface (1, 3).

The high-voltage anodic processes for coating magnesium are examples of cases where sparking on the anode surface has a practical use. These coatings resemble ceramics and are composed of tiny particles of fused material. The fused material is a reaction product of the magnesium and the ions in the bath, and its properties can be controlled, to some extent, by the composition of the bath (4). For example, in the HAE process (5), aluminate in the

bath reacts with the magnesium, yielding identifiable spinels in the coating. With the Cr-22 process (6), the use of an ammoniacal bath appears to prevent the retention of free magnesium oxide in the coating, even though this compound would be expected as a product.

Cadmium niobate, $\text{Cd}_2\text{Nb}_2\text{O}_7$, has been shown to be a material with a high dielectric constant (7), similar in many ways to barium titanate. As would be expected, considerable research has been done, both on methods of preparation and determination of properties of this material (8). Conventional high-temperature preparation methods are complicated by the fact that cadmium oxide volatilizes and is lost from the reaction mixture, making control of composition a problem (9). In the work referred to, it was found that weight losses of 10-20% occurred on firing $\text{Cd}_2\text{Nb}_2\text{O}_7$ in air in the temperature range of 1300°-1400°C. Although the authors were able to prevent weight losses by using a double crucible with a CdO seal, they still concluded that phase studies of the system $\text{CdO-Nb}_2\text{O}_5$ were ren-

dered inaccurate due to thermal decomposition of $\text{Cd}_3\text{Nb}_2\text{O}_7$.

Since it had been shown that complex oxides could be formed in anodic spark reactions, it was thought that anodizing cadmium in niobate solutions might result in the formation of cadmium niobate.

Experimental

Niobate Solution Preparation

Potassium niobate was prepared by a method which was patterned after that of Reisman, *et al.* (10). A mixture containing 50.1 mole % K_2CO_3 and 49.9 mole % Nb_2O_5 (from A. D. Mackay, Inc., 198 Broadway, New York 38, N. Y.) was placed in a platinum crucible with the Nb_2O_5 in a layer on the bottom. This was placed in an electric furnace at 800°C and the temperature was then raised to 1075°C at $5^\circ\text{C}/\text{min}$. This temperature was held for about 10 min and then was dropped at $2^\circ\text{C}/\text{min}$ to 840°C . The fusion product was removed from the furnace at this temperature and air quenched.

After quenching, the solid cake was crushed, washed with 2% K_2CO_3 solution, and ground with sufficient additional K_2CO_3 (based on the original Nb_2O_5 content) to yield a mixture containing 57.5 mole % K_2CO_3 and 42.5 mole % Nb_2O_5 . This mixture was heated at 960°C , held at that temperature 16 hr, cooled to 425°C at $2^\circ\text{C}/\text{min}$, held at 425°C 1 hr, cooled to 215°C at $2^\circ\text{C}/\text{min}$, and then allowed to cool overnight to room temperature.

This solid product was crushed and washed, as above, and ground with sufficient additional K_2CO_3 (based on the original Nb_2O_5 content) to yield a mixture containing 90 mole % K_2CO_3 and 10 mole % Nb_2O_5 . The firing cycle for this mixture was the same as that for the 57.4 mole % mixture.

The product of this fusion, when dissolved in water, yielded a solution which was straw-yellow and clear. A sample of the solution which was allowed to stand several months remained clear and appeared to be quite stable. The solution was analyzed for niobate (10) and was found to be 0.118M in KNbO_3 . KOH and possibly K_2CO_3 were also present in the solution, but their concentrations were not determined. This solution, diluted 2 to 1 (to 0.04M) was the electrolyte used for subsequent anodic oxidation studies.

Apparatus

The cell used for the anodic oxidation studies was of simple design. It consisted of a 400 ml Pyrex beaker equipped with a rhodium plated copper cooling coil, a thermometer, and a magnetic stirrer. A niobium cathode and a cadmium anode were used. Niobium was used for the cathode because it was conveniently available in this laboratory. It was considered sufficiently inert for this purpose. There was no visible evidence of attack on the cathode. Protecting the anode at the electrolyte surface is usually difficult when the anode reaction involves sparking, and this case was no exception. Masks of plastic insulating tape became charred and were undercut by the electrolyte. This resulted in their rapid failure. This problem was overcome by using

$\frac{1}{4}$ in. diameter cadmium anode rods, onto which were forced tight-fitting Teflon sleeves, restricting the spark reaction to the flat end of the anode surface. Direct current, having less than 5% ripple, was supplied to the cell by a variable rectifier.

Operating Conditions

The operating conditions used during anodizing were selected arbitrarily for the most part, but were based on previous experience and published data on anode phenomena. An electrolyte temperature of 15°C was used because it was known that, when anodic electrical barrier effects are dependent on temperature, they are usually more pronounced at lower temperatures (1). A fairly dilute solution was used because it had been observed with magnesium anodes in chromate solutions that increasing the concentration not only lowered the spark voltage, but could stifle the spark reaction completely (11). Current densities between 0.25 and 0.75 amp/in.² were used with the niobate solutions. Agitation was used to minimize temperature and concentration gradients in the cell.

Results and Discussion

Anodic Oxidation

A number of Teflon-shielded cadmium rods were anodized using the conditions given above. In addition, one rod was anodized in 0.1N K_2CO_3 at about 1 amp/in.². There were very clearly marked differences between the anode reaction of cadmium in niobate and in carbonate solutions.

In the carbonate solution, the voltage rose to 75-80 v, but would rise no higher. At this point the current increased suddenly, and this was accompanied by the formation of a bulky gelatinous film which contained about 95% water. No further work was done with this solution.

In the niobate solution, the anode voltage was initially zero, but was raised manually to maintain the anode current density in the previously stated range. From zero to 75 v, film growth seemed fairly stable and, if the voltage was not continually increased, the current dropped to nearly zero in a few minutes. The coating that formed in this range was very thin and yellow (Fig. 1A). This was thought to be some form of cadmium niobate, but it was not identified.

In the range from 75 to 85 v, the current began to increase rapidly with each small increase in voltage. In this range, a continuous evolution of gas was observed at the anode, and a faint crackling noise could be heard. This noise grew louder as the voltage was raised. Sparks were visible on the anode surface only when the cell was viewed in a darkened room. If the coating was allowed to form in this range for a few minutes, the current dropped and the smooth yellow film, formed at lower voltages, grew thicker and became darker, approaching tan (Fig. 1B).

As the voltage was raised further, the darkening and thickening of the coating continued until at 180-200 v, a third type of anode product appeared. This was a bulky, loosely held cluster of fused particles. Figure 1B shows this coating beginning

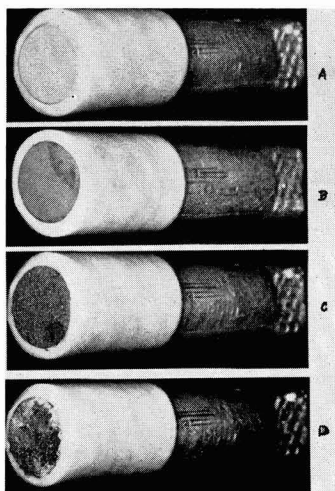


Fig. 1. Cadmium anode coatings in various stages of formation. A, 75 v; B, 75-200 v; C, 200-240 v; D, 200-240 v; prolonged anodic treatment. Magnification 4.5X before reduction for publication.

to form in one area, and in Fig. 1C the coating covers the anode surface. When the anodizing was continued and the current density was kept in the stated range, the voltage rose no higher than 240 v and fluctuated continually. Fluctuations of the current, corresponding inversely to those of the voltage, were also observed. When anodizing in this current and voltage range was prolonged, a stage was finally reached in which the fused reaction product broke away piecemeal, while the spark reaction continued at the anode surface. Figure 1D shows an anode from which material had been forming and breaking away for several hours.

Microscopic examination of all the coatings formed above 80 v in the niobate solution revealed a rough surface composed of fused particles. A sample of this is shown in Fig. 2. In this photograph, the blurred areas are due to the limited depth of focus obtainable with the magnifying camera.

An interesting phenomenon was noted in each anodizing run in niobate solution. As the anodizing continued, the solution became darker and darker. A gray-brown froth clung around the anode, and gray and yellow-brown fused solids were discharged

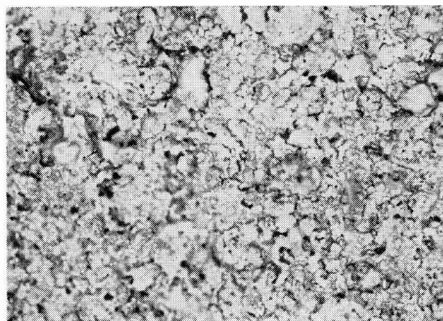


Fig. 2. Cadmium anode coating. Magnification 100X before reduction for publication.

into the solution from the anode. On standing overnight, the dark color of the solution disappeared and a small quantity of a white gelatinous product formed. This was mixed with a fused material, but was easily separated by flushing with water. The yellow-brown fused, or ceramic, material was examined as described in the following section.

Anode Product Study

A sample of the ceramic anode product was washed with distilled water and analyzed, using x-ray diffraction. No pattern was obtained. The same sample was heated for 2 hr at 650°C in an attempt to induce crystal growth. This is about 500° below the temperature at which cadmium oxide volatility becomes a problem in the usual thermal method of making cadmium niobate.

Cadmium oxide, niobium pentoxide, and a physical mixture of these two compounds were all heat treated in the same way as the anode product sample. X-ray diffraction patterns were obtained for all four materials, and also for a known sample of cadmium niobate which was obtained from the Signal Corps Laboratories at Fort Monmouth. The only pattern matching the standard was that of the crystallized anode material.

The original anode product might have been a physical mixture of cadmium oxide and niobium oxide which reacted during heat treatment to form cadmium niobate. This was discounted by the fact that the pattern for the heat-treated physical mixture of the two oxides failed to match that of the standard.

Since cadmium niobate is known to have very unusual electrical properties, attempts were made to convert the crystallized anode product to a solid wafer which could be used for electrical tests. It was desired to avoid high-temperature treatments; therefore, two samples of the crystallized anode product were pressed at room temperature, using pressures of 350,000 and 1,000,000 psi, respectively. Both samples were converted to solid brown wafers which appeared vitreous. Both wafers had small edge cracks which point in toward the center.

The central areas on both sides of each disk were painted with silver paint, and this was allowed to air dry. The wafers were dried in an oven for 24 hr at 110°C, and electrical measurements were made on them as soon as they had cooled to room temperature. The wafer pressed at 1,000,000 psi had almost zero resistance, and this appeared to be due to the silver paint having penetrated through a crack to cause a short circuit. The wafer pressed at 350,000 psi had a resistance of over 1 megohm, which was the limit of the impedance bridge. The results of the other electrical measurements on this specimen are shown in Table I.

Table I. Electrical characteristics of pressed, anodically formed cadmium niobate

	5000	10,000	20,000
Frequency (cps)	850	610	590
Capacitance ($\mu\mu\text{f}$)	0.08	0.022	0.009
Dissipation factor	890	639	618
Dielectric constant (calculated)			

d-c resistance = 1 megohm; thickness = 0.038 cm; silvered area = 0.50 cm².

Wainer and Wentworth (7) measured the dielectric constant and dissipation factor of cadmium niobate at 1000 cycles, obtaining values of 502 and 0.009. Shirane and Pepinsky (8) reported a dielectric constant of 310, measured at 10,000 cycles and room temperature. Hulm (12) obtained somewhat higher values for the dielectric constant at room temperature and noted considerable variation between samples.

The solid wafer appeared to have a strong tendency to absorb moisture. After standing for about 3 hr, exposed to a laboratory atmosphere of about 60% relative humidity, the d-c resistance was found to decrease from 1 megohm to 36,000 ohms. This and the pronounced frequency dependence of the dissipation factor were believed to indicate porosity or electrolytic impurity, or both.

Conclusions

Crystalline cadmium niobate can be prepared by a two-step process which includes: (a) the anodic oxidation of cadmium in a dilute potassium niobate solution, and (b) the heat treatment of the anode reaction product at 650°C for 2 hr.

Acknowledgment

This paper describes experimental work supported by the Ordnance Corps and conducted at Frankford Arsenal under project TB1-0004. The author wishes to express his appreciation to the Ord-

nance Corps for permission to publish this work. The author is also indebted to Dr. G. F. Nordblom, formerly of Frankford Arsenal, who first suggested the use of anodic processes to prepare ferroelectric materials.

Manuscript received Jan. 13, 1958.

Any discussion of this paper will appear in a Discussion Section to be published in the June 1959 JOURNAL.

REFERENCES

1. A. Guntherschulze, *Ann. Physik*, **34**, 657 (1911).
2. M. S. Hunter and P. Fowle, *This Journal*, **101**, 514 (1954).
3. A. Guntherschulze and H. Betz, *Z. Physik*, **78**, 196 (1932).
4. W. McNeill and R. Wick, *This Journal*, **104**, 356 (1957).
5. H. A. Evangelides, U. S. Pat. 2,723,952, Nov. 15, 1955.
6. W. McNeill, U. S. Pat. 2,778,789, Jan. 22, 1957.
7. E. Wainer and C. Wentworth, *J. Am. Ceram. Soc.*, **35**, 207 (1952).
8. G. Shirane and R. Pepinsky, *Phys. Res.*, **92**, 504 (1953).
9. L. Reed, T. Vasilos, E. D. Harris, and A. P. De Bretteville, "Dielectric and Phase Studies in the System CdO-Nb₂O₅," Signal Corps Engineering Laboratories, Fort Monmouth, N. J., Jan. 9, 1956.
10. A. Reisman, F. Holzberg, S. Triebwasser, and M. Berkenblit, *J. Am. Chem. Soc.*, **78**, 719 (1956).
11. W. McNeill, "Chromate Electrolytes for Anodizing Magnesium," Frankford Arsenal Report R-1191, March 1954.
12. J. K. Hulm, *Phys. Rev.*, **92**, 504 (1953).

Technical Notes



The Nature of Anode Slime

D. A. Vermilyea

Research Laboratory, General Electric Company, Schenectady, New York

When a metal is dissolved electrolytically the surface usually becomes covered with a dark-colored material known as "anode slime." This substance either continuously or periodically parts from the surface and falls downward through the solution. It has been thought that this anode slime comprised the impurities which were present in the metal. It is doubtful whether impurities in the metal are responsible, however, since copious quantities of anode slime are formed when silver containing less than 0.01% impurities is dissolved.

In order to determine the nature of the anode slime "high fine" silver (99.99%), obtained from Handy and Harmon Company, was dissolved anodically in a normal silver nitrate solution, pH 3, at about 1 amp/cm². The anode slime was recovered by filtration, washed, and examined. The x-ray diffraction pattern contained only the lines for metallic silver; no elements other than silver were detected

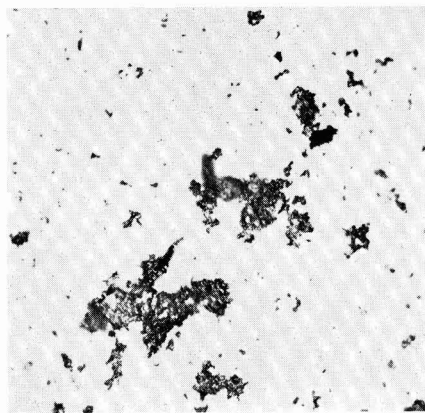


Fig. 1. Particles of anode slime from dissolution of silver. Magnification 100X.

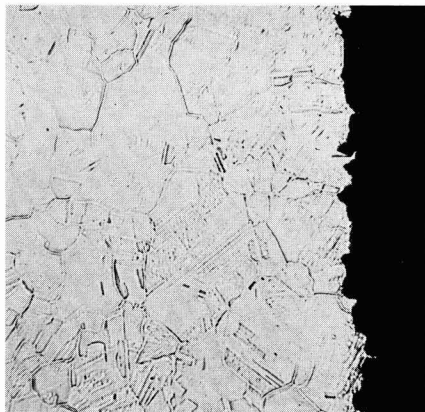


Fig. 2. Section perpendicular to the surface of a silver electrode from which silver was dissolved anodically. Magnification 500X.

by x-ray fluorescence; and chemical analysis showed that the slime was substantially all silver.

Figure 1 shows a photomicrograph of some of the slime particles. Under the microscope they appeared shiny and looked metallic. Figure 2 shows a section perpendicular to the edge of a specimen from which

some silver had been dissolved. The surface is very rough, and contains several promontories which look as though they were about to be cut off by the dissolution process.

It is concluded that the anode slime on silver consists of metallic silver; presumably the anode slime on other metals also consists of particles of the electrode metal. It seems likely that the mechanism of slime formation is as follows. Ordinary solutions contain many impurities, some of which adsorb on metal surfaces and cause "passivation." It is typical of silver particularly that electrodeposition from simple salt solutions results in the growth of only a few crystals, most of the surface of the electrode remaining inactive. It seems probable that in dissolution a similar passivation occurs, and that dissolution occurs only at isolated points. Apparently some sections of the metal surface remain passive and are cut off by dissolution from the sides, forming the silver particles which constitute the anode slime.

The experimental work described in this note was performed by W. R. Young, to whom the author is very grateful.

Manuscript received May 16, 1958.

Any discussion of this paper will appear in a Discussion Section to be published in the June 1959 JOURNAL.

Transport Numbers of the Pure Fused Salts, LiNO_3 , NaNO_3 , KNO_3 , and AgNO_3

Frederick R. Duke and Boone Owens

Institute for Atomic Research and Department of Chemistry, Iowa State College, Ames, Iowa

The alkali nitrates through potassium and silver nitrate were chosen for transport experiments as a series of salts similar in conductivity and charge type; the sizes and masses of the cations, however, are widely variant. Thus the series appears to be one in which the effects on mobility of size and mass of ions may be tested.

Experimental

The transport experiments were done in a cell which has been described previously (1). In all cases the electrodes were of solid Ag surrounded by molten AgNO_3 . When studying salts other than AgNO_3 , cells were used which contained a capillary constriction between the alkali nitrate which filled the upper portion of the cell and the AgNO_3 at the bottom in contact with the silver. The mixing that did occur took place in the capillary and is not important because it has been shown that there is very little volume change when these salts are mixed with AgNO_3 . Currents of about 50 ma for 1000 to 5000 sec were used when volume changes in the capillary were observed and several readings were taken for each salt. All salts were run at temperatures controlled to $\pm 1^\circ\text{C}$. The salts used were A. C. S. reagent grade.

Results and Discussion

In the cell $\text{Ag}; \text{AgNO}_3; \text{MNO}_3/\text{MNO}_3; \text{AgNO}_3; \text{Ag}$, the transport number of the cation M^+ is given by:

$$t^+ = \frac{1}{V_{\text{MNO}_3}} \left(\frac{\Delta V_c}{Z} + V_{\text{AgNO}_3} - V_{\text{Ag}} \right)$$

where V refers to the molar volumes, ΔV_c is the volume change of the catholyte, and Z is the current passed. The molar volumes were available from the literature (2-5).

The values of $\Delta V_c/Z$ and the resulting transport numbers are shown in Table I.

Since the membranes in all cases were made of sintered Pyrex, the transport numbers measured are those of the salt suspended in the pores of the glass;

Table I. Transport numbers and equivalent conductances of the ions and salts

Salt	λ (350°C)	V_c (cm ³) Eq.	t^+	λ + (350°C)	λ - (350°C)
LiNO_3	53.55	-0.5 ± 2.2	0.84 ± 0.06	45.0 ± 3.2	8.6 ± 3.2
NaNO_3	52.46	-2.2 ± 0.4	0.71 ± 0.01	37.2 ± 0.5	15.3 ± 0.5
KNO_3	35.55	-0.9 ± 1.3	0.60 ± 0.03	21.3 ± 1.1	14.2 ± 1.1
AgNO_3	55.82	-1.5 ± 2.6	0.72 ± 0.06	40.2 ± 3.3	15.6 ± 3.3

thus the glass takes the place of the solvent which is normally present in transport experiments, and the transport numbers are measured with respect to the glass. The rest of the apparatus and salt not in the membrane are merely conveniences to ascertain what happens in the membrane. It is assumed, in calculating mobilities of ions in fused salts, that the relative mobilities in the membrane and in the pure salt are the same; then $\lambda^* = t^+ \lambda$, where λ^* is the ionic equivalent conductivity in the pure salt, t^+ the transport number of the ion in the membrane, and λ the equivalent conductivity of the salt. Table I also contains ionic equivalent conductivities.

Since, in the membrane, the ions encounter resistance to motion by the ions immobilized at the glass surface, it might be expected that the size of the ion would be important. If, on the other hand, interactions of importance occurred only between ions of opposite charge, the interaction forces would cancel, and the controlling factor should be the momentum balance which depends on the masses of the ions. Sundheim (6) has shown that the mass dependence under these special conditions would be:

$$t_+ = \frac{m_-}{m_+ + m_-},$$

where the m 's are the equivalent weights of the ions. This transport number is of little significance because, in the general case, one would expect the two ions to impart momentum to the membrane, due to unequal interactions with the membrane.

The effect of size can be calculated; if it is assumed, for example, that the radius of the ion is the important factor, such as in Stokes law (7), the derivation below follows.

$$F_r = k r v$$

where F_r is the frictional force felt by a moving ion, k is the proportionality constant, r the ionic radius, and v the velocity of the ion. The electrical force felt by an ion in an electric field is: $F_e = E z e$, where E is the magnitude of the field, z is the valence of the ion, and e is the charge on the electron. Applying these equations to the case of the univalent salt, one arrives at the steady-state:

$$\frac{r_+}{r_-} = \frac{v_-}{v_+},$$

$$\text{and since } t_+ = \frac{v_+}{v_+ + v_-}, \text{ it follows that } t_+ = \frac{r_-}{r_+ + r_-}.$$

Table II lists the experimental transport numbers and the values calculated from the equation. TiCl

Table II. Experimental and calculated transport numbers

	t_+	r_+ (Å)	r_- (Å)	t_-
				$r_+ + r_-$
LiNO ₃	0.84 ± 0.06	0.60	2.3	0.82
NaNO ₃	0.71 ± 0.01	0.95	2.3	0.71
KNO ₃	0.60 ± 0.03	1.33	2.3	0.63
AgNO ₃	0.72 ± 0.06	1.26	2.3	0.65
TiCl	0.51 ± 0.02	1.44	1.81	0.55

The values for r_+ and r_{Cl^-} are taken from ref. (10); $r_{NO_3^-}$ is taken from ref. (11).

is included, representing a salt for which data are available (8). The agreement of experimental with calculated transport numbers is quite good, since the radii are those exhibited by certain solids rather than by liquids; and further, it is likely that, in general, the mobility depends on a more complex function of the radius than is assumed above.

The mass ratio equation agrees with the experimental data in the cases of the alkali nitrates since, for those involved here, the mass of the ion is very nearly a linear function of its radius. Salts other than univalent ones have not been included because they appear to be primarily anionic conductors (9) in spite of the small cation size or mass. Thus, it appears that the transport number is strongly dependent upon the relative charge of the cation and anion.

Manuscript received Oct. 1, 1957. It is Contribution No. 546; the work was performed in the Ames Laboratory of the U.S.A.E.C.

Any discussion of this paper will appear in a Discussion Section to be published in the June 1959 JOURNAL.

REFERENCES

1. F. R. Duke, R. W. Laity, and B. Owens, *This Journal*, **104**, 299 (1957).
2. J. Byrne, H. Fleming, and F. E. W. Wetmore, *Can. J. Chem.*, **30**, 922 (1952).
3. H. M. Goodwin and R. D. Mailey, *Phys. Rev.*, **25**, 469 (1907); *ibid.*, **26**, 28 (1908).
4. H. Bloom, I. W. Knapp, J. J. Molloy, and P. Welch, *Trans. Faraday Soc.*, **49**, 1458 (1953).
5. K. Scheel, *Z. Physik.*, **5**, 167 (1921).
6. B. R. Sundheim, *J. Phys. Chem.*, **60**, 1381 (1956).
7. M. F. R. Mulcahy and E. Heymann, *J. Phys. Chem.*, **47**, 485 (1943).
8. R. W. Laity and F. R. Duke, *This Journal*, **105**, 97 (1958).
9. E. Heymann and H. Bloom, *Nature*, **156**, 479 (1945).
10. L. Pauling, "The Nature of the Chemical Bond," 2nd ed., p. 346, Cornell University Press, Ithaca, N. Y. (1948).
11. A. F. Wells, "Structural Inorganic Chemistry," 2nd ed., p. 138, Oxford University Press, London (1950).



Report of the Chlor-Alkali Committee of the Industrial Electrolytic Division for the Year 1957

R. B. MacMullin

R. B. MacMullin Associates, Niagara Falls, New York

Jeff C. Cole

Diamond Alkali Company, Cleveland, Ohio

U. S. chlorine production in 1957 was 3,917,419 tons as compared to 3,797,702 tons for 1956. This represents an increase of only 3% above the 1956 level, whereas the trend during the past few years has been of the order of 7 or 8% increase per year. Electrolytic caustic production in 1957 increased 5% over 1956 although total caustic production increased only 2½%. Caustic soda made by the lime soda process continued to decline in 1957 and for the year represented only 7.9% of the total as compared to 10% in 1956.

The production of electrolytic potash declined somewhat in 1957. This is also true of the production of sodium metal. The total production of soda ash declined 6% in 1957, although the production of natural soda ash showed a slight gain. At the present time 87.4% of all soda ash is made by the synthetic process which now includes the manufacture of soda ash from caustic cell liquor. These results are summarized in Table I.

Chlorine produced coincidentally with caustic soda accounts for 90% of the total, as shown in Table II. Chlorine made in sodium cells accounts for 5.2%. Of the chlorine produced by brine electrolysis approximately 15.4% was made in mercury cells. In 1958 this figure is expected to increase to about 20%.

Approximately 1080 tons per day of new chlorine capacity was brought in during 1957. New chlorine

Table I. Chlor-alkali statistics, 1956 and 1957

	1957	1956
Chlorine, total tons	3,917,419	3,797,702
NaOH, electrolytic	3,975,609	3,794,963
NaOH, lime soda	341,210	422,034
NaOH, total	4,316,819	4,216,997
NaOH, per cent electrolytic	92.1	90.0
KOH, 90% basis	83,898	92,342
Na ₂ CO ₃ , synthetic	4,650,588	4,997,579
Na ₂ CO ₃ , natural	676,611	654,890
Na ₂ CO ₃ , total	5,327,199	5,652,469
Na ₂ CO ₃ , per cent synthetic	87.4	88.3
Na metal	132,977	136,018

Table II. Chlorine balance, 1957

	Tons	%
Cl ₂ equiv. of NaOH	3,523,384	90.0
Cl ₂ equiv. of KOH	47,714	1.2
Cl ₂ equiv. of Na	204,958	5.2
Cl ₂ equiv. of electrolytic soda ash	141,363	3.6
Cl ₂ equiv. of K ₂ CO ₃		
Cl ₂ equiv. of nitrosyl process		
Cl ₂ equiv. of HCl oxidation		
Cl ₂ total gas produced		

capacity is expected to increase by an additional 1400 tons in 1958. Total production capacity of chlorine for the country is expected to be of the order of 13,900 tons per day by the end of 1958. Because of the current recession it is predicted that the total chlorine production for 1958 will not exceed 4 million tons. This means that by the end of the current year production facilities for chlorine will be utilized only to the extent of about 80%. So far as we are aware no new plans for increased chlorine production have been announced since early 1957. It is assumed that the normal upward trend of chlorine production will resume at the conclusion of the present business recession.

In Canada, chlorine capacity in 1957 was of the order of 790 tons per day. This is expected to increase to approximately 945 tons per day by the end of 1958. (There will then be 12 Canadian plants.) Total Canadian production of chlorine in 1957 has been estimated at 210,000 tons.

Markets and End-Use Patterns

There have been no significant changes in the end-use pattern of chlorine and caustic soda during the year 1957. Long range trends, however, have been detected and projected into the future. Tables III and IV are quoted from a paper by Theodore Sheets, Jr.¹

The manufacture of high-energy fuels for military use could have a significant effect on the electrolytic industries. Boron fuels, for example, re-

¹ Chemical Engineering Progress, 53, 482 (1957).

Table III. Trends in chlorine use 1935-1975
(M Short Tons)

	Chemicals %		Pulp & Paper %		Sanitation %		Cotton Textiles %		Net Exports [†] %		Total Production
1935	161	48.8	109	33.0	35	10.6	19	5.8	6	1.8	330
1955	2,745.5	80.6	510	14.9	117	3.4	5.5	0.2	30	0.9	3,408
1956	3,113	82.3	527	13.9	122	3.2	4	0.1	19	0.5	3,785
1965	6,400	86.5	800	10.8	155	2.1	(7)*	(<0.1)*	45	0.6	7,400
1975	9,640	87.7	1,100	10.0	200	1.8	(10)*	(<0.1)*	60	0.5	11,000

[†] Net exports = exports minus imports.

* Absorbed in chemicals.

quire sodium hydride and boron trichloride, in turn made from sodium and chlorine. Hydrazine requires chlorine. Ammonium perchlorate requires sodium chlorate as a raw material. It is also significant that a number of industrial mergers have been formed to manufacture high-energy fuels; each group includes a chlor-alkali manufacturer.

Announcements of New Plants and Expansions

Among the new or expanded plants completed and brought into production in 1957 are the following: Allied Chemical and Dye Company, Brunswick, Ga., 260 tons per day total capacity; Columbia Southern, expansion at Lake Charles, La., 250 tons per day; Food Machinery Company, Westvaco Chemical Division, South Charleston, W. Va., rehabilitation and expansion by 90 tons to a total of 460 tons per day; Kaiser Aluminum and Chemical Corporation, Gramercy, La., 100 tons per day; Olin Mathieson Chemical Corporation, McIntosh, Ala., expansion 125 tons per day; Pennsalt Chemicals Corporation, Calvert City, Ky., expansion 100 tons per day; Weyerhaeuser Timber Company, Longview, Wash., new plant 80 tons per day.

Among the new plants scheduled to be completed in 1958 are the following: Columbia Southern, Natrum, W. Va., 160 tons per day (Uhde mercury cell); Diamond Alkali Company, Deer Park, Texas, 200 tons per day (DeNora 18 SGL); Dow Chemical Company, Plaquemine, La., 300 tons per day (Dow bipolar cell); Jefferson Chemical Company, Port Neches, Texas, 150 tons per day (Hooker S-3B cell); Wyandotte Chemical Corporation, Geismar,

La., 300 tons per day (Diamond diaphragm cell); Weyerhaeuser Timber Company, Longview, Wash., expansion 80 tons per day (DeNora cells); E. I. du Pont de Nemours, Memphis, Tenn., 100 tons per day (Downs sodium cell); Allied Chemical and Dye Company, Hopewell, Va., 90 tons per day (nitrosyl process).

In Canada, Dow has announced expansion at Sarnia, Ont.; Western Chemicals, du Vernay, Alta., is doubling its capacity to 80 tons per day in 1958; and Shawinigan Chemicals at Shawinigan Falls, Que., is building a new Krebs mercury cell plant, capacity 50 tons per day. The new Hooker plant at Vancouver, B. C., capacity 100 tons per day, commenced operations in late 1957. The Electric Reduction Company has built a new chlorate plant at Vancouver, B. C.

Diamond Alkali Company announced that it will terminate its lease on the Pine Bluff, Ark., Arsenal chlor-alkali facility as of April 27, 1958.

Chemical Salt Production Company, Salt Lake City, jointly owned by Hooker Electrochemical Company and Pennsalt Chemicals Corporation, is now producing chemical grade salt which is to be shipped to the owners' plants in the Tacoma-Seattle area.

Technical Developments

An outstanding paper describing horizontal and vertical mercury cell development in Europe and the United States was presented by Mr. H. A. Sommers, Air Products, Incorporated at the American Institute of Chemical Engineers meeting, Seattle,

Table IV. Trends in caustic soda—End-use
(M Short Tons)

	1935		1955		1965		1975	
		%		%		%		%
Chemicals	118	16.5	1,050	26.9	2,350	31.0	4,000	36.0
Rayon	158	22.0	695	17.8	680	9.0	780	6.9
Film	—	—	—	—	320	4.2	420	3.8
Pulp and paper	43	6.0	258	6.6	480	6.3	680	6.1
Export	71	9.9	227	5.8	330	4.3	450	4.0
Petroleum refining	90	12.6	215	5.5	335	4.4	460	4.1
Lyes and cleaners	31	4.3	160	4.1	295	3.9	390	3.5
Cotton textiles	34	4.7	137	3.5	190	2.5	250	2.2
Soap	96	13.4	82	2.1	60	0.8	55	0.5
Reclaimed rubber	11	1.5	27	0.7	10	0.1	—	—
Vegetable oils	9	1.3	24	0.6	35	0.5	45	0.4
All others (including metallurgical uses)	55	7.8	1,030	26.4	2,515	33.0	3,670	32.5
Metallurgical uses	—	—	—	—	(600)	(7.9)	(1,200)	(10.7)
Total production	716	—	3,905	—	7,600	—	11,200	—

Wash., June 1957. This article was published in full in the September and October issues of *Chemical Engineering Progress*, Vol. 53, p. 409 and 506. The October publication is an exhaustive tabular compilation of chlorine producing companies in the United States and Europe as of June 1, 1957 and proposed expansions by 1958. The data includes company names, plant locations, capacity, type of cells, and in some instances the number of cells and amperage.

Three important papers were presented at a symposium on "Trends in the Chlor-Alkali Industry" at the Baltimore meeting of the American Institute of Chemical Engineers in September 1957. The titles included the following: "End-Use" by T. A. Sheets, Jr., Diamond Alkali Company; "Technology" by

R. B. MacMullin, R. B. MacMullin Associates; and the "Inter-relationship Between the Chlor-Alkali and the Soda Ash Industries" by M. E. Clark, Frontier Chemical Company and C. F. Gerlach, Wyandotte Chemicals Corporation. The first and third of these papers have been published in *Chemical Engineering Progress*, Vol. 53, p. 482 and 537.

Some new data on the thermodynamic properties of chlorine and hydrochloric acid were published by C. J. Dobratz, *Chemical Engineering*, Vol. 65, No. 3, p. 144 (1958).

Manuscript received May 13, 1958. This paper was prepared for delivery before the New York Meeting, April 27-May 1, 1958.

Any discussion of this paper will appear in a Discussion Section to be published in the June 1959 JOURNAL.



Ottawa Meeting, September 28-October 2, 1958



Royal Canadian Air Force Photograph

Parliament Hill in Ottawa; Chateau Laurier on right

The Fall Meeting of the Society will be held at the Chateau Laurier in Ottawa, Ont., Canada, from September 28 to October 2, 1958. Under the chairmanship of Dr. John Convey, the Local Convention Committee of the Ontario-Quebec Section has prepared a program which promises to make the meeting a memorable one.

Accommodations are plentiful, although not all are in the headquarters hotel. For this reason, you are urged to mail your room reservation forms promptly, and to mention that

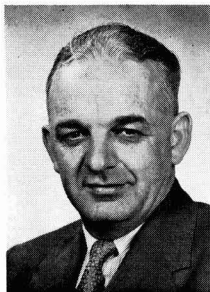
you are planning to attend The Electrochemical Society Convention. As registration and other fees should be paid in Canadian funds, visitors from the U.S.A. are urged to obtain Canadian funds before crossing the border.

The members of the Ottawa Local Committee are: John Convey, Chairman; T. H. Hawkins, Hotel; R. R. Rogers, Finance; Morris Cohen, Registration; W. R. Inman, Entertainment; R. A. Campbell, Publicity; J. S. McCree, Tours; and Miss F. E. Goodspeed, Ladies' Committee Liaison.

Members of the Ladies' Committee are: Mrs. John Convey, Chairman; Mrs. R. A. Campbell, Mrs. Morris Cohen, Mrs. T. H. Hawkins, Mrs. W. R. Inman, Mrs. R. R. Rogers, and Mrs. P. L. Stevenson.

Technical Program

The technical program is, of course, the responsibility of the various Divisions. Sessions will be conducted by the Battery, Corrosion, Electrodeposition, Electronics-Semiconductors, Electrothermics and Metallurgy, and Theoretical Electrochemistry Divisions. The high lights of the Electrodeposition sessions will be symposia on Electrodeposition on Uncommon Metals and Electrodeposition from Fused Salts. The Corrosion, Theoretical Electrochemistry, and Battery Divisions are jointly sponsoring a symposium on Films Formed in Contact with Liquids. The Corrosion Division has scheduled three general sessions. The Electronics Division-Semiconductor Group has scheduled symposia on Thermo-electric Materials and Device Design; Structural Chemistry, Preparation, and Properties of Compound Semiconductors; Physics and Chemistry of Silicon and Germanium Crystals; PN Junctions in Silicon and Germanium Crystals; and Surface Treatments and Device Technology. The Electrothermics and Metallurgy Division has scheduled symposia on Properties of Graphite; Arc Phenomena; Arc Applications, Oxidation; and Electric Smelting.



John Convey



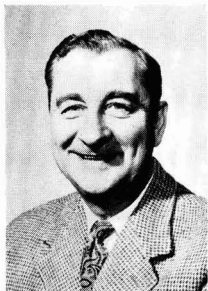
T. H. Hawkins



R. R. Rogers



Morris Cohen



W. R. Inman



R. A. Campbell



J. S. McCree



F. E. Goodspeed



Mrs. John Convey

The complete program appeared in the August JOURNAL (pp. 145C-169C).

Buffet Supper

On Monday evening, September 29, an opportunity will be provided for the registrants to relax and become better acquainted with one another at an informal Buffet Supper at HMCS Carleton on the shore of beautiful Dow's Lake in the western part of the city. Cocktails will be served beforehand, and there will be light entertainment following the dinner.

Society Luncheon and Acheson Medal Banquet

The Society Luncheon will be held on Monday, September 29, in the Ballroom of the Chateau Laurier. The Acheson Medal Award Banquet will take place on Tuesday, September 30, also in the Ballroom. At the banquet, cocktails will be served at 6:30 followed by dinner at 7:30 P.M.; dress is optional. Following the presentation of the Award, the guests are invited to linger for a program of entertainment.

Division Luncheons and Business Meetings

The Battery Division Luncheon and Business Meeting and Presentation of the Research Award of the Battery Division to Dr. John J. Lander will be held Tuesday, September 30, at 12:15 P.M. in Salons B-D. The

Corrosion Division Luncheon and Business Meeting will be on Wednesday, October 1, at 12:15 P.M. in the Banquet Room. The Electrodeposition Division Luncheon and Business Meeting will be on Wednesday, October 1, at 12:15 P.M. in Salons B-D.

Plant Trips

An unusual plant visit is in store for those who plan to spend Friday, October 3, at Atomic Energy of Canada Ltd. at Chalk River, Ont. On the same day, another group will visit the plant of Dominion Magnesium Ltd. at Haley, Ont., where magnesium is being produced by the Pidgeon electrothermic process.

Please register for trips early in the week. Each trip on Friday is limited to 40 persons; applications to see the atomic reactors at the Chalk River Plant had to be filed by July 30.

Most of the Canadian Government's scientific research work is centered in Ottawa, and visits have been arranged to laboratories of the National Research Council and the Dept. of Mines and Technical Surveys. A trip also has been arranged to visit the Dept. of Chemical Engineering and Chemistry of Ottawa University. These tours will be held on Thursday afternoon, October 2. At the National Research Council, visitors will see some of the work in progress in the Divisions of Applied Chemistry, Radio and Electrical Engineering, Building Research, and Mechanical Engineering. At the

Mines Branch of the Dept. of Mines and Technical Surveys, they will visit laboratories in the Divisions of Mineral Dressing and Process Metallurgy, Physical Metallurgy, Industrial Minerals, and Fuels.

Ladies' Program

A particularly interesting program is in store for the ladies. On Monday, September 29, they are invited to attend a conducted tour of the Canadian Parliament Buildings, under the distinguished patronage of Senator Mrs. F. E. Inman. A sight-seeing tour of the colorful Gatineau Hills on the Quebec side of the Ottawa River has been arranged for Tuesday, September 30, which will include lunch at the Country Club Lodge. On Wednesday, October 1, a visit will be made to one of Canada's scenic and exclusive clubs, the Seigniori Club, located about 50 miles due east of Ottawa, on land formerly held by a French seigneur. This locale perpetuates for us the memory of old French Canada. In addition, the ladies are invited to attend the Society Luncheon and Buffet Supper on Monday and the Banquet on Tuesday. A morning Coffee Hour will be a daily event.

It is suggested that each lady provide herself with walking shoes in order to enjoy the tours to the fullest extent.

The weather in Ottawa in early October is usually pleasant with temperatures in the range of 50°-60°F.

June 1959 Discussion Section

A Discussion Section, covering papers published in the July-December 1958 JOURNALS, is scheduled for publication in the June 1959 issue. Any discussion which did not reach the Editor in time for inclusion in the December 1958 Discussion Section will be included in the June 1959 issue.

Those who plan to contribute remarks for this Discussion Section should submit their comments or questions in triplicate to the Managing Editor of the JOURNAL, 1860 Broadway, New York 23, N. Y., *not later than March 2, 1959*. All discussion will be forwarded to the author, or authors, for reply before being printed in the JOURNAL.

J. J. Lander to Receive Battery Division's First Research Award

The Battery Division's first Research Award goes to Dr. John J. Lander, director of electrochemical research at the Delco-Remy Division of General Motors Corp. In naming Dr. Lander to its highest honor, the Battery Division pays tribute to his pioneering work on the kinetics of the anodic corrosion of lead, specifically for his paper in the June 1951 issue of this JOURNAL entitled "Anodic Corrosion of Lead in Sulfuric Acid Solutions." This work is one of a series of papers which helped to clarify many things which for years have been part of the art of battery technology. The Research Award will be presented to Dr. Lander at the Battery Division's Luncheon to be held during the Society meeting in Ottawa, September 28-October 2, 1958.

Dr. Lander, born in Elicottville, N. Y., in 1918, received a B.S. degree in chemistry from Canisius College, Buffalo, N. Y., and a M.S. and a Ph.D. degree in physical chemistry from the University of Maryland in 1942 and 1948, respectively. During the war, he served as a lieutenant in the U. S. Navy, being stationed at the Edgewood Arsenal and the Naval Research Lab. Following the war, he continued with the Naval Research Lab. until 1956, serving as a research chemist in the Electrochemistry Section of the Chemistry Division. From 1956 to 1958 he was research manager of the Battery Division of the Electric Auto-Lite Co.



J. J. Lander

In June 1958, he joined the Delco-Remy Division of General Motors Corp. as director of electrochemical research.

The Research Award of the Battery Division of The Electrochemical Society was established for the purpose of stimulating battery research and encouraging the preparation of high-quality papers for the JOURNAL of The Electrochemical Society. It is planned to select, every two years, the author or authors of a recent paper relating to electrochemical cells or batteries published in the

JOURNAL. The paper is selected primarily on the basis of scientific merit and importance. This includes originality of concept and experimental approach, thoroughness of experiments, and logic of conclusions. Clarity of presentation also is considered. The Research Award consists of an engraved scroll to each author of the chosen paper, along with prepaid membership in the Society and subscription to the JOURNAL as follows: single author—life membership and subscription; two authors—ten years' prepaid membership and subscription to each; three authors—seven years' prepaid membership and subscription to each.

The Research Award winner is chosen by a committee of five appointed by the Battery Division Chairman, consisting of the Chairman, the Divisional Editor, and three other members of the Division. The selection is approved by the Battery Division Executive Committee and the recommendations submitted to the Society Board of Directors for final approval. The present Award Committee consists of C. K. Morehouse, Chairman; U. B. Thomas, W. C. Vosburgh, E. F. Willihnganz, and W. S. Herbert. This group has been responsible for planning the Research Award and selecting the first recipient. The selection of Dr. Lander's paper was based on a review of over seventy papers published during the last ten years.

High Lights of the Board of Directors' Meeting

(Held April 27, 1958, Hotel Statler, New York, N. Y.)

The Secretary reported that, in the minutes of the previous Board Meeting, the name, B. E. Conway, appearing in the list of those present should have been John Convey. The minutes were approved as corrected.

The President announced that the Asia Foundation had sent the Society a check to subsidize the dues for our India Section members.

It was voted that The Electrochemical Society should participate in the Office of Critical Tables' Advisory Board, which has been set up by the National Academy of Sciences-National Research Council, and Dr. Ernest Yeager was appointed as our representative.

Dr. Henry B. Linford, Secretary of the Society, was appointed to act as the Society's representative at the Fiftieth Anniversary Celebration of

the Founding of the American Institute of Chemical Engineers, to be held during June 1958 in Philadelphia. The Resolutions Committee has prepared formal greetings to be presented at that celebration.

It was voted that Dr. W. C. Gardner perform, under the title of Acting President, the duties of the President's office until Dr. Sherlock Swann, Jr., is able to assume these duties.

The Treasurer presented the financial statement for the fiscal year ending March 31, 1958, and pointed out that the current value of our General Portfolio of Investments is \$70,000, of which \$22,000 was added during the year. Calculated on the basis of the full \$70,000 for the entire year, the earnings amounted to more than 3½%; at the same time,

the value of the securities decreased but \$330. The Treasurer advised that the possibility of adding to our Reserve Fund at a slower rate be considered.

The Secretary announced that the winner of the Young Author's Prize for 1957 was Dr. Paul Ruetschi. The Francis Mills Turner Memorial Award winner was Dr. A. C. Makrides; honorable mention was given to Dr. Milton Stern and Mr. K. M. Carlsen.

Recommendations were made for future meeting sites. The possibility of holding the Spring 1963 Meeting in Roanoke, Va., with alternates of New Orleans or Baton Rouge, will be investigated. It was felt that for the New York Meeting to be held in the fall of 1963, Atlantic City or Asbury Park should be considered.

Also, it was suggested that the 1965 Spring Meeting be held in the Mohawk-Hudson Section—Albany, Schenectady, or Saratoga, N. Y. For the Fall 1965 Meeting, it was suggested that either Minneapolis or Pittsburgh be selected.

The Board approved the establishment of an award to be given by the Battery Division in Ottawa. It was voted that names of famous scientists should not be used to designate unendowed divisional awards.

It was voted that all nonmember authors of papers presented at a national meeting shall be entitled to register at the members' rate. The sponsoring Division may choose to pay the registration fees of certain invited speakers. The Instructions to Members Inviting Speakers will be rewritten in line with this change in policy.

Recommendations made by the Ways and Means Committee to modify the Abstract of Rules and Regulations of The Electrochemical Society by declaring certain sections obsolete and amending others were approved.

The Executive Secretary was authorized to undertake the necessary negotiations to withdraw the microfilming right from Ashley-

Ratcliff and extend this to University Microfilms; also, the Executive Secretary is to negotiate with the Johnson Reprint Service for an agreement to reprint out-of-date issues of the JOURNAL.

The Acheson Award Committee reported that Dr. William J. Kroll has been selected as the recipient of the Acheson Award to be presented at Ottawa in the fall of 1958. Dr. Kroll was elected as the Perkin Medalist for 1958 by the Society of Chemical Industry, and was presented with this Medal in New York City on January 10, 1958.

Dr. Thurnauer, Chairman of the Sustaining Membership Committee, reported that, as the result of a campaign started after the Buffalo Meeting in October 1957, we now have a total of 14 new Sustaining Members. This campaign will be continued after the New York Meeting.

Dr. Koerker, Chairman of the Membership Committee, reported that as of April 1, 1958, the total membership of the Society was 2,784. This includes all categories and represents an 11% increase over the previous year's April 1 total.

Robert K. Shannon,
Executive Secretary

Secretary-Treasurer — Lawrence Young, Dept. of Chemistry, British Columbia Research Council, University of British Columbia, Vancouver 9, B. C.

George B. Adams, Jr.,
Past Chairman

Division News

Battery Division

The Nominating Committee of the Battery Division have nominated a slate of candidates for officers of the Division, subject to the election which will be held at the Division Luncheon and Business Meeting, Tuesday, October 1, 1958, in Ottawa:

For Chairman—J. C. White, Naval Research Lab.

For Vice-Chairman—E. J. Ritchie, Eagle-Picher Co.

For Secretary-Treasurer (one to be elected)—
Charles H. Clark, Signal Corps Engineering Lab.

Paul S. Brooks, National Carbon Co.

For Members-at-Large (two to be elected)—

Bernard Agruss, National Lead Co.

T. P. Dirkse, Calvin College
Arthur Fleischer, Thomas A. Edison Lab.

W. J. Hamer, Bureau of Standards

W. S. Herbert, Ray-O-Vac Co.
C. K. Morehouse, RCA Research Lab.

Additional nominations may be made by any member of the Division, either in writing to the Division Chairman, or from the floor at the election, provided the nominee's willingness to serve if elected has been obtained. The Nominating Committee members were: N. C. Cahoon, Chairman; A. F. Daniel, J. J. Lander.

E. J. Ritchie, *Sec.-Treas.*

E & M Symposium on Mechanical Properties of Intermetallic Compounds

The Electrothermics and Metallurgy Division announces a Projected Symposium on "Mechanical Properties of Intermetallic Compounds" to be held during the 115th Meeting of The Electrochemical Society in Philadelphia, Pa., May 3-7, 1959.

For the purposes of this Symposium, intermetallic compounds will be held to comprise all intermediate phases in binary or higher order sys-

Section News

San Francisco Section

The last regular meeting of 1957-1958 was held on May 28, 1958 at the University of California's International House in Berkeley. The technical program featured a talk by Dr. David R. Stern, assistant manager of research for the American Potash & Chemical Corp., on "Lithium in Electrochemistry."

The speaker began by reviewing the history, raw materials, and producers of lithium chemicals; non-electrochemical applications were discussed briefly.

The electrochemical production of lithium metal from a fused LiCl-KCl eutectic was described and various cell designs were shown. In view of the high value of lithium chemicals, it was pointed out that chemical utilization is more important than current efficiency in this electrolysis. Lithium alloys can be produced directly by electrochemical reduction.

Lithium salt additives in electrolytic processes (both aqueous and fused salt) may have various beneficial effects, e.g., a decrease in melting point, viscosity, or polarization, an increase in conductivity or cell capacity, etc.

Lithium compounds find uses in secondary batteries (Edison Cell) as well as in primary cells (e.g., low-temperature dry cells). Electrothermic applications include the electric melting of glasses and welding fluxes.

It was pointed out that the availability of lithium chemicals has been increasing and the prices decreasing, thus making possible new applications all the time.

An interesting question and discussion period followed the formal part of the talk.

Morris Feinleib, *Chairman*

Pacific Northwest Section

The following recently were elected new officers of the Pacific Northwest Section for 1958-1959:

Chairman—Henry J. Wittrock, Dept. of Metallurgical Research, Kaiser Aluminum & Chemical Corp., Spokane 69, Wash.

Vice-Chairman—Glen C. Ware, Nonferrous Metals Branch, Region II, Bureau of Mines, Albany, Ore.

tems of true metals, including superlattices. Interstitial compounds of metals and nonmetals, such as the carbides, nitrides, borides, etc., will not be considered.

It is hoped to include papers covering the following topics:

Mechanical Properties of Intermetallic Compounds

Fundamental Behaviors: Deformation Modes; Initiation and Propagation of Fracture; Effects of Crystal Structure; Dislocations in Intermetallic Compounds; Influence of Point Defects; Radiation Damage.

Phenomenology: Effects of Processing Variables; Temperature Dependence of Mechanical Properties; Effects of Impurities; Effects of Alloying; Effects of Stress State and Strain Rate.

Experimental Techniques: Testing Techniques Applicable to Brittle Compounds; Preparation of Intermetallic Compounds with Reference to Mechanical Property Studies, e.g., Single Crystal, and High-Purity Samples.

Titles and authors of proposed papers should be sent immediately, and triplicate copies of 75-word abstracts by January 2, 1959, to the Secretary-Treasurer of the Electrothermics and Metallurgy Division (please underline the name of the author who will present the paper):

Dr. J. H. Westbrook
Research Lab.
General Electric Co.
P.O. Box 1088
Schenectady, N. Y.

Arrangements can be made for authors residing outside the United States who wish to have papers presented *in absentia*.

Industrial Electrolytic Division

At the New York Meeting of the Society in May, the following new officers of the Industrial Electrolytic Division were elected for 1958-1959:

Chairman—J. C. Cole, Diamond Alkali Co., 300 Union Commerce Bldg., Cleveland 14, Ohio

Vice-Chairman—W. D. Sherrow, Great Lakes Carbon Corp., Niagara Falls, N. Y.

Secretary-Treasurer—R. F. Bechtold, Dow Chemical Co., Western Div., P. O. Box 351, Pittsburg, Calif.

Walter J. Sakowski, Olin Mathieson Corp., Niagara Falls, N. Y., continues to represent the Division's membership interests.

J. C. Cole, *Chairman*

New Members

In July 1958, the following were elected to membership in The Electrochemical Society by the Admissions Committee:

Active Member Sponsored by a Sustaining Member

Albert V. Collins, McGean Chemical Co., Box 2277 Brooklyn Station, Cleveland, Ohio (Electrodeposition)

Active Members

Charles T. Brown, Battelle Memorial Institute; Mail add: 196 Highfield Dr., Columbus 14, Ohio (Electrodeposition)

Fred P. Burns, Chatham Electronics, Div. of Tung Sol Electric; Mail add: 17 Sheridan Rd., Summit, N. J. (Electronics)

Sidney Burger, S. Burger, Inc.; Mail add: P. O. Box 127, Bound Brook, N. J. (Electronics)

Albert J. Cook, International Business Machines Corp.; Mail add: 16

Peter Cooper Dr., Poughkeepsie, N. Y. (Electric Insulation, Electronics, Theoretical Electrochemistry)

Barlane R. Eichbaum, International Business Machines Corp.; Mail add: 52 Homer Pl., Poughkeepsie, N. Y. (Electric Insulation, Electronics, Electrothermics & Metallurgy, Theoretical Electrochemistry)

Warren T. Eriksen, Raytheon Manufacturing Co.; Mail add: Old Farm Circle, R.F.D. #2, Wayland, Mass. (Electronics)

Jack E. Field, E. I. duPont de Nemours & Co.; Mail add: 60 Delvin Terrace, Wilmington 5, Del. (Electronics)

Reinhard Glang, Diamond Ordnance Fuze Lab.; Mail add: 5601 13th St., N.W., Washington 11, D. C. (Electronics)

Ernest Jost, Metals and Controls Corp., Attleboro, Mass. (Corrosion, Electrodeposition, Electrothermics & Metallurgy, Theoretical Electrochemistry)

Tomoo Kirihara, Columbia University, School of Mines; Mail add: c/o Mrs. Elisa Capobianco, 811 Riverside Dr., New York 32, N. Y. (Electrothermics & Metallurgy)

Robert K. Kulp, Electro Metallurgical Co.; Mail add: 333 Buffalo Ave., Niagara Falls, N. Y. (Electrothermics & Metallurgy)

Sheldon L. Matlow, Hoffman Electronics, Semiconductor Div., 930 Pitner, Evanston, Ill. (Electronics)

William J. Moroney, C.B.S.—Hytron; Mail add: 175 Topsfield Rd., Danvers, Mass. (Electronics)

James R. Nall, Diamond Ordnance Fuze Lab.; Mail add: 3321 Pendleton Dr., Silver Spring, Md. (Electronics)

Robert N. O'Brien, University of Alberta, Dept. of Chemistry, Edmonton, Alberta, Canada (Theoretical Electrochemistry)

Manuscripts and Abstracts for Spring 1959 Meeting

Papers are now being solicited for the Spring Meeting of the Society, to be held at the Sheraton Hotel in Philadelphia, Pa., May 3, 4, 5, 6, and 7, 1959. Technical sessions probably will be scheduled on Electric Insulation, Electronics (including Luminescence and Semiconductors), Electrothermics and Metallurgy (including a Projected Symposium on "Mechanical Properties of Intermetallic Compounds"), Industrial Electrolytics, and Theoretical Electrochemistry.

To be considered for this meeting, triplicate copies of abstracts (*not to exceed 75 words in length*) must be received at Society Headquarters, 1860 Broadway, New York 23, N. Y., *not later than January 2, 1959*. Please indicate on abstract for which Division's symposium the paper is to be scheduled, and underline the name of the author who will present the paper. Complete manuscripts should be sent in triplicate to the Managing Editor of the JOURNAL at the same address.

★ ★ ★

The Fall 1959 Meeting will be held in Columbus, Ohio, October 18, 19, 20, 21, and 22, 1959, at the Deshler-Hilton Hotel. Sessions will be announced in a later issue.

By action of the Board of Directors of the Society, all prospective members must include first year's dues with their applications for membership.

Also, please note that, if sponsors sign the application form itself, processing can be expedited considerably.

Mary Jo Pribble, Marietta College, Dept. of Chemistry, Marietta, Ohio (Battery)

Simon A. Prussin, Pacific Semiconductors, Inc., 10451 W. Jefferson Blvd., Culver City, Calif. (Electronics)

Robert L. Rouse, Associated Electrical Industries; Mail add: 53 Alexandra Rd., Reading, Berkshire, England (Electronics)

Kenneth Speigel, C.B.S.—Hytron, Advanced Development Lab., Newburyport, Mass. (Electronics)

William C. Spindler, U. S. Naval Ordnance Lab.; Mail add: Box 232, Norco, Calif. (Battery)

Sydney Wagner, R.C.A. Victor Co., Ltd., Research Labs., 1001 Lenoir St., Montreal 30, P. Q., Canada (Electronics)

Leo Wootntr, Radio Corp. of America; Mail add: 3416 Home Ave., Marion, Ind. (Electronics)

Associate Member

Alan J. Carlan, Hoffman Semiconductor Div.; Mail add: 1807 Monroe St., Evanston, Ill. (Electronics, Theoretical Electrochemistry)

Student Associate Member

George Economy, Ohio State University; Mail add: 179 W. Frambes, Columbus 1, Ohio (Theoretical Electrochemistry)

Reinstatements to Active Membership

John Betley, Lansdale Tube Co., Div. of Philco Corp.; Mail add: 44 Green St., Lansdale, Pa. (Electronics)

Charles A. Escoffert, International Rectifier Corp.; Mail add: 7913 Beland Ave., Los Angeles 45, Calif. (Electronics)

Transfer from Associate to Active Membership

Edmund R. Hogan, Jr., National Carbon Co., Div. of Union Carbide Corp.; Mail add: 329 Orchard Rd., Grand Island, N. Y. (Industrial Electrolytic)

Deceased Members

John J. Chapman, Baltimore, Md.
Arthur R. Ferguson, Indianapolis, Ind.

Polykarp Herasymenko, New York, N. Y.

Harvey C. Waechter, Lewiston, N. Y.

Personals

Harley C. Lee, vice-president and director of Basic Inc., Cleveland, Ohio, recently was awarded the Benjamin G. Lamme Medal of Ohio State University, one of that institution's highest honors. The gold medal is awarded each year to an alumnus of Ohio State in recognition of "meritorious achievement in engineering or the technical arts." Widely recognized in steel and other industries for his pioneering research and development work in the field of basic refractories, and holder of many patents, Mr. Lee earned his bachelor's degree in mining engineering from Ohio State in 1927.

Charles Sheer, former arc research department head, has been named chief scientist of Vitro's West Orange Lab. The laboratory is one of three facilities operated by Vitro Labs., a division of Vitro Corp. of America. In his new post, Dr. Sheer will be responsible for scientific guidance and general consultation in high-intensity arc research and development. Active for almost 25 years in arc research, Dr. Sheer is co-inventor of the Sheer-Korman Process employed in various high-temperature chemical and metallurgical applications.

Frank P. Schiro, formerly manager of Govt. Sales and Application Engineering Depts. of Mallory Battery Co., Cleveland, Ohio, has joined ACR Electronics Corp., 551 W. 22 St., New York City, as vice-president of sales.

Roger Whaley Sanderson

Roger Whaley Sanderson, a senior member of the Research Labs. of the General Electric Co. Ltd., Wembley, England, died recently at the age of 58.

Mr. Sanderson was educated at King Edward's School, Birmingham, and entered Birmingham University in 1918, gaining an honors degree in physics and chemistry in 1920. He then did research work for the Dept. of Scientific and Industrial Research in the university, and joined the staff of the G.E.C. Research Labs. in 1923. He was responsible for research and development work on primary batteries until 1957 when he took charge of a newly formed group working on corrosion problems.

He was a member of The Electrochemical Society and the Institute of Metal Finishing. He served on

various B.S.I. Committees and was permanent chairman of the Battery Committee of the International Electrotechnical Commission.

News Items

ECS Members Among Those Awarded Citations of Honor

At the June 14 dedication of the Dana Science Building of Indiana Technical College, Fort Wayne, Ind., "Citations of Honor" were awarded to "100 Midwestern leaders in science, engineering, and industry" from the five-state area, Indiana, Ohio, Illinois, Michigan, and Kentucky.

Members of The Electrochemical Society who received awards were: George W. Heise, (retired) associate director of research, National Carbon Research Labs., Cleveland, Ohio; Clyde E. Williams, president, Clyde Williams & Co., Columbus, Ohio; and Mars G. Fontana, professor of metallurgical engineering, Ohio State University, Columbus, Ohio.

Symposium on "Electrolytic Cells"

A symposium on "Electrolytic Cells" will be held at the Central Electrochemical Research Institute, Karaikudi, India, during the fourth week in December 1958, the exact date to be announced.

The scope of the symposium is as follows: 1. industrial electrolytics; 2. electrometallurgical processes; 3. other miscellaneous applications; 4. recent advances in fundamental aspects of electrolytic cells.

Papers may be contributed dealing with the design, operation, chemical control, and other aspects of electrolytic cells which generally fall within the scope of the above sections.

Abstracts of papers (not exceeding 100 words) should be sent to the convenor of the symposium, Dr. H. V. K. Udupa, Assistant Director, Central Electrochemical Research Institute, Alagappa College P.O., Karaikudi, S. Rly., India, *not later than September 15, 1958*, and com-

1957 Bound Volume Available

A limited number of the bound volume of 1957 JOURNALS (Vol. 104) are available from Society Headquarters, 1860 Broadway, New York 23, N. Y., at \$18.00 per copy to nonmembers, including subscribers, and \$12.00 per copy to ECS members, subject to prior acceptance.

plete papers (not exceeding 3000 words) by November 15, 1958. Arrangements can be made for presentation of papers of those unable to attend the symposium.

H. E. Head Elected AES President

At its Annual Meeting held in May, the governing council of the American Electroplaters' Society elected Herberth E. Head, Chrysler Corp., Detroit, as the society's National President succeeding Francis T. Eddy, president, Technicraft Labs., Inc., Thomaston, Conn. Mr. Head had served as First Vice-President during the society's previous fiscal year.

A native of Owensboro, Ky., now residing in Detroit where he is an engineer with the Chrysler Corp., Mr. Head has been associated with the automotive industry for nearly 40 years, the bulk in electroplating.

Mr. Head's other professional affiliations include The Electrochemical Society, the American Society for Testing Materials, the Society of Automotive Engineers, the Engineering Society of Detroit, and the Seahorse Institute (Corrosion).

Union Carbide Has Spent over \$60,000,000 on Five-Year Research Construction Program

During the past five years, Union Carbide has spent over \$60,000,000 on the expansion of research and development facilities, according to Morse G. Dial, president. Included in this program are seven new research and development laboratories and extensive new research facilities at four other existing laboratories. As a result of this construction program, the corporation has doubled its research and development operating budgets during this five-year period and, in 1957, expenditures amounted to approximately \$65,000,000. Mr. Dial also stated that research expenditures for 1958 will continue at the same level as in 1957.

Dr. Augustus B. Kinzel, vice-president of research at Union Carbide, pointed out that the research program includes the Union Carbide Research Institute. Dr. Kinzel said,

JOURNAL ELECTROCHEMICAL SOCIETY

Wanted to Buy.

Back sets, volumes, and issues of this JOURNAL and TRANSACTIONS.

Especially volumes 1, 3 and from volume 60 to date.

We pay good prices.

Buy also Technical and Scientific Periodicals.

E. O. ASHLEY, 27 E. 21 St., N. Y. 10, N. Y.

Changes in E & M Program, Ottawa Meeting

The paper by R. P. Morgan and T. E. Butler, "Arc Behavior in Variable Pressure Systems" (Abstract No. 134), has been withdrawn from the Electrothermics and Metallurgy Symposium on Arc Phenomena.

In its place on Tuesday, Sept. 30, at 10:55 A.M., H. V. Kinsey will present a paper by J. W. Suiter, "Some Effects of Pressure on Consumable Electrode Arc Melting."

"The Institute was formed a year ago to supplement our basic research for the corporation. We have always held that an aggressive fundamental research program is essential to our corporate growth, and in past years have expanded our basic research program to keep it commensurate with the increasing size of our corporation and its broader interests. The Institute is now operating in small temporary quarters in White Plains, N. Y., and has been assigned space in the corporation laboratory facilities now under construction at Sterling Forest, N. Y."

At Sterling Forest, Union Carbide is building one of the largest privately owned nuclear research laboratories in the country. In a temporary laboratory on the site, a staff of scientists and engineers is now seeking answers to some vital scientific and economic questions concerning the utilization of atomic energy. Their research includes studies of ways to expand the use of radioisotopes in industry and to industrialize the by-products of nuclear energy. In close association with this nuclear research laboratory, a new ore research organization at the same location is working to develop more efficient methods of detecting, mining, and extracting profitable mineral raw materials for industry.

Other new Union Carbide research laboratories recently completed, or nearing completion, include: a laboratory at Parma, Ohio, concerned principally with physical sciences and their application to chemical problems; a laboratory at Speedway, Ind., working on crystal growth, flame-plating, and other super high-temperature arc studies; and a plastics research laboratory at Bound Brook, N. J., just being occupied. New research facilities have also been added at the corporation's metals research laboratories at Niagara Falls, N. Y., and the cryogenics (low temperature) and inorganic chemical research center at Tonawanda, N. Y. The Tonawanda facilities now have a new radiation

The paper by E. A. Gulbransen and K. F. Andrew, "Oxidation Studies on the Iron-Chromium-Aluminum Heater Alloys," will be presented at 3:00 P.M. on Wednesday, Oct. 1, 1958, before the Electrothermics and Metallurgy Symposium on Oxidation. The August issue of the JOURNAL containing the Program also lists it for presentation before the Corrosion General Session on Wednesday, Oct. 1.

laboratory, using a 4200-curie cobalt 60-source to conduct radiation experiments.

Aluminum Industry's Newest Reduction Plant Now in Production

The nation's second largest aluminum reduction plant is now in production, Ormet Corp. announced recently. Full-scale operation at the \$110,000,000 Ormet facility is scheduled for the end of the year.

Ormet is owned jointly by Olin Mathieson Chemical Corp. and Revere Copper and Brass Inc.

Located between Clarington and Hannibal, Ohio, the new facility has an annual capacity of 180,000 tons of primary aluminum. When in full production, Ormet will be the nation's fourth largest aluminum producer.

Ormet was formed in August 1956 to construct, own, and operate the primary aluminum production facilities for the two companies. Of the 180,000 tons of aluminum to be produced annually by Ormet, Olin Mathieson will receive 120,000 tons and Revere 60,000.

Enthone Products to be Manufactured in Italy

Enthone, Inc., of New Haven, Conn., a subsidiary of American Smelting and Refining Co., has announced the licensing of Compagnia Italiana Galvanotecnica of Milano to manufacture, distribute, and service the complete line of Enthone metal finishing chemicals in Italy. The Italian firm is well known in the plating industry and has a competent staff of engineers and chemists to provide technical assistance in the use of Enthone products. Their headquarters is at Viale Pasubio 8, in Milan.

With the completion of this arrangement, Enthone products are now manufactured in five European countries and distributed throughout Western Europe. In addition to Italy, manufacturing operations are conducted by firms in England, France, Sweden, and West Germany.

New Translation Service Initiated by SLA Translation Center

The Special Libraries Association Translation Center, located at the John Crerar Library in Chicago, has announced that it can now furnish, on a subscription basis, printed catalog cards for current scientific and technical material which has been translated into English from all languages, including Russian. This latest effort of the Center to facilitate the exchange and growth of scientific knowledge in the Western World will make available in easy-to-use, up-to-date card form the thousands of citations given in the Center's bibliographical journal, *Translation Monthly*.

Four types of subscriptions to translation catalog cards are available: 1. full coverage of *Translation Monthly* (approximately 12,000 titles yearly); 2. coverage of all translations currently received by the Center (approximately 6750 titles yearly); 3. coverage of all Russian translations received by the Center (approximately 3100 titles yearly); 4. coverage of all titles in specific subject fields.

Special Libraries Association is an international organization of profes-

sional librarians and information experts who serve industry, business, scientific research, educational and technical institutions, government, newspapers, and other organizations. Since 1909, the Association has promoted the collection, organization, and dissemination of information in specialized fields and has published professional and bibliographical books and journals. The development of the Translation Center is one of its most recent and significant projects.

The SLA Translation Center was established at the John Crerar Library in October 1953, and its size, scope, and services have developed at a remarkable rate. A staff of four is now kept busy serving the scientific community by accumulating, cataloging, and circulating translations and copies of translations.

In less than five years, the original collection of 932 translations has increased to more than 20,000 items, and approximately 6750 titles are being added annually. At the request of the National Science Foundation, the SLA Translation Center took over, in January 1957, the Russian translations then housed in the Scientific Translations Center at the

Library of Congress. This added 4000 Russian items to the collection and, since then, Russian material has been received regularly—about 3000 titles a year—as have translations from all other languages.

Further information about the SLA Translation Center and its services may be obtained from: The SLA Translation Center, The John Crerar Library, 86 E. Randolph St., Chicago 1, Ill.

English Edition of Japanese Journal

The first English edition issue of the *Journal of the Electrochemical Society of Japan* was published recently. Since 1933, the society has published the journal in Japanese with a few lines of English abstract. In 1956, the English abstracts were expanded to a full page per report. This year, the society undertook the publication of an English quarterly edition. The first English quarterly edition, 52 pages, contains English translations of 15 reports of original Japanese works included in Vol. 26, No. 1-3 (1958) of the journal.

The overseas membership fee is \$5.00 per year and the price of a single copy of the English edition journal is \$1.50, including postage.

Standard Samples of Phosphors

The National Bureau of Standards recently made available 14 standard samples of phosphors selected in cooperation with The Electrochemical Society. The samples were prepared under the supervision of Dr. A. F. Forziati in the dental research laboratory and may be obtained from the Standard Sample Section, National Bureau of Standards, Wash-

ington 25, D. C. The phosphor samples are for industrial and research use in quality control and development of improved phosphors for radar screens, television sets, and radioactivity counters and detectors. The main concern in preparing the samples was to achieve uniformity of characteristics and, thus, to provide a fixed basis for comparison with other phosphors.

The 14 standard samples of phosphors that have thus far been prepared are listed in Table I, together with their symbolic formulas, weights, and prices. The spectral emission of these phosphors varies from the ultraviolet through the blue and red regions of the spectrum when excited by ultraviolet radiation (2537Å or 3650Å) or by cathode rays.

Table I. Phosphor standard samples

Sample No.	Name	Symbolic formula	Remarks	Approx. wt in grams	Price per sample
1020	Zinc sulfide phosphor	ZnS:Ag	Blue component of P-4 phosphor	14	\$3.00
1021	Zinc silicate phosphor	Zn ₂ SiO ₄ :Mn	P-1 phosphor as used in cathode-ray tubes	28	3.00
1022	Zinc sulfide phosphor	ZnS:Cu	P-2 phosphor	14	3.00
1023	Zinc-cadmium sulfide phosphor	ZnCdS:Ag	Yellow component of P-4 phosphor	14	3.00
1024	Zinc-cadmium sulfide phosphor	ZnCdS:Ag	Orange component of P-4 phosphor	14	3.00
1025	Zinc phosphate phosphor	Zn ₃ (PO ₄) ₂ :Mn	Red component of P-22 phosphor	28	3.00
1026	Calcium tungstate phosphor	CaWO ₄ Pb	—	28	3.00
1027	Magnesium tungstate phosphor	MgWO ₄	—	28	3.00
1028	Zinc silicate phosphor	Zn ₂ SiO ₄ :Mn	As used in fluorescent lamps	28	3.00
1029	Calcium silicate phosphor	CaSiO ₃ Pb,Mn	—	14	3.00
1030	Magnesium arsenate phosphor	(MgO) _x (As ₂ O ₅) _y :Mn	—	28	3.00
1031	Calcium halophosphate phosphor	3Ca ₂ (PO ₄) ₂ ·Ca(F, Cl):Sb, Mn	—	28	3.00
1032	Barium silicate phosphor	BaSi ₂ O ₇ :Pb	Near ultraviolet emission	28	3.00
1033	Calcium phosphate phosphor	Ca ₃ (PO ₄) ₂ :Tl	Erythral ultraviolet emission	38	3.00

Correspondence should be addressed to: Masao Oyaizu, Secretary, the Electrochemical Society of Japan, 3, 1-chome, Yuraku-cho, Chiyoda-ku, Tokyo, Japan.

Sylvania Announces New Silicon Rod for Transistor Research

Sylvania Electric Products Inc. has announced a new form for silicon which facilitates floating zone purification of the semiconductor material and expedites precise laboratory analysis.

Robert Beatty, general sales manager of Sylvania's Chemical and Metallurgical Division, said that cast silicon polycrystalline rods, high in purity and with a density near theoretical, have been developed by the company in diameters ranging from 4 mm to 15 mm. The rods are ready for floating zone purification, according to Mr. Beatty, without further processing.

The Sylvania sales executive said the new small-diameter rods are available in three standard grades based on resistivity, from solar grade to over 100 ohm cm p-type or 40 ohm cm n-type.

Sylvania silicon is available also as polycrystalline, stalagmatic rod 1½ in. in diameter.

Literature from Industry

New Automatic Activation Makes Yardney Primary and Secondary Batteries Interchangeable, a technical bulletin just issued by Yardney Electric Corp., 40-50 Leonard St., New York City, describes a new activating method which allows Yardney primaries to be activated and operated in any position.

Cerium, Lanthanum, Didymium, and other rare earth metals and alloys are available in the form of ingot, rod, pellet, turnings, or powder. Bulletins on properties and useful applications in the metallurgical and electronic industries are available from Dept. 59, New Process Metals, Inc., 45-65 Manufacturers Place, Newark 5, N. J.

The ABCs of Colloidal Dispersions, a new booklet, has been issued by Acheson Colloids Co., Port Huron, Mich., Div. of Acheson Industries, Inc., manufacturers of the 'dag' family of dispersions designed for a wide variety of industrial uses. Sections of the booklet include "What is Graphite?," "What is Colloidal Graphite?," "Why is a Colloidal Dispersion Better Than a Dry Powder?,"

Lepel
HIGH FREQUENCY INDUCTION HEATING UNITS

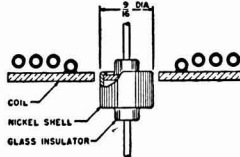
BRAZING
BOMBARDING
SOLDERING
MELTING
HARDENING
ANNEALING

The Lepel line of induction heating equipment represents the most advanced thought in the field of electronics as well as the most practical and efficient source of heat yet developed for industrial heating.

If you are interested in induction heating you are invited to send samples of the work with specifications. Our engineers will process and return the completed job with full data and recommendations without any cost or obligations.

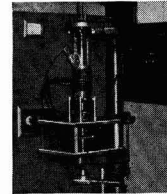
TYPICAL INDUCTION HEATING APPLICATIONS IN THE MANUFACTURE OF TRANSISTORS

SOLDERING TRANSISTOR ASSEMBLIES BY INDUCTION HEATING



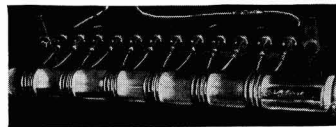
Concentrator-type coil creates high intensity, restricted heating at joint of nickel shell and tinned glass, thus causing solder to flow for permanent seal.

SINGLE CRYSTAL PULLER



General arrangement for pulling single crystals. Induction heating coil is shown surrounding quartz tube containing crucible with molten germanium in suitable atmosphere.

MULTIPLE ZONE REFINING



Induction heating apparatus used in zone refining. The six coils shown provide simultaneous molten zones in the ingot as it passes through the tube containing the protective atmosphere.

Electronic Tube Generators from 1 kw to 100 kw.
Spark Gap Converters from 2 kw to 30 kw.

WRITE FOR THE NEW LEPEL CATALOG . . . 36 illustrated pages packed with valuable information.

All Lepel equipment is certified to comply with the requirements of the Federal Communications Commission.

LEPEL HIGH FREQUENCY LABORATORIES, INC.
55th STREET and 37th AVENUE, WOODSIDE 77, NEW YORK CITY, N. Y.

"Why Is Graphite Dispersed in Various Fluids?," "What is Molybdenum Disulfide?," and "What Other Solids Do We Disperse?," among others. For a copy of the "ABCs" booklet, write Acheson Colloids Co., Port Huron, Mich.

Book Reviews

Mathematics of Physics and Modern Engineering, by I. S. Sokolnikoff and R. M. Redheffer. Published by McGraw-Hill Book Co., Inc., New York, 1958. 810 pages; \$9.50.

This impressive volume—a successor to the senior author's "Higher Mathematics for Engineers and Physicists"—is intended to provide the student with most of the mathematical equipment needed in engineering at its present stage of development. Elementary calculus is the only prior knowledge assumed. The authors tell us that their book will suffice for a four-semester course meeting three hours a week, and this may be an understatement.

The emphasis is, appropriately, on the use of advanced mathematical methods to achieve acceptable solutions of problems, rather than on mathematical developments for their own sake. The evaluation of the errors incurred in approximate calculations receives continual attention. Though difficult proofs are often omitted, there is no carelessness about stating the conditions under which propositions are true; the authors, themselves mathematicians, have not forgotten that application without understanding is sterile if not dangerous, and the reader has every opportunity to perceive the beauty as well as the utility of the subject.

An attempt to mention every commendable feature would be futile when there are so many; perhaps a few should be cited. The distinction between mean and point-wise convergence of Fourier series is discussed at some length, and point-wise convergence is proved for the class of series usually encountered. The Fourier transform is introduced as a means of solving differential equations, in analogy to solution by series. The stability of solutions of differential equations is discussed, though not with the thoroughness which it seems to deserve. A method is given for appraising the error in the solution of a differential equation which is itself only approximate. The discussion of partial differential equations goes as far as possible with arbitrary functions before series are introduced.

In a treatise of such size and scope, it is always possible to find shortcomings, which is to say that every reader would have written the book in a somewhat different way. The faults seem to be those of imitation rather than of original commission. The most convincing reason for confining attention to analytic functions of a complex variable—that this class includes all the functions which can be written explicitly in terms of z , without the separate introduction of x and y , or, equivalently, of z and z^* —is overlooked, as usual. The teacher of thermodynamics or of electronics will deplore, once again, the failure to introduce such nota-

tions as $\left(\frac{\partial f}{\partial x}\right)$ and to present the techniques of manipulating partial

derivatives when the selection of independent variables is subject to frequent shifts. The relegation to an appendix of Laplace transforms, so beloved of engineers, is surprising.

Despite the title, the problems which are not purely mathematical are almost all based on engineering applications, and the preface makes it clear that this is a text designed for use in engineering schools. Some problems taken from modern physics might have broadened its appeal, while incidentally contributing to the general education of engineering students. This omission does nothing to lessen the value of the book to the pure scientist as a work of reference. The price seems very reasonable by contemporary standards.

John Avents

Cuneo Press finds "Plus-4" Copper Anodes keep working until they're "so thin that they almost float"

In the big, busy rotogravure cylinder plating room of The Cuneo Press, Inc., Chicago, the acid-copper tanks are operating 24 hours a day.

Supplying precision cylinders to meet weekly deadlines in printing some 13 million copies of weekly magazines and pictorial sections for newspapers calls for maximum reliability and efficiency in every phase of the operation.

Late in 1954, Cuneo first tried "Plus-4" Anodes, Anaconda's phosphorized copper anodes. After more than three years of experience, they report the following advantages:

1. Solution is more easily maintained and balanced—with consider-

able saving in solution dumped and acid added.

2. Practically no sludge—tanks are drained only half as often as with ordinary anodes.

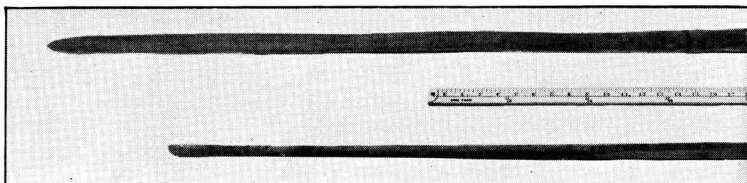
3. 15 per cent more usable copper. "Plus-4's" corrode so evenly (see below) that only slender ribbons remain. Though these do not actually float, they become so light that they no longer maintain proper contact with the anode cradle.

Write for information on how you can obtain a test quantity to supply one tank. Address: The American Brass Company, Waterbury 20, Conn. In Canada: Anaconda American Brass Ltd., New Toronto, Ont.

58137

ANACONDA®

"PLUS-4"® ANODES Phosphorized Copper
MADE BY THE AMERICAN BRASS COMPANY



Progress in Semiconductors, Vol. 2.

Edited by Alan F. Gibson, P. Aigrain, and R. E. Burgess. Published by John Wiley & Sons, Inc., 1957. 280 pages; \$10.50.

This volume is the second in the promised annual series of selected research papers in this ever-growing field of applied electronics, and the critical remarks directed at the first volume (1956) still are valid. The book is a rather loose assembly of specialized research papers with a bare minimum of introduction. An attempt is made by the editor in the preface to coordinate and show some of the high lights in their relative importance but the overburdened general reader will find the reading not easy, due to the compressed form and report style of writing. Special-

ized researchers, however, will find some quite complete papers comprising an immense amount of able research work.

The paper by F. A. Connel and E. W. Saker, although dealing with the newer applications (of semiconducting compounds) for transistor-type devices using aluminum, gallium, indium, phosphorus, arsenic, and antimony instead of the conventional germanium and silicon, constitutes, in the words of the authors, only a part of the whole range of compound semiconductors.

"Semiconductor Alloys" by F. Herman, M. Glicksman, and R. H. Parmenter presents some interesting definitions almost in the style of a monograph but requires knowledge of the specialized language of this literature.

J. H. Crawford and J. W. Cleland explain "Radiation Effects" and ably survey this field to show the effect of particle bombardment to produce acceptor- and donor-states in germanium and in silicon. "The Production of High Quality Germanium Single Crystals" by L. G. Cressel and J. A. Powell is a somewhat easier presentation and a valuable review of importance to the practical crystal-grower and experimenter. It is supplemented by good pictures showing, also, crystal growing furnaces in diagrams and pictures of crystal surfaces (etched), but references are only up to 1955.

The article on "Lifetimes of Free Electrons and Holes in Solids" by A. Rose is of theoretical nature, describing a general model from which the carrier lifetime in a very wide range of materials can be deduced. It also tries to include the transition from semiconductors to insulators.

"Impurities in Germanium" by W. Crawford Dunlap, Jr., tries to give as complete a story of this all-important factor as can be done in the limited space. The studies are concerned only with specific impurity effects in germanium which produce major, easily detectable effects.

"High Electric Field Effects" by J. B. Gunn is a theoretical presentation using a great deal of mathematics to explain the behavior of junctions, the effects of higher electric fields on carrier velocity, and interrelated current densities. The effect of luminosity due to so-called "avalanche" multiplication is shown in two good photographs. Further "Theories of Electroluminescence" are expanded by D. Curie from Paris, France (Laboratoire de Luminescence), with pertinent theoretical explanations in a very compressed form, not easily followed by outsiders.

Summarizing, a lot more coordination and editing is needed to make a readable book out of this loose array of highly compressed articles. As it stands, the general reader will soon find himself stranded. On the other hand, the specialized researcher familiar with the terms, language, and history of the semiconductor field will find the composition stimulating.

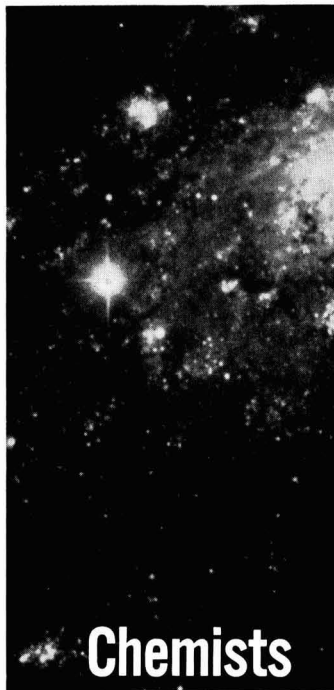
Oscar Morgenstern

The Metallurgy of Vanadium, by William Rostoker. Published by John Wiley & Sons, Inc., New York, 1958. 185 pages; \$8.50.

This is a book about a metal that has not as yet found any industrial application. However, one need but



Putting finishing touches on a copper cylinder for one of the weekly newspaper rotogravure sections shown in the background. Below: Typical "fish" from Cuneo's tanks. The top one is 80" long, weighs 2 lb. 3 oz.—original 85-lb. anode was 1" x 3" x 88½". Lower "fish" is 71" long, weighs 1 lb. 4 oz.—original 74-lb. anode was 1" x 3" x 76".



Chemists Chemical Engineers

Boeing has rewarding research openings in the area of inorganic finishes, for chemists or chemical engineers experienced in electroplating and anodic finishing. The work deals with research studies on the effects of process variables upon structural properties of the base metals and development of new plating techniques. Experience in electrochemistry is desirable but not essential.

Send your inquiry to:

Mr. Stanley M. Little
Department EC-1
Boeing Airplane Co.
P. O. Box 3822
Seattle 24, Wash.

BOEING

recall the recent history of titanium and zirconium and the current exploitation of niobium to realize that metallic vanadium may one day be employed outside of the laboratory.

The author has extracted the important information from the available literature and has organized it in admirable fashion. The result is a smooth story with none of the usual drawbacks of a literature survey. In addition, each of the ten chapters is well documented and is accompanied by a comprehensive bibliography. The material is arranged logically, beginning with a description of the extraction and reduction of the metal and followed by sections on the properties of vanadium and its alloys, their fabrication and finishing, and their resistance to corrosive media. The book ends with chapters on metallography and the use of vanadium as an alloy addition.

Since most of the work on which the book is based was performed during the past few years, one may wonder a little about the motivation for so intensive an effort. Although not specifically stated, it would appear that the purpose has been an exploration directed toward a goal of elevated temperature strength combined with a relatively low density. The value of such a combination in high-speed aircraft or missiles is obvious. It is too soon to predict the ultimate success of the endeavor, but this book is an excellent interim report.

M. Kolodney

Ion Exchange Resins, 2nd Edition, by Robert Kunin. Published by John Wiley & Sons, Inc., New York, 1958. xiii + 466 pages; \$11.00.

Ion Exchange Resins, by J. A. Kitchener. Published by John Wiley & Sons, Inc., New York, 1957. vii + 109 pages; \$2.00.

The second and thoroughly revised edition of the well-known book by Robert Kunin has more than doubled its size, indicating the great increase in both theoretical knowledge and practical application that has occurred in the field of ion exchange resins during the eight-year interval between editions. Addressed to both the newcomer and the advanced worker, this book might well be considered the standard reference book of ion exchange resins. It is thorough in its coverage from the early history of ion exchange resins to the most recent applications in

analytical chemistry and chromatography, hydrometallurgy, ion exchange catalysis, and ion exchange membranes, in addition to the classical problem of water treatment. A wealth of data is presented through the 234 figures and 76 tables; there is scarcely a page in which the reader is not presented with some graphical illustration. Thorough digestion of this book could well make anyone an expert in the field.

Moreover, it is gratifying to see that the material devoted to the increasingly numerous applications of ion exchange resins now exceeds that devoted primarily to theoretical matters. Of special importance to those considering installation of ion exchange equipment is the amplified section on the design and economics of ion exchange units showing sample calculations for a typical water softening problem. Although the literature abounds in technical data for the ion exchange process, up to now little has been written on the economics of its use.

Another unusual and valuable feature is the "laboratory manual" in the chapter on "Methods of Studying Ion Exchange Resins" which gives specific procedures for determining the properties of ion exchange resins. Heretofore, it was only in specific research papers that this information could be found. The chapter on "Miscellaneous Applications" is perhaps of greatest interest to the general reader since it points out the directions along which ion exchange studies are advancing in medicine, atomic energy, agriculture, and non-aqueous media. Any one of these will probably rate a chapter in some future edition.

The book is thoroughly documented. There is a 34-page section containing 1170 references dating as late as 1956.

The smaller of the two books is one of the Methuen Monographs on Chemical Subjects. It is difficult to see to what reader the book is directed. The small size allows only a bare mention of the applications of ion exchange resins which is found in the last third of the book, but there is included an interesting tabulation of these applications. The physical chemistry and kinetics of the ion exchange process are considered in some detail. For someone not in the ion exchange field and who does not intend to go into the field but wishes to obtain a smattering of it, this book might be one to be taken along on a holiday.

W. L. Miller

Announcements from Publishers

"Decontamination of Stainless Steel," Atomic Energy Commission (AEC) Report ANL-4970,* Jan. 1953. 14 pages; 50 cents.

"Disposal of Radioactive Liquid Wastes from the Uranium Recovery Plant," AEC Report HW-54721,* June 1957. 33 pages; \$1.00.

"Electrolytic Recycle Method for the Treatment of Radioactive Nitric Acid Waste," AEC Report KAPL-1721,* June 1957. 81 pages; \$2.00

"Dissolution of Metals in Fused Fluorides," AEC Report ORNL-1877* (Revised), Oct. 1955. 13 pages; 50 cents.

"The Concentration of U²³⁵ by Chemical Exchange in Combination with Countercurrent Electromigration," AEC Report Y-488* (Revised), Aug. 1949. 44 pages; \$1.25.

"Summary of Development and Evaluation of Insulating Type Refractory Coatings," S. Sklarew,

* Order from Office of Technical Services, U. S. Dept. of Commerce, Washington 25, D. C.

C. A. Hauck, and A. V. Levy, Marquardt Aircraft Co., for Wright Air Development Center, U. S. Air Force, Oct. 1956. Report PB 121759,* 96 pages; \$3.75.

"Ceramic Reinforced Alloys and Plated Cermets," M. T. Curran and others, The New York State College of Ceramics, for Wright Air Development Center, U. S. Air Force, May 1957. Report BP 131188,* 49 pages; \$1.25.

"Quantitative Analysis," by Willis C. Pierce, Donald T. Sawyer, and Edward L. Haensch. Published by John Wiley & Sons, Inc., New York, 1958. 497 pages; \$5.75.

"Aliphatic Fluorine Compounds," by Alan M. Lovelace. Published by Reinhold Publishing Corp., New York, 1958. 370 pages; \$12.50.

This comprehensive treatment of the preparation and properties of aliphatic fluorine compounds is of special interest to those in the protective coatings division, but there is a tremendous amount of worthwhile material for both engineers and organic chemists. References are through 1955 with some papers as late as 1956 and 1957.

"Progress in Plastics," Proceedings of British Plastics Convention, July 1957. Edited by Philip Morgan. Published by Philosophical Library, Inc., New York, 1957. 394 pages; \$22.50.

This is the fourth in the "Plastics Progress Series." Articles of interest to Society members may include those on polymerization of olefins, effect of crystallinity on permeability of polythene, factors influencing long-term stress properties of polythenes, high-impact rigid vinyl materials, recent developments in fluorine polymers, and relative merits of epoxide polyesters and phenolic resins in glass-reinforced plastics.

"Encyclopedia of Chemical Reactions, Vol. VII," by C. A. Jacobson and C. A. Hampel. Published by Reinhold Publishing Corp., New York, 1958. 479 pages; \$12.75.

Vol. VII covers strontium, sulfur, tantalum, technetium, tellurium, terbium, thallium, thorium, thulium, tin, and titanium. Although admittedly incomplete, the volume contains over 1700 abstracts of articles on reacting these elements and their compounds, complete with references. There are separate indexes covering reagents and products.

Employment Situation

Please address replies to box shown, c/o The Electrochemical Society, Inc., 1860 Broadway, New York 23, N. Y.

Position Wanted

Chemist-Electrochemist. Situation wanted—Age 36, B.S. degree. Experienced in plating and finishing processes, development-research, process design, production, and control. Extensive experience in metalizing and plating on plastics, printed circuitry, automatic plating, electroless plating, noble metals, cleaning. *Reply to Box 364.*

Advertiser's Index

American Brass Company 196C-197C	
Bell Telephone Laboratories, Inc.	185C
Boeing Airplane Company.....	198C
Enthone, Incorporated	Cover 4
Grace Electronic Chemicals, Inc.	186C
Great Lakes Carbon Corporation	Cover 2
Lepel High Frequency Laboratories, Inc.	195C
Lockheed Missile Systems Division	199C
Stackpole Carbon Company.....	183C

ELECTROCHEMISTS SOLID STATE CHEMISTS

■ Ph.D.'s or equivalent experience for research and development. Work on long-range problems in energy sources, fuel cells, dynamic reserve batteries, and solid state devices. Some positions are in fundamental research; others in development.

Positions are available at the San Francisco Peninsula facilities near Stanford University.

For those attending the Electrochemical Society Convention in Ottawa, Canada, September 29, contact Dr. Morris Eisenberg, Solid State Electronics Department, or write Research and Development Staff, Lockheed Missile Systems Division, Sunnyvale 35, California.

Lockheed

MISSILE SYSTEMS DIVISION

SUNNYVALE, PALO ALTO, VAN NUYS, SANTA CRUZ, COOKE AFB, CALIF.
CAPE CANAVERAL, FLORIDA • ALAMOGORDO, NEW MEXICO



The Electrochemical Society

INSTRUCTIONS TO AUTHORS OF PAPERS

Address all correspondence to the Editor,
JOURNAL OF THE ELECTROCHEMICAL SOCIETY,
1860 BROADWAY, NEW YORK 23, N. Y.

FORM

Manuscripts submitted for publication should be in triplicate to expedite review. They should be typewritten, double-spaced, with 2½-4 cm (1-1½ in.) margins.

Title should be brief, followed by the author's name and his business or university connection.

Abstract of about 100 words should state the scope of the paper and give a brief summary of results.

ILLUSTRATIONS

Drawings will be reduced to column width, 8.3 cm (3¼ in.), after reduction should have lettering at least 0.15 cm (1/16 in.) high. Original drawings in India ink on tracing cloth or white paper are preferred. Curves may be drawn on coordinate paper only if the paper is ruled in blue. All lettering must be of lettering-guide quality. See sample drawing on reverse page.

Photographs must be glossy prints and mounted flat.

Captions for all figures must be included on a separate sheet. Captions and figure numbers should not appear in the body of the figure.

General—Figures should be used only when necessary. Omit drawings or photographs of familiar equipment. Figures from other publications are to be used only when the publication is not readily available, and should always be accompanied with written permission for reprinting.

SYMBOLS

If more than a few symbols are used, these should be defined in a list at the end of the paper, for example:

$a, b \dots$ = empirical constants of Brown equation
 f_i = fugacity of pure i th component, atm
 D_e = bulk diffusion coefficient, cm²/sec

REFERENCES

Literature and patent references should be listed at the end of the paper on a separate sheet, in the order in which they are cited. They should be given in the style adopted by *Chemical Abstracts*. For example:

R. Freas, *Trans. Electrochem. Soc.*, **40**, 109 (1921).

H. T. S. Britton, "Hydrogen Ions," Vol 1, p. 309, D. Van Nostrand Co., New York (1943).

H. F. Weiss (To Wood Conversion Co.), U. S. Pat. 1,695,445, Dec. 18, 1928.

Metric units should be used throughout but, where desirable, English units may be given in parentheses.

Corrosion rates in the metric system should preferably be expressed as milligrams per square decimeter per day (mdd), and in the English system as inches penetration per year (ipy).

In reporting electrode potentials, the sign of the standard Zn/Zn⁺⁺ electrode potential should be taken as negative; Cu/Cu⁺⁺ as positive.

UNITS OF MEASUREMENT

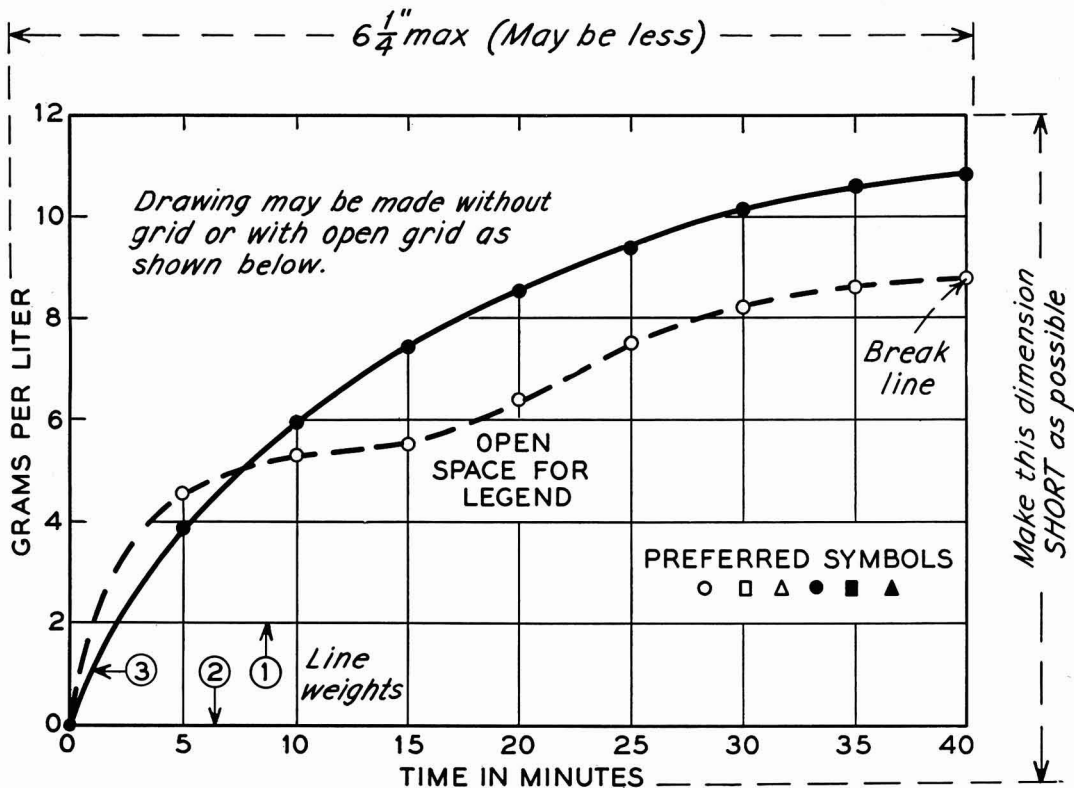
ABBREVIATIONS

Abbreviations should conform with the American Standards Association's list of "Abbreviations for Scientific and Engineering Terms."

GENERAL

Authors should be as brief as is consistent with clarity, and must omit all material which can be regarded as familiar to specialists in the particular field.

The use of proprietary names, trade-marks, and trade names should be avoided if possible. If used, these should be capitalized so that the owner's legal rights are not jeopardized.



Remarks: Line weight 2 is used for borders and zero lines. When several curves are shown, each may be numbered and described in the caption. Lettering shown is approximately 1/8 in. In plotting current or potential as ordinate, increasing negative values should go down.

SAMPLE CURVE DRAWING FOR REDUCTION TO $\frac{1}{2}$ SIZE

The Electrochemical Society

Patron Members

Aluminum Company of Canada, Ltd.,
Montreal, Que., Canada
International Nickel Company, Inc.,
New York, N. Y.
Olin Mathieson Chemical Corporation,
Niagara Falls, N. Y.
Industrial Chemicals Division, Research
and Development Department
Union Carbide Corporation
Divisions:
Electro Metallurgical Company,
New York, N. Y.
National Carbon Company,
New York, N. Y.
Westinghouse Electric Corporation,
Pittsburgh, Pa.

Sustaining Members

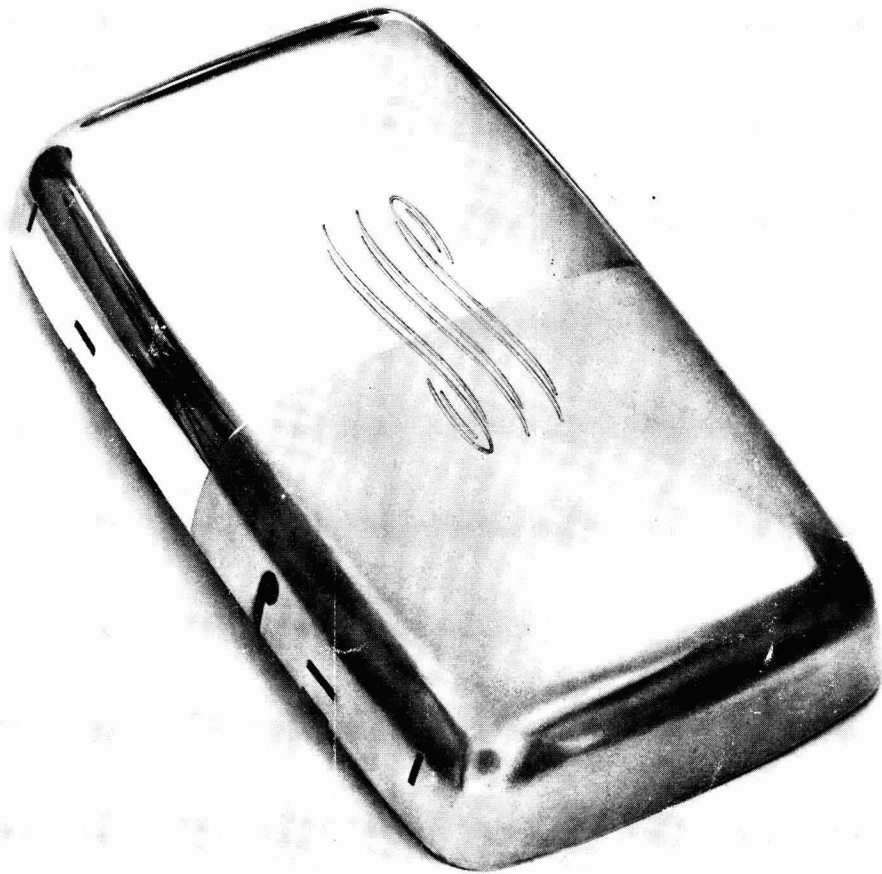
Air Reduction Company, Inc.,
New York, N. Y.
Ajax Electro Metallurgical Corporation,
Philadelphia, Pa.
Allied Chemical & Dye Corporation
General Chemical Division,
Morristown, N. J.
Solvay Process Division,
Syracuse, N. Y. (3 memberships)
Alloy Steel Products Company, Inc.,
Linden, N. J.
Aluminum Company of America,
New Kensington, Pa.
American Machine & Foundry Company,
Raleigh, N. C.
American Metal Company, Ltd.,
New York, N. Y.
American Platinum Works, Newark, N. J.
(2 memberships)
American Potash & Chemical Corporation,
Los Angeles, Calif. (2 memberships)
American Zinc Company of Illinois,
East St. Louis, Ill.
American Zinc, Lead & Smelting Company,
St. Louis, Mo.
American Zinc Oxide Company,
Columbus, Ohio
M. Ames Chemical Works, Inc.,
Glens Falls, N. Y.
Auto City Plating Company Foundation,
Detroit, Mich.
Bart Manufacturing Company, Bellville, N. J.
Bell Telephone Laboratories, Inc.,
New York, N. Y. (2 memberships)
Bethlehem Steel Company,
Bethlehem, Pa. (2 memberships)

Boeing Airplane Company, Seattle, Wash.
Burgess Battery Company, Freeport, Ill.
(4 memberships)
C & D Batteries, Inc., Conshohocken, Pa.
Canadian Industries Ltd., Montreal, Que.,
Canada
Carborundum Company, Niagara Falls, N. Y.
Catalyst Research Corporation, Baltimore,
Md.
Chrysler Corporation, Detroit, Mich.
Ciba Pharmaceutical Products, Inc., Summit,
N. J.
Columbian Carbon Company, New York,
N. Y.
Columbia-Southern Chemical Corporation,
Pittsburgh, Pa.
Consolidated Mining & Smelting Company of
Canada, Ltd., Trail, B. C., Canada
(2 memberships)
Continental Can Company, Inc., Chicago, Ill.
Cooper Metallurgical Associates, Cleveland,
Ohio
Corning Glass Works, Corning, N. Y.
Crane Company, Chicago, Ill.
Diamond Alkali Company, Painesville, Ohio
(2 memberships)
Dow Chemical Company, Midland, Mich.
Wilbur B. Driver Company, Newark, N. J.
(2 memberships)
E. I. du Pont de Nemours & Company, Inc.,
Wilmington, Del.
Eagle-Picher Company, Chemical Division,
Joplin, Mo.
Eastman Kodak Company, Rochester, N. Y.
Electric Auto-Lite Company, Toledo, Ohio
Electric Storage Battery Company,
Philadelphia, Pa.
The Eppley Laboratory, Inc., Newport, R. I.
(2 memberships)
Federal Telecommunication Laboratories,
Nutley, N. J.
Food Machinery & Chemical Corporation
Becco Chemical Division, Buffalo, N. Y.
Westvaco Chlor-Alkali Division, South
Charleston, W. Va.
Ford Motor Company, Dearborn, Mich.
General Electric Company, Schenectady,
N. Y.
Chemistry & Chemical Engineering
Component, General Engineering
Laboratory
Chemistry Research Department

(Sustaining Members cont'd)

- General Electric Company (cont'd)
Metallurgy & Ceramics Research
Department
- General Motors Corporation
Brown-Lipe-Chapin Division, Syracuse,
N. Y. (2 memberships)
Guide Lamp Division, Anderson, Ind.
Research Laboratories Division, Detroit,
Mich.
- Gillette Safety Razor Company, Boston, Mass.
Gould-National Batteries, Inc., Depew, N. Y.
Great Lakes Carbon Corporation, New York,
N. Y.
- Hanson-Van Winkle-Munning Company,
Matawan, N. J. (3 memberships)
Harshaw Chemical Company, Cleveland,
Ohio (2 memberships)
Hercules Powder Company, Wilmington, Del.
Hooker Electrochemical Company, Niagara
Falls, N. Y. (3 memberships)
Houdaille-Hershey Corporation, Detroit,
Mich.
- Hughes Aircraft Company, Culver City,
Calif.
- International Business Machines Corporation,
Poughkeepsie, N. Y.
- International Minerals & Chemical
Corporation, Chicago, Ill.
- Jones & Laughlin Steel Corporation,
Pittsburgh, Pa.
- K. W. Battery Company, Skokie, Ill.
- Kaiser Aluminum & Chemical Corporation
Chemical Research Department,
Permanente, Calif.
Division of Metallurgical Research,
Spokane, Wash.
- Keokuk Electro-Metals Company, Keokuk,
Iowa
- Libbey-Owens-Ford Glass Company, Toledo,
Ohio
- P. R. Mallory & Company, Indianapolis, Ind.
McGean Chemical Company, Cleveland, Ohio
Merck & Company, Inc., Rahway, N. J.
Metal & Thermit Corporation, Detroit, Mich.
Minnesota Mining & Manufacturing
Company, St. Paul, Minn.
- Monsanto Chemical Company, St. Louis, Mo.
Motorola, Inc., Chicago, Ill.
- National Cash Register Company, Dayton,
Ohio
- National Lead Company, New York, N. Y.
National Research Corporation, Cambridge,
Mass.
- Norton Company, Worcester, Mass.
- Olin Mathieson Chemical Corporation,
Niagara Falls, N. Y.
High Energy Fuels Organization
(2 memberships)
- Pennsalt Chemicals Corporation,
Philadelphia, Pa.
- Philips Laboratories, Inc., Irvington-on-
Hudson, N. Y.
- Pittsburgh Metallurgical Company, Inc.,
Niagara Falls, N. Y.
- Poor & Company, Promat Division,
Waukegan, Ill.
- Potash Company of America,
Carlsbad, N. Mex.
- Radio Corporation of America, Harrison, N. J.
Ray-O-Vac Company, Madison, Wis.
- Raytheon Manufacturing Company,
Waltham, Mass.
- Reynolds Metals Company, Richmond, Va.
(2 memberships)
- Schering Foundation, Inc., Bloomfield, N. J.
Shawinigan Chemicals Ltd., Montreal, Que.,
Canada
- Speer Carbon Company
International Graphite & Electrode
Division, St. Marys, Pa. (2 memberships)
- Sprague Electric Company, North Adams,
Mass.
- Stackpole Carbon Company, St. Marys, Pa.
(2 memberships)
- Stauffer Chemical Company, Henderson,
Nev., and New York, N. Y. (2 memberships)
- Sumner Chemical Company, Division of
Miles Laboratories, Inc., Elkhart, Ind.
- Superior Tube Company, Norristown, Pa.
- Sylvania Electric Products Inc., Bayside,
N. Y. (2 memberships)
- Sarkes Tarzian, Inc., Bloomington, Ind.
- Tennessee Products & Chemical Corporation,
Nashville, Tenn.
- Texas Instruments, Inc., Dallas, Texas
- Titanium Metals Corporation of America,
Henderson, Nev.
- Udylite Corporation, Detroit, Mich.
(4 memberships)
- Upjohn Company, Kalamazoo, Mich.
- Victor Chemical Works, Chicago, Ill.
- Wagner Brothers, Inc., Detroit, Mich.
- Weirton Steel Company, Weirton, W. Va.
- Western Electric Company, Inc., Chicago, Ill.
- Wyandotte Chemicals Corporation,
Wyandotte, Mich.
- Yardney Electric Corporation, New York,
N. Y.

How to make metal stripping an exact science: What metal do you want to strip? There are eight metal strippers in the Enthone "ENSTRIP" series, which, in most cases, will do the specialized job thoroughly, quickly, economically. If one of these standard strippers won't precisely cover your requirements, there are special Enthone research developments available. Write us about your particular needs or problems. Include a sample of your product if possible. We'll be glad to recommend the best methods to follow. Enthone, Inc., 442 Elm Street, New Haven 11, Conn.



ENTHONE, INC. IS A SUBSIDIARY OF AMERICAN SMELTING AND REFINING COMPANY

ENTHONE